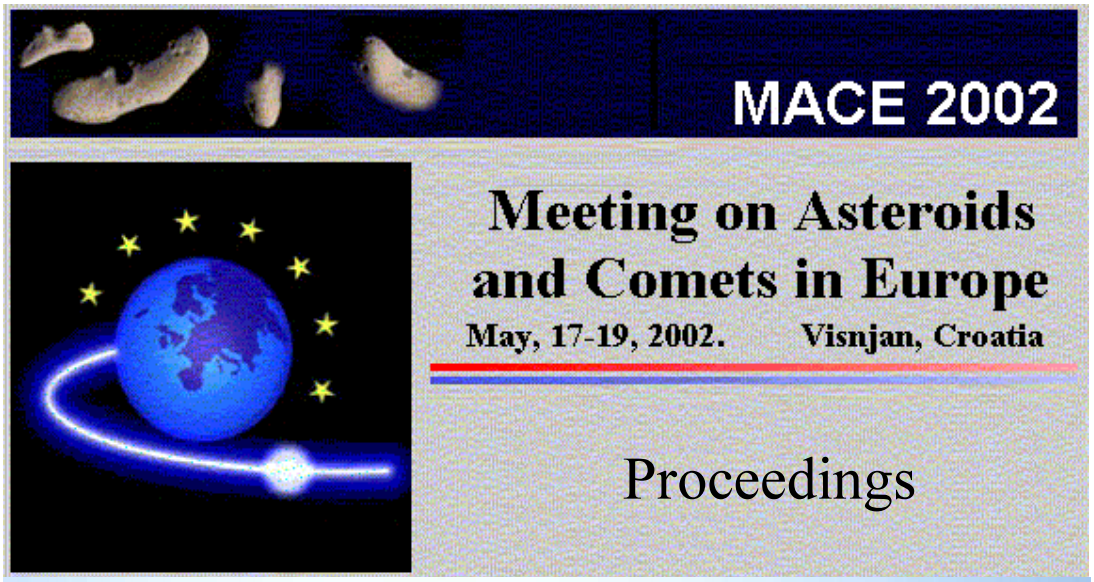

Meeting on Asteroids and Comets in Europe

May, 17-19, 2002. Visnjan, Croatia

Proceedings

MACE 2002

Meeting on Asteroids and Comets in Europe
May, 17-19, 2002. Višnjan, Croatia

SCIENTIFIC AND ORGANIZING COMMITTEE

Luciano Bittesini	(Farra d'Isonzo Observatory) Italy
Korado Korlević	(Višnjan Observatory) Croatia
Jaime Nomen	(Ametlla de Mar Observatory) Spain
Petr Pravec	(Ondrejov Observatory) Czech R.
Herbert Raab	(Linz Observatory) Austria
Jure Škvarc	(Črni vrh Observatory) Slovenia
Stefano Sposetti	(Gnosca Observatory) Switzerland
Reiner Stoss	(Starkenburg Observatory) Germany
Juraj Toth	(Modra Observatory) Slovakia
Željko Andreić	(Proceedings Editor - Institute R. Boskovic) Croatia

LOCAL ORGANIZING COMMITEE

Korado Korlević
Petar Radovan
Ivo Fatorić
Mario Dobrilović
Marino Bravar
Reiner Stoss
Luciano Bittesini
Željko Andreić
Ivo Topolnjak
Robin Paulović
Nevia Poropat
Petar Deklich
Jadranka Škropeta
Petar Poleti
Bravar Elena
Mario Jurić
Ivan Turčin
Ana Bonaca
Ana Bedalov
Petra Korlević
Vanja Brčić
Damir Matković
Valentina Drljača

Table of contents

GIA - GRUPPO ITALIANO ASTROMETRISTI

Luciano BITTESINI
CCAF - 595 Farra Observatory (Italy)

Argument of this presentation is the Italian Astrometrists Group, an informal club of public and private amateur observatories that actively participate at the astrometric work in the world. I like to underline "informal" because there is nothing that links all of us, other than the friendship, the kind of work we do and the word "GIA".
This partnership started in 1989, when I read on a Italian astro-magazine about a Roman that was searching close to him people to do astrometry. I had a lot of time to spend in Rome during my stand-by service, so I called Silvano CASULLI in Colleverde and we soon became family friends.
CASULLI at that time was in touch with Tonino VAGNOZZI of Stroncone observatory and with Ermes COLOMBINI of S.Vittore; in Italy they were doing photographic astrometry like Johann BAUR at Chions, Ulisse QUADRI in Bassano Bresciano and Luciano LAI in Cavriana.
This group became naturally the spring from where we started to take experiences, software and operating instructions (think that the computers we had where the firsts Texas, HP, Commodore or Apple II).
Many of us built the blink-comparators to identify the moving objects and some measuring machines to derive the positions between the stars, others started writing software.
In 1991 started the revolution when we bought the first three ST4's to have a better guide while taking pictures of faint moving objects. After less than a year we ordered the first two ST6's and then we started our asteroid fight sending in March 1993 our first discovery positions.
The first observatory we talk about is Colleverde di Guidonia, just outside the big Rome highway ring; Silvano CASULLI works there from a balcony at 5th floor with another balcony above him, thus he can see only less than half east sky with a lot of light pollution southwards. Nevertheless he continues to follow and discovery minor bodies reaching magnitudes well above 19. m with 0.4m f/3.2 Newton and ST4 ST6 cameras.
Just few kilometers apart lies Mentana with Stefano VALENTINI: since 1994 he joined GIA group writing a lot of software for astrometry: he started with the one for Windows 3.1 and then made an integration of many packets for Windows 95; now he has more complex version able to do even precoveries on old plates; all this software is available to every one asks it him.
Next observatory is Stroncone, just above the south hills of Terni, about 100 km north of Rome. Tonino VAGNOZZI and many other friends had built here a fully automatic telescope capable of high performance due to site elevation, about 800 meters and due to the absence of light pollution southward.
This site has been home of a continuos upgrading of software files that allowed all GIA, since 1992, to read catalogs, blink pictures and compute positions in a very sophisticated manner. _ 0.50m f/3.2 Ritchey-Chretien ST4 ST6
Few kilometers to the east Polino that just started astrometric work. _ 0.40m f/5 Newton ST4 ST6
Going northbound, on the Appennini chain north-west of Florence and north-east of Pisa you may find one of the two observatories of GIA open to the public, S. Marcello. These observatories make a strong activity with students, school groups and common people on a regular basis monthly and even by appointment with teachers: they host even "open nights" during selected astronomical events. Here has been discovered the first Amor in Italy, 1994 QC. _ 0.40m f/5 Newton-Cassegrain ST4 ST5 new telescope and dome
More close to Florence works one of the few ladies of the GIA, Maura TOMBELLI, who with his instrument actually follows NEOs and comets, but time ago worked with S. Marcello and even with Asiago observatory, a professional structure of Padua University, where she contributed to discover about 80 objects. _ 0.30m f/5.7 Schmidt-Cassegrain ST6
Another 100 km northbound, half of the climb of the hill that overstays Bologna, operates the older staff of the italian astrometrists: founded by Ciro VACCHI, that left all of us two years ago, more than 80, with a severe deformity at his legs due to a poliomyelitis while young, and Giorgio SASSI, he more than 80 too and still active, took CCD pictures that Ermes COLOMBINI, in Modena, interested in numerical computations of orbits, identifies and collects data from . _ 0.45m f/5 Newton 0.32m f/2.5 Schmidt ST6
I like to remember that VACCHI and SASSI passed through all the steps of making a telescope, updating it, applying electronics, taking film pictures, processing them, applying a CCD, taking CCD pictures with a computer and interfacing and operating a telescope by computer: all handmade by them. If you go to visit them you may recap all the history of astrometry.
North of Milan, between the two branches of Como lake (humanists here may remember Alexander MANZONI, a famous Italian writer with his "Promessi Sposi" "Betrothed") at about 1500 m of elevation stays a dome where the team of Sormano most of the time follows NEOs.
Even here there is people that develops software to follow fast moving objects, to make a preliminary identification, to compute ephemeris and orbits. _ 0.50m f/4.2 Ritchey-Chretien ST4 ST6
In their web site they have a page dedicated to the objects that need more observations and when the observation arc is big enough they compute the real values of approach to the Earth (MOID), from the past century to the next two, in order to make easier the precoveries on old plates.
In the next years they are planning a new 600 mm telescope and a 2048x2048 CCD.

If we go to the east just south of Verona we meet the observatory of Luciano LAI, another of the "film astrometrists".
He started in Cavriana observatory (571), about 20 km to the west of his actual site, with the discovery of Verona and with a Jupiter observation program born after a request of the French Dragesco, to continue an older program of Lowell Observatory. The program ended after 4 years with the advent of planetary probes when all instruments where ready and well calibrated to operate: LAI said that probably Dragesco may had some other problems causing his withdrawal from the project.
After this research he moved to his home in Dossobuono where he continues experimenting with optics, electronics and CCDs while doing astrometry. _ 0.40m Newton f/5 ST4 ST6
Passing Venice eastwards, after 100 km we reach Remanzacco (Udine) where Giovanni Sostero to the comet astrometry prefers to do, with remarkable results, photometry with standard BVRI and interference filters.
Few kilometers east is Farra where stays the last Italian observatory: we are open to the public like S. Marcello and our annual rate of visitors is above 2000, included more than 50 classes of schools (we have students visiting us from elementary to high-school). There are two main telescopes: the one you see in the slide below a dome is the former one of Mr. Baur and makes all the astrometric work while the other, under a box with a sliding roof, it's a new 300, completely automatic, that will be used for visual observation during visiting times and for automatic research at the end of the guest sessions. _ 0.40m f/4.5 Newton-Cassegrain 0.30m f/4 Newton ST4 ST6
The last of us is not Italian, it stays here: Korado KORLEVIC worked hard to teach mathematics in a polytechnic middle-school, organizing every year many stages of astronomy for his students and for all others that come from the whole Croatia; after the war they remained the only working observatory in this country. Now he left his job in the public education and acts as mentor for high IQ students classes held at the observatory. They participate to our meetings and activities and contribute with software, telescope interfacing and observing time. I like to remenber that in the scoreboard of this observatory there are three comets_ 0.41m f/4.3 Newton-Ross ST6 2048x2048

DETECTING AND MEASURING FAINT POINT SOURCES WITH A CCD

Herbert Raab[a,b]

[a] Astronomical Society of Linz, Sternwarteweg 5, A-4020 Linz, Austria

[b] Herbert Raab, Schönbergstr. 23/21, A-4020 Linz, Austria; herbert.raab@utanet.at

Stars, Asteroids, and even the (pseudo-)nuclei of comets, are point-sources of light. In recent times, most observers use CCDs to observe these objects, so it might be worthwhile to think about some details of detecting and measuring point sources with a CCD. First, this paper discusses the properties of point-sources, and how they can describe them with a small set of numerical values, using a Point Spread Function (PSF). Then, the sources of noise in CCD imaging systems are identified. By estimating the signal to noise ratio (SNR) of a faint point source for some examples, it is possible to investigate how various parameters (like exposure time, telescope aperture, or pixel size) affect the detection of point sources. Finally, the photometric and astrometric precision expected when measuring faint point sources is estimated.

Introduction

Modern CCD technology has enabled amateur astronomers to succeed in observations that were reserved to professional telescopes under dark skies only a few years ago. For example, a 0.3m telescope in a backyard observatory, equipped with a CCD, can detect stars of 20^{mag}. However, many instrumental and environmental parameters have to be considered when observing faint targets.

Properties of Point Sources

In long exposures, point sources of light will be "smeared" by the effects of the atmosphere, the telescope optics, vibrations of the telescope, and so forth. Assuming that the optics are free of aberrations over the field of the CCD, this characteristic distribution of light, called the "Point Spread Function" (PSF) is the same for all point sources in the image. Usually, the PSF can be described by a symmetric Gaussian (bell-shaped) distribution (figure 1) [1]:

$$I_{(x,y)} = H \times e^{\frac{(x-x_0)^2+(y-y_0)^2}{2\partial^2}} + B \qquad (1)$$

$I_{(x,y)}$ is the intensity at the coordinates (x,y), which can be measured form the image. By fitting the PSF to the pixel values that make up the image of the object (figure 1), the quantities x_0, y_0, I, ∂ and B can be found, which characterize the point source as follows:

- **Position**
  The position of the object in the CCD frame can be expressed in rectangular coordinates (x_0, y_0), usually along the rows and columns of the CCD. Fitting a PSF to the image will allow to calculate the position of the object to a fraction of the pixel size.

- **Intensity**
  The height of the PSF (H) is proportional to the magnitude of the object. The total flux of the objects corresponds to the integrated volume of the PSF, less the background signal (see below).

- **Width**
  In equation 1, the width of the Gaussian PSF is characterized by the quantity □. In astronomy, the width of the PSF is frequently specified by the so-called "Full Width Half maximum" (FWHM). As the name implies, this is the width of the curve at half its height. The FWHM corresponds to approximately $2.355 \times \partial$. Although a number of factors control the FWHM (like focusing, telescope optics, and vibrations), it is usually dominated by the seeing. The FWHM is the same for all point-sources in the image (if optical aberrations can be neglected). Most notably, it is independent of the brightness of the object. Bright stars appear larger on the image only because the faint outer extensions of the PSF are visible. For faint stars, these parts drown in the noise and are therefore not visible.

- **Background**
  During the exposure, the CCD not only collects signal from the object, but also light from the sky background and the thermal signal generated within the detector. These signals result in a pedestal (B) on which the PSF is based. Ideally, the background signal is the same over the whole field for calibrated images. In practice, however, it will vary somewhat over the field.

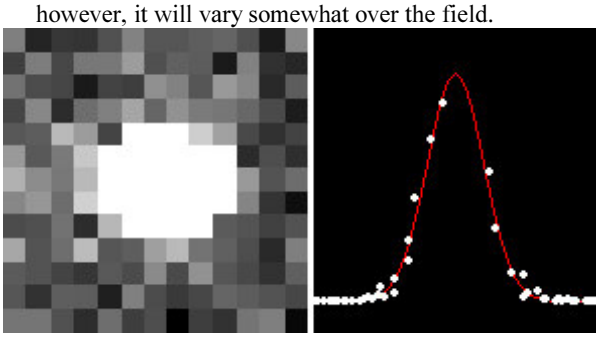

Figure 1: Image of a star on a CCD (left), and the Gaussian PSF fitted to the image data (right).

Signal and Noise

As briefly mentioned above, the CCD not only collects light from celestial objects, but also some unwanted signals. The thermal signal, for example, can be subtracted from the

image by applying a dark frame calibration, but the noise of the thermal signal remains even in the calibrated image. In addition to the thermal noise, the readout noise is generated in the detector. External sources of noise are the photon noise in the signal from the sky background, as well as the photon noise in the signal of the object under observation. The Poisson noise in a signal (that is: the standard deviation of the individual measurements from the true signal) can be estimated as the square root of the signal, i.e.

$$\sigma = \sqrt{N} \qquad (2)$$

where S is the signal (for example, the thermal signal), and σ is the noise level in that signal (in that example, the thermal noise). The total noise from the four independent noise sources mentioned above add in quadrature to give the total noise:

$$\sigma = \sqrt{\sigma_B^2 + \sigma_S^2 + \sigma_T^2 + \sigma_R^2} \qquad (3)$$

where σ is the total noise, σ_B is the background noise, σ_s is the object noise, σ_T is the thermal signal, and σ_R is the readout noise. The Signal Noise Ratio (SNR) can be calculated from:

$$SNR = \frac{S}{\sigma} \qquad (4)$$

Where S is the signal from the object, and σ the total noise. By combining equations 2 to 4, it is possible to calculate the SNR in one pixel:

$$SNR = \frac{S}{\sqrt{S + B + T + \sigma_R^2}} \qquad (5)$$

Here, S is the signal from the object collected in the pixel, B the signal from the sky background and T the thermal signal collected by the pixel, respectively, and σ_R is the readout noise for one pixel. If equation 5 is applied to the brightest pixel in the image of the object, the result is the Peak SNR for that object. The Peak SNR is important, as software (or humans) can detect faint objects only if at least the brightest pixel has a SNR over some threshold that is set to avoid false detections in the image noise. Usually, a Peak SNR of ~3 is considered to be a marginal detection. In other words, this would correspond to the limiting magnitude of the image.
For unfiltered or broadband images, the dominant source of noise is usually the sky background, even under very dark skies. With modern, cooled CCDs, the instrumental noise is generally less important, and object noise is only significant for very bright objects.

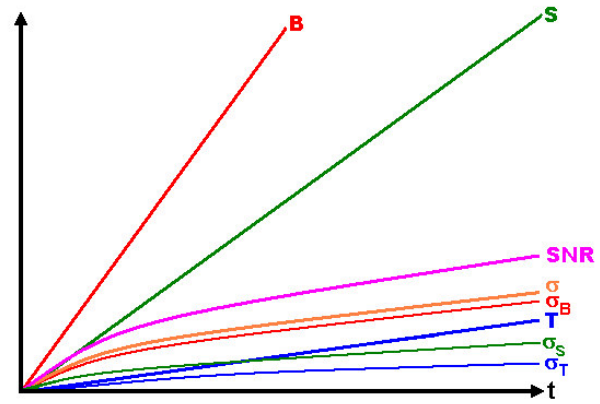

Figure 2: Growth of Signal, Noise, and Signal to Noise Ratio with increasing exposure time.

Figure 2 shows the growth of Signal, Noise, and Signal to Noise Ratio (SNR) with increasing exposure time t. Note that, in this example, the background signal B is stronger than the signal S from the object under observation. The background noise is σ_B, the object noise is σ_S. The readout noise is independent of the exposure time and it is therefore not drawn. (For sky-limited exposures, it can practically be neglected.) The signal S grows linear with increasing exposure time, as do the background signal B and the thermal signal T. Fortunately, the background noise ($\sigma_B = \sqrt{B}$) and the thermal noise ($\sigma_T = \sqrt{T}$) grow slower. Doubling the exposure time will increase all signals (S,B,T) by a factor of 2, but the noise levels (σ_s, σ_B, σ_T, σ) by a factor of only √2, so the SNR increases by $2 \div \sqrt{2} = \sqrt{2}$. With increasing exposure, the faint object will obviously emerge from the noise, even though the background signal is always stronger than the signal from the object in this example.

Estimating the Signal to Noise Ratio

With a few, mostly very simple calculations, it is possible to estimate the Signal to Noise Ratio that can be expected for a stellar object of known magnitude with a certain equipment. In this chapter, one example is described in some detail. Further examples in the following chapter will be used to compare various telescope setups, and the gain (or loss) in the SNR.
The telescope used in this example is a 0.6m f/3.3 reflector, with a central obstruction of 0.2m. As a detector, a CCD with 24µm square pixels (corresponding to 2.5" at the focal length of 1.98m), a dark current of one electron per second per pixel, a readout noise of ten electrons per pixel, and a mean quantum efficiency of 70% over the visible and near infrared portion of the spectrum (400nm to 800nm) is used [2]. We assume a stellar object of 20^{mag} as the target of the observation, the brightness of the sky background to be 18^{mag} per square arc second, and the FWHM of the stellar image to be 4". In that spectral range, we receive about 4×10^{10} photons per second per square meter from a star of 0^{mag} [3]. A difference of 1^{mag} corresponds to a factor of 2.5 in the brightness, so there will be only $4\times10^{10} \div 2.5^{20}$, or about 440 photons per second per square meter from our target. The light collecting area of the 0.6m telescope is 0.25m2, so it will accumulate 11'000 photons in a 100

second exposure. With a quantum efficiency of 0.7, this will generate about 7'700 electrons in the CCD.
Assuming that the PSF of the object can be described with equation 1, and that the peak brightness is located exactly at the centre of one pixel, this pixel collects about 29% of the total light, or about 3'190 photons, which will generate 2'233 electrons in that pixel. The Poisson noise of this signal is $\sqrt{2'233} \sim 47$.
In analogy to the stellar flux, we can estimate the flux from the sky background (18^{mag} per square arc second) to be $4 \times 10^{10} \div 2.5^{18}$, or about 2'748 photons per second per square meter. The telescope therefore collects about 68'700 photons from each square arc second during the exposure. Each pixel covers 6.25 square arc seconds, and therefore, about 429'375 photons from the sky background will be collected during the exposure in each pixel. This will generate about 300'563 electrons, with a Poisson noise of ~ 548 electrons.
During the exposure, the dark current will generate 100 electrons in each pixel, and the dark noise is therefore $\sqrt{100} = 10$. The readout adds further 10 noise electrons.
Using equation 3, the total noise in the brightest pixel can be calculated by adding the object noise in the brightest pixel, the sky noise, the dark noise and the readout noise in quadrature, i.e. $\sqrt{(472 + 5482 + 102 + 102)} \sim 550$. The Peak Signal Noise Ratio is now found to be $2'233 \div 550 \sim 4.1$. Obviously, the 20^{mag} object is only marginally detected in this example.
Although this is a simplified calculation (e.g., no attempt to correct for atmospheric extinction was made, and no attention was given to the saturation of pixels, etc.), it is still a reasonable estimate. Some further telescope setups will be compared in the next chapters, and the results are compared. All calculations are summarized in table 1 in the Appendix.

Exposure Time

In the previous chapter, a star of 20^{mag} is only marginally detected with a 0.6m f/3.3 telescope in a 100 second exposure. In the next example, the exposure time is extended to 600 seconds to increase the Signal Noise Ratio of the object. The calculation, which is summarized as example 2 in table 1 in the Appendix, shows that the SNR of the brightest pixels increases from 4.1 to 10.0. It has been noted previously that increasing the exposure time by a factor of n will raise the SNR by a factor of $\sqrt{n}$. In this example, the exposure time has been increased by a factor of 6, and the SNR was raised by a factor of $\sqrt{6} \sim 2.45$.
The limiting magnitude of an image can be defined by the brightness of the stars reaching some minimal SNR, for example, 3.0. A factor of 2.5 in brightness corresponds to one magnitude, which closely matches the increase in SNR due to the longer exposure. To increase the limiting magnitude by one full magnitude, the exposure time would have to be extended by a factor of 6.25, i.e., to 625 seconds. Pushing the limiting magnitude down by one more magnitude, another increase by a factor of 6.25 would be necessary: the exposure time would increase to about 3900 seconds, or 65 minutes (figure 3).

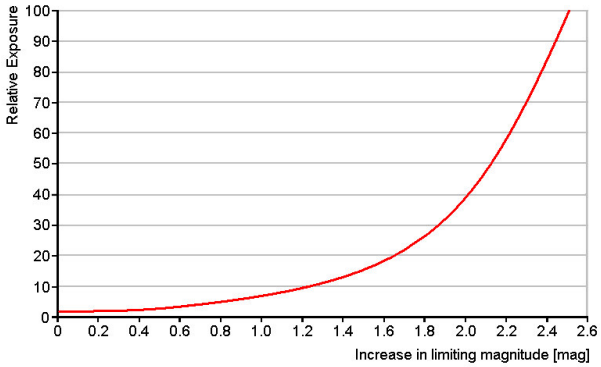

Figure 3: Relative exposure time required for increasing the limiting magnitude.

Telescope Aperture

In the next example, we will expand the telescope aperture from 0.6m (as used in the previous examples) to 1.5m, with a central obstruction of 0.5m in diameter and a focal length of 7m. For the environment (sky background, seeing) and the detector, the same values as in the previous examples are used, and a exposure time of 100 second (as in example 1) assumed. The result of the calculation, which is summarized as example 3 in table 1 in the Appendix, is somewhat surprising: Although the 1.5m telescope has 6.25 times more light collecting area than the 0.6m instrument, the Peak SNR is now only 3.4. Compared to the Peak SNR of 4.1 that was found for the 100 second integration with the 0.6m telescope, this is a loss of $\sim 0.2^{mag}$ in limiting magnitude.
How can this be? Due to the long focal length of the telescope, each pixel now covers only 0.71" × 0.71". Compared to the 0.6m telescope from the previous examples (pixel size 2.5" × 2.5"), this is only 8% of the area. By combining the increased light collecting power, and the smaller pixel scale, we find that each pixel receives only about $6.25 \times 0.08 \approx 0.5$ times the light collected in one pixel of the CCD by the smaller telescope. As both the light from the object and from the sky background (the dominant source of noise in these examples) drop by the factor of 0.5, the SNR should decrease approximately by a factor of $0.5 \div \sqrt{0.5} \sim 0.7$. The true factor found by comparing the SNR calculated in examples 1 and 3 is only about 0.8, because the PSF is a non-linear function (equation 1), concentrating more light in the centre of the pixel than in the outer regions that were lost due to the smaller angular size of the pixels in that example.
Does this mean that it makes no sense to use larger telescopes? Of course not! Apparently, the problem is related to the pixel scale, so pixel binning might be of some help: By using 2 × 2 binning (example 4), a Peak SNR of 6.4 is obtained, which corresponds to an increase in limiting magnitude of about 0.5^{mag} as compared to the 0.6m telescope in example 1, or of 0.7^{mag} as compared to the 1.5m telescope with the CCD used without binning (example 3).
Scaling the FWHM from 4" to 2" (by improving the telescope optics, the focusing, the mechanics or the seeing, if possible in some way) would be even better than binning: The peak SNR would grow to 12.7, and the gain in limiting

magnitude is about 1.2^{mag}, as compared to example 1, or 1.4^{mag} as compared to example 3.

Pixel Size and Sampling

Apparently, the relative size of the pixel to the FWHM of the stellar images is an important factor in obtaining the highest possible SNR. By performing calculations similar to the SNR estimates in the previous chapters, it can be shown that the highest Peak SNR is obtained when the pixels are about 1.2 × FWHM in size (figure 4).

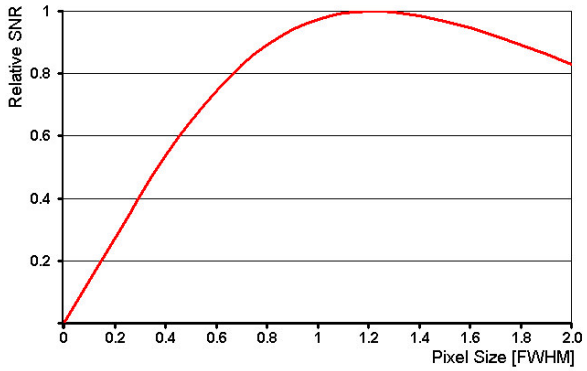

Figure 4: Variation of peak SNR for various pixel scales. The pixel size is measured in units of FWHM.

With such large pixels, most of the photons are collected by the single pixel on which the PSF of the stellar image is centred, whilst only the fainter, noisy "wings" of the PSF fall on the neighbouring pixels, resulting in a high SNR. However, with almost all the light concentrated in a single pixel, it would be very difficult to distinguish real objects from image artefacts (like hot pixels or cosmic ray strikes), and it is impossible to calculate the precise position of the object to sub-pixel accuracy.

To retain the information of the objects on the CCD image, the scale must be chosen so that the FWHM of stellar sources spans at least 1.5 to 2 pixels [4]. This scale is called "critical sampling", as it preserves just enough information that the original PSF can be restored by some software analysing the image. With even larger pixels (i.e., less than 1.5 pixels per FWHM), the PSF can not be restored with sufficient precision, and astrometric or photometric data reduction is inaccurate, or not possible at all. This situation is called "undersampling". In the other extreme ("oversampling") the light of the object is spread over many pixels: Although the PSF of stellar objects can be restored with high precision in this case, the SNR is decreased (figure 5).

Critically sampled images will give the highest SNR and deepest limiting magnitude possible with a given equipment in a certain exposure time, without loosing important information contained in the image. For applications that demand the highest possible astrometric or photometric precision, one might consider some oversampling. The same is true for "pretty pictures", as stars on critically sampled images look rather blocky.

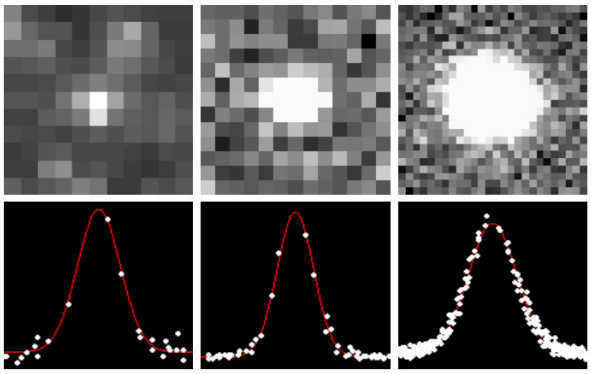

Figure 5: Undersampled (left), critically sampled (center) and oversampled (right) stellar images (top row), and the PSF fitted to the image data (bottom row).

Error Estimates

Fitting a PSF profile to a faint, noisy detection is naturally less precise than for bright stellar images with a high SNR (figure 6). Position and brightness calculated for faint detections are therefore expected to be less precise than for bright objects.

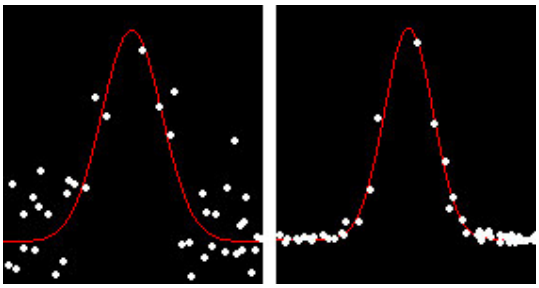

Figure 6: Gaussian PSF fitted to a faint (Peak SNR ~4) and a bright (Peak SNR ~100) stellar image.

The fractional uncertainty of the total flux is simply the reciprocal value of the Signal to Noise Ratio, 1 ÷ SNR (sometimes also called the Noise to Signal Ration). By converting this uncertainty to magnitudes, we get:

$$\sigma_{PHOT} = \frac{Log(1+\frac{1}{SNR})}{Log(2.5)} \qquad (6)$$

Here, σ_{PHOT} is the one-sigma random error estimated for the magnitude measured, and SNR is the total SNR of all pixels involved (e.g., within a synthetic aperture centred on the object). By modifying equation 5, we can find this value from:

$$SNR = \frac{S}{\sqrt{S + n \times \left(B + T + \sigma_R^2\right)}} \qquad (7)$$

In this formula, S is the total integrated signal from the object in the measurement (i.e., within the aperture), and n is the number of pixels within the aperture. The other quantities are identical to equation 4. It should be noted that, as both S and n will change with the diameter of the aperture, the total SNR varies with the diameter of the

photometric aperture, so photometry can be optimised by choosing the appropriate aperture [5].

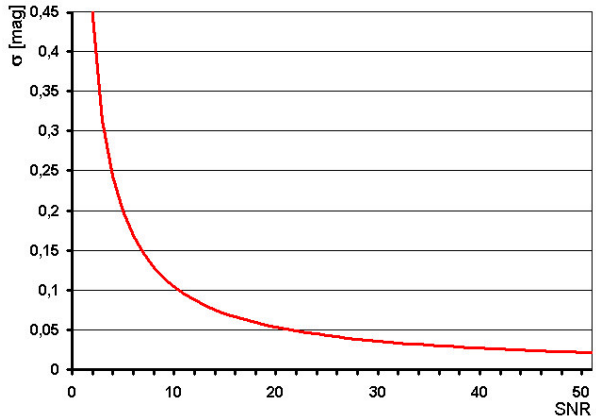

Figure 7: The photometric error (in stellar magnitudes) expected for point-sources up to a SNR of 50.

Figure 7 shows the expected uncertainty in the magnitude for point up to SNR 50, as calculated from equation 6. Equation 6 only estimates the random error in photometry due to image noise. It does not account for any systematic errors (like differences in spectral sensitivity of the CCD and the colour band used in the star catalogue) that might affect absolute photometric results.

Provided that the stellar images are properly sampled, the astrometric error can be estimated using this equation [6]:

$$\sigma_{AST} = \frac{\sigma_{PSF}}{SNR} \qquad (8)$$

Here, σ_{AST} is the estimated one-sigma error of the position of the object, σ_{PSF} the Gaussian sigma of the PSF (as in equation 1), and SNR is the Peak Signal to Noise Ratio of the object. Note that σ_{AST} will be expressed in the same units as σ_{PSF} (usually arc seconds), and that σ_{PSF} can be calculated from FWHM÷2.355.

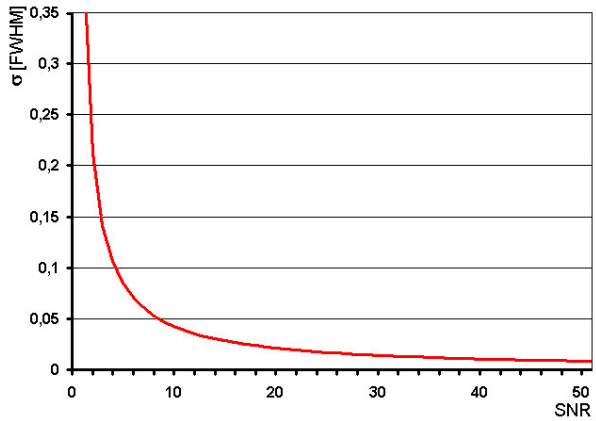

Figure 8: The astrometric error (in units of the FWHM) expected for point-sources up to a Peak SNR of 50.

Figure 8 shows the expected uncertainty in the position (in units of FWHM) for point up to SNR 50, as calculated from equation 8. Again, equation 8 only estimates the random error in the stellar centroid due to image noise. It does not account for any systematic errors (introduced by the astrometric reference star catalogue, for example) that might affect absolute astrometric results.

Returning to example 1, the astrometric one-sigma error expected for the point source with a Peak Signal to Noise Ratio of 4.1 and a FWHM of 4" can now be estimated to ~0.4", using equation 8. Adopting a photometric aperture with a diameter of 3 × FWHM (covering 18 pixels), a total Signal to Noise Ratio of about 3.3 is found by using equation 7. From equation 6, the photometric error is estimated to ~0.3^{mag}.

An astrometric error of ~1" is acceptable, particularly if it is a observation of a minor planet with a uncertain orbital solution or a large sky-plane uncertainty (for example, as in the case of late follow-up or recovery observations). Observations of the light curve of a minor planet usually require a precision of 0.05^{mag} or better, corresponding to a SNR of 20 or higher. Obviously, photometric observations are much more demanding than astrometry.

Summary and Conclusions

This paper first described the characteristics of a Gaussian Point Spread Function, and the sources of noise in the imaging system. A few examples, estimating the Signal to Noise Ratio obtained for faint point sources with various telescope setups, highlighted that environmental conditions, telescope equipment, and CCD detector must harmonise to operate at peak performance. Finally, the astrometric and photometric error expected when measuring faint point sources was estimated.

Useful astrometric results can be obtained even for very faint targets at the limit of detection, particularly if the sky-plane uncertainty for the object under observation is large. For photometric studies, a higher SNR is desirable.

References

1. Auer, L. H.; van Altena, W. F.: Digital image centering II, Astronomical Journal, 83, 531-537 (1978)

2. Scientific Imaging Technologes, Inc: SITe 512 × 512 Scientific-Grade CCD

3. Berry, R; Burnell, J.: The Handbook of Astronomical Image Processing, Willmann-Bell, Inc. (2000)

4. Howell, S. B.; Koehn, B; Bowell, E.; Hoffman, M.: Detection and Measurement of poorly sampled Point Sources images with 2-D Arrays, The Astronomical Journal, **112**, 1302-1311 (1996)

5. Naylor, T.: An optimal extraction algorithm for imaging photometry, Monthly Notices of the Royal Astronomical Society, **296**, 339-346 (1998)

6. Neuschaefer, L. W.; Windhorst, R.A.: Observation and Reduction Methods of deep Palomar 200 inch 4-Shooter Mosaics, The Astrophysical Journal Supplement Series, **96**, 371-399 (1995)

Share for central Pixel	**0.29**	**0.29**	**0.027**	**0.104**	**0.104**
Object Flux in centr. Pixel	**3'190 γ**	**19'140 γ**	**1'865 γ**	**7'184 γ**	**7'184 γ**
Signal to Noise Ratio Estimation					
	Example 1	Example 2	Example 3	Example 4	Example 5
Telescope					
Mirror Diameter	**0.60 m**	**0.60 m**	**1.50 m**	**1.50 m**	**1.50 m**
Obstruction	**0.20 m**	**0.20 m**	**0.50 m**	**0.50 m**	**0.50 m**
Light Collecting Area	**0.25 m2**	**0.25 m2**	**1.57 m2**	**1.57 m2**	**1.57 m2**
Local Length	**1.98 m**	**1.98 m**	**7.00 m**	**7.00 m**	**7.00 m**
Focal Ratio	**3.30**	**3.30**	**4.67**	**4.67**	**4.67**
Detector					
Pixel Size	**24 µm**	**24 µm**	**24 µm**	**48 µm**	**24 µm**
Pixel Scale	**2.50 "/Pixel**	**2.50 "/Pixel**	**0.71 "/Pixel**	**1.42 "/Pixel**	**0.71 "/Pixel**
Dark Current	**1 e^-/s/Pixel**	**1 e^-/s/Pixel**	**1 e^-/s/Pixel**	**4 e^-/s/Pixel**	**1 e^-/s/Pixel**
Readout Noise	**10 e^-**	**10 e^-**	**10 e^-**	**20 e^-**	**10 e^-**
Quantum Efficiency	**70 %**	**70 %**	**70 %**	**70 %**	**70 %**
Integration Time	**100 s**	**600 s**	**100 s**	**100 s**	**100 s**
Object and Sky					
Object Magnitude	**20 ^{mag}**	**20 ^{mag}**	**20 ^{mag}**	**20 ^{mag}**	**20 ^{mag}**
Sky Background	**18 ^{mag}/□"**	**18 ^{mag}/□"**	**18 ^{mag}/□"**	**19 ^{mag}/□"**	**19 ^{mag}/□"**
FWHM	**4"**	**4"**	**4"**	**4"**	**2"**
SNR Calculation					
Object Flux	**11'000 γ**	**66'000 γ**	**69'080 γ**	**69'080 γ**	**69'080 γ**
Object Signal	**7'700 e^-**	**46'200 e^-**	**48'356 e^-**	**48'356 e^-**	**48'356 e^-**
Object Signal in centr. Pixel	**2'233 e^-**	**13'394 e^-**	**1'305 e^-**	**5'029 e^-**	**5'029 e^-**
Object Noise in centr. Pixel	**47 e^-**	**116 e^-**	**36 e^-**	**71 e^-**	**71 e^-**
Background Flux	**429'375 γ/pixel**	**2'576'250 γ/pixel**	**217'487 γ/pixel**	**869'948 γ/pixel**	**217'487 γ/pixel**
Background Signal	**300'648 e^-/pixel**	**1'803'375 e^-/pixel**	**152'241 e^-/pixel**	**608'964 e^-/pixel**	**152'241 e^-/pixel**
Background Noise	**548 e^-/pixel**	**1342 e^-/pixel**	**390 e^-/pixel**	**780 e^-/pixel**	**390 e^-/pixel**
Dark Current	**100 e^-/pixel**	**600 e^-/pixel**	**100 e^-/pixel**	**400 e^-/pixel**	**100 e^-/pixel**
Dark Noise	**10 e^-/pixel**	**25 e^-/pixel**	**10 e^-/pixel**	**20 e^-/pixel**	**10 e^-/pixel**
Noise in centr. Pixel	**550 e^-**	**1342 e^-**	**392 e^-**	**783 e^-**	**397 e^-**
Peak SNR	**4.1**	**10.0**	**3.4**	**6.4**	**12.7**

Table 1: Summary of the SNR calculations mentioned in the text. Example 1 is described in some detail in the paper. Note that, for example 4, the pixel size listed in the table is not the physical size, but the site of the 2×2 binned pixel, and all other data refer to the binned pixel.

PRECISION IN ASTROMETRY AND PHOTOMETRY : AN AMATEUR APPROACH

Bernard Christophe, 65 Bld de Courcelles,75008 Paris , France

bchristo@club-internet.fr

Abstract :

When studying the rotation of asteroids it is necessary to get a great number of images of the same stars field. In fact, we also have access to the precision in the measurement of position and of magnitude of the stars of the field.
I would like to give some further explanations : Indeed, if a hundred images of the same area are recorded and if it is possible to measure, in each picture, a hundred stars by using sofware like IRIS, as well as the USNO catalog. We do get, for each star showing on several images, an interesting number of measurements of positions and magnitude. Consequently, it is possible to calculate the average and the rms of measured RA, De, Mag for each of these stars.
The average measurements could be used to update catalogs, whereas the rms value gives you an information on the obtained precision. I have performed this kind of survey with 100 images of an area surrounding the Asteroid 14923 1994TU3. Results are not « absolute » but depend on how images were obtained. I will present some conclusions and raise some questions.

Principles of the measuments :

Let's make the assumption that we have 100 stars in the field of view, each star being affected by some noise (this noise is caused by fluctuations of the background, pixelisation, turbulences, etc..).
If all the stars have the same position noise - say 1 sec of arc rms, the grid defined by the 100 stars will bear an rms position noise of only 0.1 sec of arc (1sec of arc divided by the root of 100). Now if I compare the position of one star with the grid defined by the 100, the rms measured will be a little bit over 1 sec of arc, the error coming through grid noise is negligeable.
I compare positions with the USNO catalog in order to get more informations but it is not really necessary for obtening measurement precision.
By using 100 pictures, you get a very good confidence in the average and in the rms value for positions and magnitudes.

Conditions of observation :

I used a home made newtonian 60 cm telescope, 335 cm focal length.
The conditions of observation are 70 Km North of Paris at a low altitude, very near of what you can have in a plain area. (during these observations the seeing was rather good : 2sec of arc - the target was near the zenith).
The CCD camera used is an Hi-sis 22, equiped with a Kodak Kaf 400 - no filter and binning configuration 2*2.

This gives a 1 sec of arc resolution and a field of view of 6*4 min of arc.

Exposure time is chosen at 100sec for not saturating the 13mag star in the field and also to get sharp stars and maximize the signal to noise ratio.

Target :

Observation of the rotation of 14923 1994TU3 Mag 15.6 21h23m29s 31°39 (2000) near dzeta Cygni (Fig 1) This Asteroid was chosen for the following reason :

- no curves of rotation were available ,
- its angular mouvement will keep it in the small field of view during the 4 hour time of observation,
- its predicted mag of 15.6 is within a range of good precision, as we will see.

100 pictures were saved , Fig 2 shows one of these pictures (n°82). Fig 3 is the sum of all the pictures, on which we can see the mouvement of the asteroid and also some very weak stars around mag 21.

Fig 4 shows the USNO-A.2 stars (around 150) of the same field of view.

CCD camera sofware :

I use Qmips 32 to acquire the pictures and IRIS to process them.
Each picture is corrected for offset dark and flat. After that I will use the automatic astrometric process of the software. When one picture has been processed, the software will deliver a list of the detected stars with their positions and magnitude, compared with the USNO reference stars.

Fig 5 gives an exemple of these detected stars list and Fig 6 gives the catalog reference stars list.

IRIS also gives access to the signal to noise ratio for different stars.
Fig 7 shows S/N compared with magnitude.
The noise was around 4 LSB and the dynamic range of the 12 bit camera is 4096. A star mag 13 is at the limit of saturation and a star mag 18 is detected with an S/N of 10.

I developped a few softwares in Basic, to aggregate these stars lists, to match stars and for each one of the common stars on the 100 pictures to calculate :

- the average positions and the rms
- the average magnitude and the rms

Results :

Fig 8 shows a list of differences between the reference positions of USNO stars and the average position obtained. These differences are quite large, sometimes over 0.5 sec of arc, which means that the USNO catalog is getting old and should be tuned up.

Fig 9 gives the rms of the measured RA and De versus magnitude .
Fig 10 gives the rms versus S/N
Fig 11 gives the rms of the measured magnitude versus magnitude
Fig 12 gives the rms versus S/N.

I would like to emphasize that, between magnitude 13 and 17 and for an observation time of 100s, we obtain :
rms value in RA and De better than 0.1 sec of arc
rms value in Magnitude better than 0.05 mag.

This means that if we take only one picture at 95% of confidence we will be at + or - 0.2 sec of arc and at + or – 0.1 mag, around mag 18 respectively + or – 0.4 sec of arc , + or – 0.3 mag.
If we increase the observation time or if we take N pictures, these precisions will be improved by the root of N.

If we want to reach 0.01mag, we would need 2500s and for 0.01 sec of arc, we would need 10000s of observation time.

Conclusions :

I think that reaching a precision of 0.1 sec of arc in 100 s of observation is a very interesting and encouraging result. This means that amateur astronomer can do a lot of astrometric work. To do so, we need an improved reference catalog.
For the magnitude measurements, the dispersion is quite large because we face many problems about the R and B mag of the catalog and the spectral CCD response.
In the future I hope that we will get a catalog with not only a position precision of 0.01 sec of arc but also with reference filtered magnitudes.

I would like to comment the avantages of the techniques above mentionned :
-They are quite simple to implement and they would enable anybody to get his own precision curves,
- It is also an absolute way of comparing different softwares, CCD, binning, etc…

These results raise some questions :
Are the curves coherent with the ratio signal to noise (see the article by Herbert Raab) ?
Are some other parameters significant (CCD uniformity ….) ?
Can we improve the situation ?
What should be done on the telescope on the camera on the software ?

ADAS, ASIAGO-DLR ASTEROID SURVEY

Cesare Barbieri[a], Giuliano Pignata[b], Gerhard Hahn[c], Stefano Mottola[c], Martin Hoffmann[d], Riccardo Claudi[b], Sara Magrin[a], Ivano Bertini[a], Luciano Salvadori[a], Massimo Calvani[b]

[a]Department of Astronomy, University of Padova, vicolo Osservatorio 2, 35122 Padova, barbieri@pd.astro.it

[b]Astronomical Observatory of Padova

[c]DLR Institute of Space Sensor Technology and Planetary Exploration, Berlin (Germany)

[d]Institute for Geology, Geophysics and Geoinformatics, Freie Universität Berlin (Germany)

***ADAS, the Asiago-DLR Asteroid Survey**, is the joint program among the Department of Astronomy and Astronomical Observatory of Padova and the DLR Berlin, dedicated to the search of asteroids. The Minor Planet Center has attributed to ADAS the survey code 209. On the Web, ADAS is described in:* **http://planet.pd.astro.it/planets/adas**.*

The project is carried out since the end of December 2000 with the S67/92cm telescope at Asiago - Cima Ekar equipped with the SCAM-1 camera of DLR, in Time Delay Integration mode, in a strip from –5° to +15° around the celestial equator. The camera has a front illuminated Loral chip of 2048x2048 pixels of 15 micrometers each, covering a field of 49'x49' with a resolution of 1".4/pixel.

This paper presents the main results obtained till March 15, 2002, when the telescope has been closed for a complete overhaul. ADAS will resume presumably at the end of June 2002.

Introduction

The project to adapt a CCD camera to the S67/92 cm Schmidt telescope at Cima Ekar (Fig. 1) is a joint collaboration between the Department of Astronomy and the Astronomical Observatory of Padova on one side, and DLR Berlin on the other. The main scientific driver is the discovery and follow up of moving objects (asteroids, NEOs, NEAs, TNOs, KBOs, etc.). Hence the name **ADAS: Asiago-DLR Asteroid Survey** given to the project. The Minor Planet Center has attributed to ADAS **the survey code 209.** An updated view of ADAS can be found on the Web site: **http://planet.pd.astro.it/planets/adas**

Other scientific programs will be possible: no filter is at moment provided, but a filter wheel device is available and it will be mounted in the near future.

DLR has provided the SCAM-1 camera (which can be operated both in Time-Delay Integration mode and in normal mode), the software for image acquisition and quick look (Astph32), and for astrometry and automatic detection of moving objects by comparing 3 frames (Rackis, see Fig. 2).

Fig. 1 – The SCAM camera head and its electronics attached to the NW side of the S/67-92cm telescope at Cima Ekar.

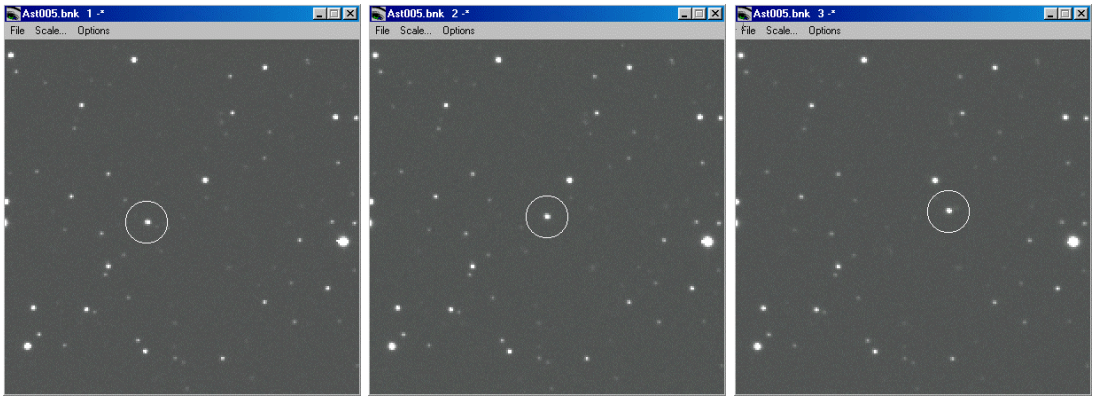

Fig. 2 – Three images for the detection of an asteroid.

Photometry and centroiding of all stars on the frame is accomplished by using Sextractor, a public domain software package developed by E. Bertin and S. Arnouts (1996, [1]).

The thick front-illuminated CCD is a grade A 2048x2048 LORAL chip with a pixel size of 15x15 µm (1".437x1".437 on the sky), and covers an area of 49x49 arcmin (0.67 sq deg). In TDI, the effective exposure time for each star is of 196s at the equator. The camera is equipped with a Vincent 45 precision shutter, the shortest exposure time being 0.1 sec; because the diameter of the shutter is of 45 mm, a slight vignetting is introduced. The chip is refrigerated by a two-stage cooling device, where the primary stage is a Peltier cooler and the secondary one consists of a closed-circuit liquid refrigerator. The achieved CCD operational temperature is –63 °C. A complete characterization of the chip and its electronics was performed thanks to the kind help of Catania Astrophysical Observatory (Claudi et al. 2002 see Fig. 3, [2]).

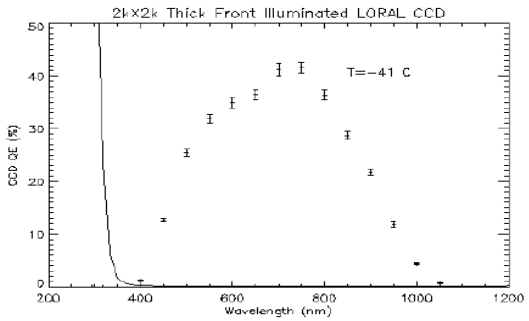

Fig. 3 – The quantum efficiency of the Loral chip. The continuous curve is the "opacity" of the BK7 dewar window (Claudi et al. 2002)

The system obtained useful data since December 21st,2000. Till the middle of February 2001, the focal plane was folded to the CCD camera via a (slightly undersized) flat metal mirror kindly provided by Officine Galileo (Firenze); the mirror is a spin-off of the very successful prototype built for the Halley Multicolour Camera on board GIOTTO, now produced in large quantities for several non-astronomical applications. A new flat mirror in glass, with larger dimensions in order to collect all the light beam, and excellent optical quality (see Fig. 4), was produced by Ottica ZEN (Venezia); it was installed at the telescope the 21st of February 2001.

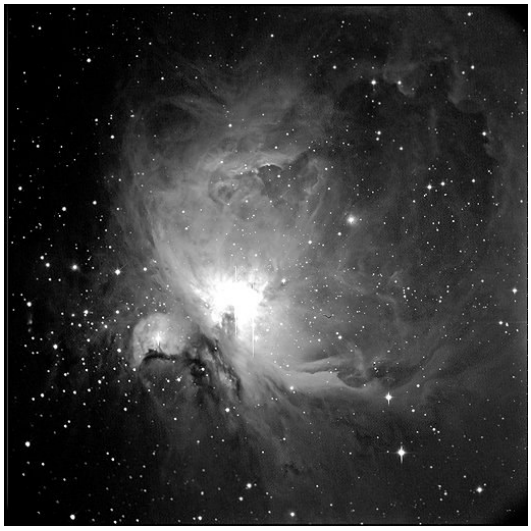

Fig. 4 – M 42, 15^{S}, unfiltered

Several tools for ADAS have been adapted from available software packages. The astrometric residuals are evaluated by a comparison with the asteroids positions (MPC format) in the **asteroid server** developed by **J. Skvarc** through the web interface: **http://astro.ago.uni-lj.si/asteroids/residuals.html**
This service uses several programs and information sources developed by different people. The asteroid database is maintained at **Lowell Observatory** by **E. Bowell**. Propagation of asteroid positions is done by a program called **Orbfit,** part of a NEO information tool **NEODyS** developed by the **Orbfit consortium**. Identification of the asteroids is made using the MPC tool:

MPChecker http://cfaps8.harvard.edu/~cgi/CheckSN?s=m

The asteroid positions are referred to the USNO SA2.0 and to the GSC 1.1 Astrometric Catalogues.

1 – The First Phase, 20 Dec. 2000 – 20 Feb. 2001, normal imaging mode

The first phase of our work, using the metal mirror, lasted from Dec. 20, 2000 through Feb. 20, 2001. Although the optical quality had not reached its optimal value, the limiting magnitude was already sufficiently faint to give hope to have a competitive system. For instance, the faintest observed object the very first night was 1998 KN45, V(JPL) = 19.94 (there is no

filter in front of the CCD, the effective band is essentially V+R), with an exposure time of 80 sec. In this first part of the ADAS program, we have essentially operated in guided mode.

2 – The Second Phase, since 21 Feb. 2001 till 15 March 2002, TDI mode

The second phase of ADAS started on 21 Feb 2001, when the new excellent glass mirror was mounted. The optical quality improved and the alignment of the CCD columns with the Hour Angle was optimized, so that the TDI scan mode could be implemented.

With the TDI technique and 30 min long scans, we cover a field of 6.15 sq deg for 3 times in 1.7 hours, approximately 3.6 sq deg/h. In winter time (10h observing runs), the total surveyed field has been of 36.0 sq deg; in summer time (6h observing runs) the total surveyed field has been of 21.6 sq deg.

The image quality can be maintained good only in the interval of declination (-5°,+10°), on higher declination the curvature of the sky becomes noticeable, but several data were nevertheless obtained at Hour Angles not too far from the meridian. The observing time was divided essentially among 2 different programs:

1. survey of asteroids around the meridian, in particular around Saturn's Lagrangian points and near the opposition
2. survey of asteroids at small solar elongations.

For both point we give a detailed account in paragraph 3 and 4.

The area covered in TDI mode is shown in Fig. 5.

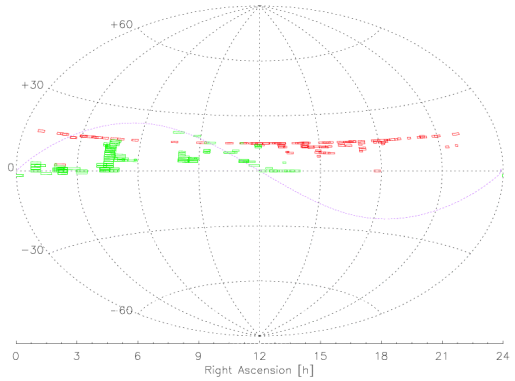

Fig. 5 – Area of sky covered in TDI mode, the fields observed at small solar elongation are red colored while the fields observed around the meridian are green**.**

Table 1 gives the statistics of the results obtained to date.

Table 1 – The results obtained from December 2000 to March 2002.

New Designations: 221
Total number of Positions: 13372
New Objects' Positions: 1523
Single-Night Positions: 3314
New orbits: 121
Special asteroids discovered: 3 Trojans, 1 Hilda, 1 Hungaria
2 Mars crossers: 2002 AN7,2002 CS

3 – Observing around the meridian

Table 2 gives the results obtained by observing at Hour Angles close to the meridian.

Table 2 – Observational statistics around the meridian

Ecliptic Latitude	Surveyed (sq deg)	Detected asteroids	Asteroids per sd deg
-15o< β < 15o	625.6	3877	6.20
β > 15o	263.2	542	2.06

total number of detected asteroids: 4419
surveyed area: 888.8 sq deg
asteroids per sq deg: 4.97
smallest angular displacement rate: 4.5 arcsec/h.
smallest angular displacement: 2.5 arcsec

The astrometric and photometric precision achieved can be best estimated by comparing our positions and magnitude with those of some 181,000 astrometric catalog stars (see Fig. 6, Fig. 7, and

Table 3).

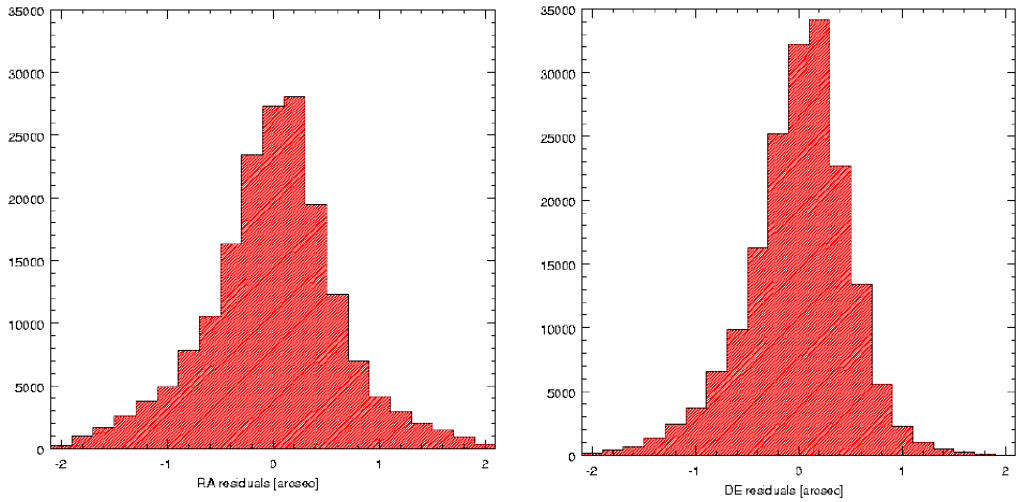

Fig. 6 – Distribution of astrometric residuals relative to reference stars.

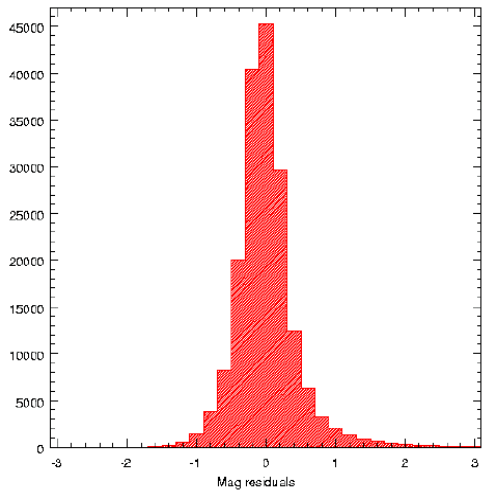

Fig. 7 – Distribution of photometric residuals relative to reference stars.

Table 3 - Internal errors of photometry and astrometry

$\overline{R_\alpha} \pm \sigma_\alpha$	$\overline{R_\delta} \pm \sigma_\delta$	$\overline{R}_m \pm \sigma_m$
0.00 ± 0.62	0.00 ± 0.49	0.01 ± 0.46

Notice that the errors in RA are larger than those in Dec due to the TDI mode.

Comparing the positions with those given by the MPC for the *numbered asteroids* in common, the errors will comprise therefore all sources of internal (including centroiding and timing errors on our images) and external factors (astrometric catalog errors, orbital uncertainties). The results for objects observed around the meridian are given by Table 4 and Fig. 8.

Table 4 – The astrometric quality for numbered asteroids observed around the meridian.

Residuals (arcsec)	N° of observations	Percentage
< 0.2	342	14.0 %
< 0.5	1382	56.7 %
< 1.0	2249	92.2 %
< 2.0	2426	99.5 %
> 2.0	12	0.5 %
All observations	2438	

Average RA residual	-0.04 ± 0.48 arcsec
Average DEC residual	0.20 ± 0.34 arcsec
Average total residual	0.52 ± 0.35 arcsec

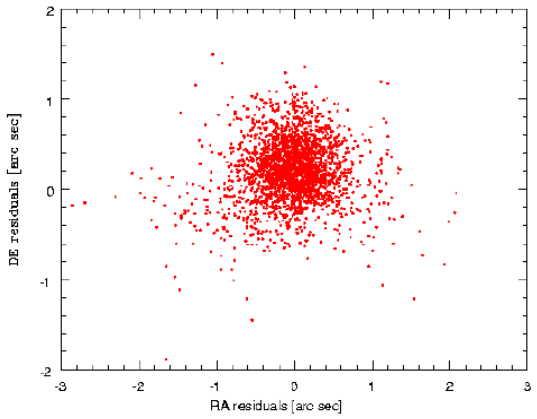

Fig. 8 – The distribution of the astrometric residuals of numbered asteroids observed by ADAS around the meridian.

Fig. 9 shows the magnitude distribution of all asteroids detected till now.

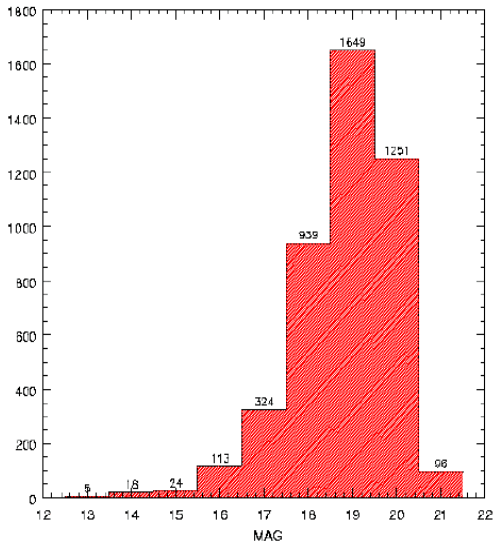

Fig. 9 – The magnitude distribution of all asteroids detected by ADAS around the meridian.

4 – Observing at small solar elongations

Several studies have shown the presence of a bias between the observed Aten-NEA fraction and the real one (Boattini and Carusi 1998, [3], Michel et al. 2000 [4]). This bias is due to the fact that the large asteroid surveys observe near the opposition, where Atens spend the least of their time. Moreover some studies (Tabachnick and Evans 2000, [5]) have pointed out the existence in the inner solar system of quite stable dynamical zones (e.g. around the Lagrangian points of Venus and Earth), but until today no asteroid with orbit completely inner to that of the Earth has been discovered: this type of asteroids can be detected only with observations at small solar elongations. We have drawn in Fig. 10 and in a simple model of magnitude variation of any given asteroid of mag. H as function of its position and phase angles. Notice that the objects become fainter and fainter going to smaller elongations, while the explored volume of inner solar system becomes larger.

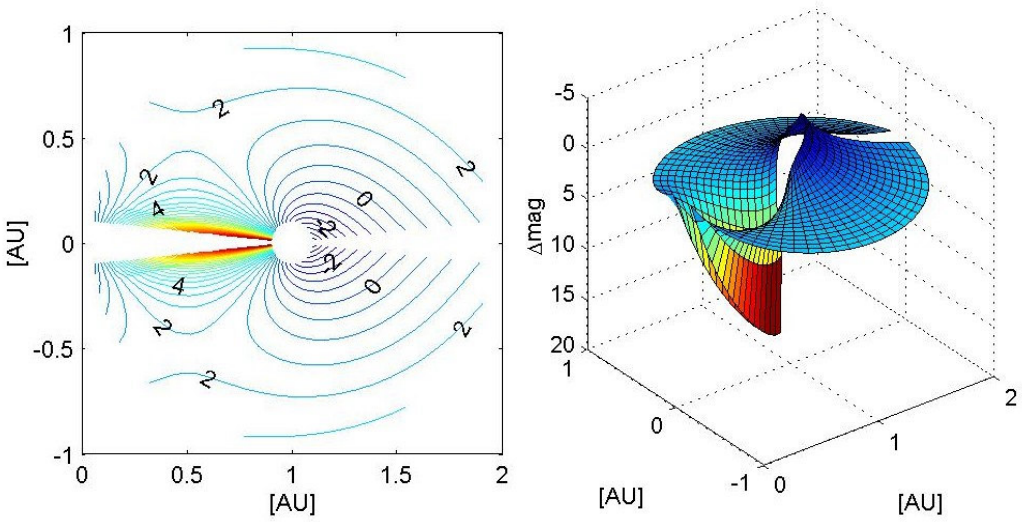

Fig. 10 – Difference between the absolute magnitude H and the observed magnitude m for a given asteroid, as function of its position, represented both in 2- and in 3-D. The Earth is in (0,0), the Sun in (1,0). The curves are separated by 0.5 magnitudes.

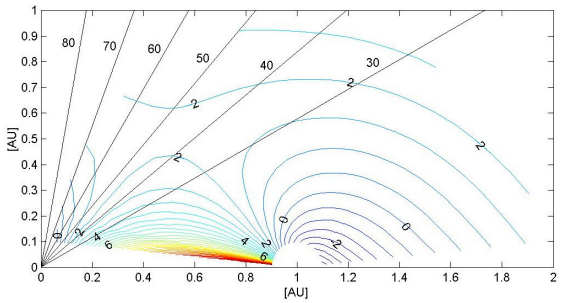

Fig. 11 – Same as in Fig. 10, together with the reference lines showing solar elongations.

On the other hand, the search of objects at small solar elongations is carried out under non-optimal observing conditions, and in some cases exclude the ecliptic plane, considerably lowering the total number of observable asteroids (Tholen et al 1998, [6]).

This expectation is born out by the available data as shown in Table 5:

Table 5 – Observational statistic at small solar elongations

Ecliptic latitude	Solar elongation (deg)	Surveyed (sq deg)	Detected asteroids	Asteroids per sd deg
-15o< β < 15o	[40,50[	9.8	8	0.82
	[50,60[	2.6	10	3.85
	[60,70[	26.1	29	1.11
	[70,80[	24.9	70	2.81
	[80,90[	60.3	91	1.51
	[0,90[	123.7	208	1.68
β > 15o	[40,50[	42.5	2	0.05
	[50,60[	75.8	1	0.01
	[60,70[	39.2	2	0.05
	[70,80[	68.4	3	0.04
	[80,90[	83.7	6	0.07
	[0,90[	309.6	14	0.05

total number of detected asteroids: 222
surveyed area: 433.3 sq deg
asteroids per sq deg: 0.51

Fig. 12 and Table 6 give the astrometric precision. Fig. 13 gives the photometric distribution.

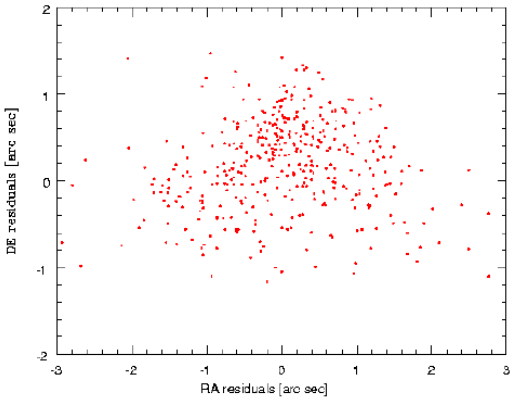

Fig. 12 – The distribution of the astrometric residuals of numbered asteroids observed by ADAS at small solar elongations.

Table 6 – The astrometric precision of numbered asteroids at small solar elongations

Residuals (arcsec)	N° of observations	Percentage
< 0.2	10	2.5 %
< 0.5	70	17.4 %
< 1.0	252	62.7 %
< 2.0	387	96.3 %
> 2.0	15	3.7 %
All observations	402	

Average RA residual	0.01 ± 0.92 arcsec
Average DEC residual	0.19 ± 0.53 arcsec
Average total residual	0.94 ± 0.52 arcsec

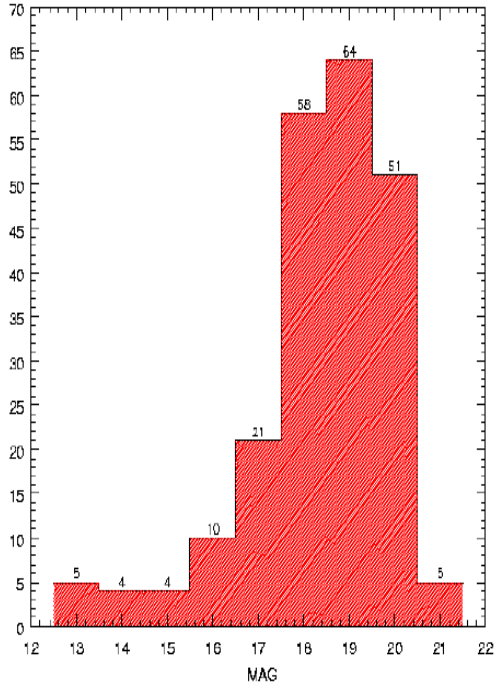

Fig. 13 – The magnitude distribution of all asteroids detected by ADAS at small solar elongations.

The loss in accuracy and magnitude is plainly evident.

5 - Further developments

Several improvements will be carried out in the central part of 2002:

1. a filter wheel with several broad band filters is under construction,
2. full automatization of the telescope and dome. New motors and cabling will be installed.
3. a new control room at the ground floor, capable to host several persons

It is expected to resume the observations in June 2002.

Acknowledgements

Thanks are due to the technical staff of the Padova – Asiago Observatory for the excellent work on the telescope and dome, and of the Catania Astrophysical Observatory for the kind helping characterizing the CCD and associated electronics. The development of the control software for the filter wheel is also under preparation at Catania.
Mr. S. Dalle Ave kindly helped with the observations.

References

1. Bertin, E., Arnouts, S. 1996, *Sextractor: Software for source extraction*, Astron. & Astrophys. Suppl. v. 117, pp.393-404.

2. Claudi R.U., Pignata, G., Strazzabosco, D., Bonanno, G., Belluso, M., Bruno, P., Cali, A., Cosentino, R., Timpanaro, M.C., Scuderi, S. 2002, *CHARACTERIZATION OF THE 67/90 SCHMIDT TELESCOPE CCD Padova and Asiago Observatories*, Technical Report n. 19, January 2002

3. Boattini, A., Carusi, A., 1998 *Aten: Importance among Near-Earth-Asteroids and search strategies,* Vistas in Astronomy Vol. 41, No. 4, pp. 527-541

4. Michel, P., Zappala, V., Cellino, A., Tanga, P. 2000, *Estimated Abundance of Aten and asteroids evolving on orbits between Earth and Sun,* Icarus, Volume 143, Issue 2, pp. 421-424

5. Tabachnick, S. A., Evans N. W. 2000, *Asteroids in the inner Solar system – I. Existence,* Monthly Notices of the Royal Astronomical Society, Volume 319, Issue 1, pp. 80-94.

6. Tholen, D. J., Whiteley, R. J. 1998, *Results From NEO Searches At Small Solar Elongation,* American Astronomical Society, DPS meeting #30, #16.04; Bulletin of the American Astronomical Society, Vol. 30, p.1041

OCCULTATION PREDICTIONS OF KBOS AND OTHER UNUSUAL OBJECTS

Mike Kretlow [a]

[a] Michael Adrian Observatory, Fichtenstrasse 7, D-65468 Trebur, Germany, e-mail: mkretlow@gmx.de

Kuiper Belt Objects (KBOs)[1] are of special interest for our understanding of the solar system and his formation. We do not know many of these objects nor do we know very much about them (therefore a KBO flyby of the Pluto Express space mission is planned if suitable candidates could be found). The observation of stellar occultations by KBOs could provide us with valuable physical data like their diameter. Candidates of such events are presented.

[1] *also known as Transneptunian Objects (TNOs)*

Introduction

In our current general understanding of the solar system, the region beyond Neptune is populated with ~10^5 Kuiper Belt Objects (KBOs) with diameter D > 100 km (Jewitt, Luu, Trujillio 1998). This region was first postulated by Edgeworth and Kuiper in 1949 and 1951, respectively. In 1992, the first KBO (1992 QB1) was discovered (Jewitt and Luu, 1993). At present only a fractional part of these KBOs and of other "unusual" objects like Centaurs are known.

With exception of Chiron, Pluto and Charon no occultation by KBOs or Centaurs has ever been observed. Physical data, in particular the diameter, can only estimated by formulas where the geometric albedo has to be assumed (in general 4%) or was provided independently by combining thermal and visual measurements. But because we deal with faint objects (m_R ~ 22-23), this is a difficult task and big telescopes are needed. Only for a few objects like the Centaur (10199) Chariklo and the KBO (20000) Varuna direct measurements of the albedo were performed. The observations of star occultations by such objects could give us valuable information about their diameter (with highest accuracy), shape, albedo (can simply be calculated if the diameter is known) and perhaps the presence of companying moons or even an atmosphere. As known, the present atmosphere of Pluto was discovered during an occultation.

Results and discussion

The author searched for occultations by KBOs and other unusual objects like Centaurs for the years 2002 & 2003. These predictions were carried out by an own program, which is also used for the annual prediction of occultations by minor planets, distributed by IOTA/ES. In a first step, all objects were selected from the list of TNOs and Centaurs published on the webpage of the Minor Planet Center (MPC 2002) for which at least 3 oppositions were observed. For these candidates full perturbed (M-v) apparent ephemeris were computed. Then a search for occultations of Tycho catalog stars was performed by a second program. During this calculation, an estimate of the diameter (assuming an albedo of 4%) according to the formula given by Trujillo et al. (2001) was used for the calculation of the expected occultation duration. From all events found by the program, those were selected for which the observation conditions will be reasonable, i.e. magnitude drop at least 0.5mag and elongation from the Sun > 30 deg. The results will be published on the web (Kretlow 2002) and in the proceedings of this meeting.

Conclusions

The observation of occultations of KBOs/Centaurs could provide us with important information about their main physical parameters. Possible candidates were presented. It should be mentioned, that the accuracy of the prediction will increase significantly, if last-minute (or better last-days) astrometry of high accuracy will be available to the calculators. On the other hand, the width of the ground track is expected to have a width of several hundred km, so hopefully an occultation by a KBO could be timed in the near future.

References

Jewitt,D., Luu,J., Trujillo,C., AJ 115, 2125 (1998)
Jewitt,D., Luu,J., Nature, 730, 352 (1993)
Trujillo,C., Luu,J., Bosh,A.S., Elliot,J.L., AJ 122, 2740 (2001)
MPC 2002, http://cfa-www.harvard.edu/iau/lists/MPLists.html
Kretlow 2002, http://www.minorplanets.org

THE MAGNITUDE ALERT PROJECT (MAP)

Gérard FAURE
(gpmfaure@club-internet.fr)

Minor Planet Section of the Association Of Lunar and Planetary Observers
(http://www.lpl.arizona.edu/~rhill/alpo/minplan.html)

AUDE (Association des Utilisateurs de Détecteurs Electroniques)
(http://www.ccdaude.com)

Many old numbered asteroids visually observed in the seventies and eighties showed discrepancies between predicted and observed magnitudes, which were be annually noted in a report in the Minor Planet Bulletin during many years.
Lawrence GARRETT, one of the coordinators of the Minor Planet Section of the ALPO (Association of Lunar and Planet Observers, in USA) proposed in 1996 an alert program which would inform observers of asteroids of suspected error immediately, rather then just publishing results annually, thanks to the new use of Internet.
In this way, more observations would be obtained, allowing to better refine the suspected errors observed.
The MAP was created by in late 1996.
As member of the Minor Planet Section and member of the French network AUDE (Association des Utilisateurs de Détecteurs Electroniques, id est Electronic Detectors User's Association), I joined the MAP at the end of 1997 to contribute to its development and to relay AUDE measures to Lawrence GARRETT.
Together, Lawrence and myself share ideas on improving, publication, and promotion of the MAP.
While Lawrence issue MAP alerts and reviews, I handle the data received from each observer in the MAP Database and furnish each month the MAP Observation Program.
The objective of the MAP (Magnitude Alert Project) is to pursue the search and the follow-up of asteroids with magnitude discrepancy. The goal is to improve their H absolute magnitude, with an accuracy of about a tenth of magnitude.
By the obtaining of visual or CCD magnitude measures, then by their global analysis for each asteroid, it is possible to revise the H magnitude which will permit the future calculations of more accurate ephemeride V magnitudes.
Despite the difficulties to obtain asteroid magnitudes measures, notably by the lack of very accurate star catalogues, this Amateur Project permitted up to now to find more than two hundred asteroids with errors of magnitude apparently greater than 0.3 magnitude.
The MAP is an opportunity to the visual and CCD amateur Observers to do an useful work with simple means.
Two articles already have been published in the Minor Planet Bulletin in 1999 and 2001. They concerned 40 asteroids observed at least by three observers, often during two or more oppositions, with similar results for each of them.
A revision of the H absolute Magnitude also was proposed.

The origins of the project

Many old numbered asteroids visually observed in the seventies and eighties showed discrepancies between predicted and observed magnitudes, which were annually noted in the reports from Frederick Pilcher in the Minor Planet Bulletin during many years.
Some of these discrepancies were important , up to 3 magnitudes !
The most significant errors were reported in a table of the paper "1000 and more" in "The Minor Planet Bulletin" of October-December 1998.
Some of these important errors of H magnitude were corrected by the Minor Planet Center before 1998.

Table 1: "selection of great discrepancies of magnitude seen visually from 1980 to 1997"

SELECTION OF GREAT MAGNITUDE DISCREPANCIES VISUALLY SEEN FROM 1980 TO 1997							
ASTEROIDS	MAG.DIF. SEEN	DATES	NAME OF OBSERVER	MAG. B(1,0) EMP87	MAG. H 88-91	MAG. H 92-97	REMARKS
	(F=fainter/B=brighter than predicted in the annual EMP)						
316 Goberta	1.2 +B	88/11/11	PILCHER	11,5	11,5	9,8	Correction on EMP92
473 Nolli	1.0 +F	88/02/10	HARVEY	-	10,0	12,3	Correction on EMP92
1206 Numerowia	1.6 +F	89/10/22	HARVEY	12,4	9,5	11,2	Correction on EMP92
1212 Francette	2.0 +F 0.8 +F 2.2 +F	80/02/12 83/08/09 85/10/10	PILCHER FABRE HARVEY	8,0	9,4	9,5	Correction on EMP87 (Var.>= 0,04 Mag)
1293 Sonja	1.8 +F 1.3-1.6 +F	92/11/08 96/08/09	HARVEY FAURE	15,4	14,0	12,0	Error on EMP92
1656 Suomi	1.0 +F 1.1 +F	87/11/21 96/02/24	HARVEY FAURE	15,4	13,1	12,4	Error on EMP87-92 Var. 0,09/011 Mag
1663 Van Den Bos	1.5 +B	90/11/12	HARVEY	14,9	13,7	12,2	Correction on EMP92
1890 Konoshenkova	1.0 +F	95/12/21	HARVEY	12,6	11,2	10,8	Error on EMP92 ?
2143 Jimarnold	2.5 +F	97/08/31	FAURE	15,3	14,1	11,2	Correction on EMP98
2183 Neufang	1.0 +F	90/06/20	HARVEY	12,6	11,4	11,5	Var. > 0,1 Mag
2491 Tvashtri	1.5 +F	87/01/03	HARVEY	14,6	13,7	13,7	
2791 Paradise	1.3 +F	88/01/24	HARVEY	13,0	11,5	12,2	Var. 0,25 Mag
3578 Carestia	1.8 +F 1.9 +F 3.0 +F 3.1 +F	91/10/04 91/10/13 96/07/22 96/09/04	FAURE HARVEY GARRETT GARRETT	-	10,5	8,1	Error on EMP89/92 Var 0.25 Mag Correction on EMP98
3873 Roddy	1.4 +F 1.3-1.6 +F	92/12/03 96/06/11	HARVEY FAURE	-	13,1	11,8	Error on EMP92
4116 Elachi	1.2 +F	94/03/16	HARVEY	-	13,3	13,0	
4729 1980 RO2	1.3 +B	90/10/17	HARVEY	-	-	13,1	
4744 1988 RF5	1.2 +F	91/01/26	HARVEY	-	11,6	10,9	Error on EMP92 ?
5641 Mc Cleese	1.7 +F	95/03/25	HARVEY	-	-	12,7	
5905 Johnson	1.1-1.4 +F	95/08/02	HARVEY	-	-	13,0	

Lawrence GARRETT, one of the Coordinators of the Minor Planet Section of the ALPO (Association of Lunar and Planet Observers, in USA) proposed in 1996 an alert program which would inform observers of asteroids of suspected error immediately, rather then just publishing results annually, thanks to new use of Internet.

In this way, more observations would be obtained, allowing to better refine the suspected errors observed by the ALPO observers.

The map birth

The MAP was created by Lawrence Garrett in late 1996.
It is an Amateur Project which would permit to do an Astronomical work even with simple means.
As Member of the Minor Planet Section and Member of the French network AUDE (Association des Utilisateurs de Détecteurs Electroniques, id est "Electronic Detectors User's Association"), I joined the MAP at the end of 1997 to contribute to its development and to relay AUDE measures to Lawrence GARRETT.
The objective of the MAP (Magnitude Alert Project) is to search and to do the follow-up of asteroids with magnitude discrepancy.
The goal is to improve their H absolute magnitude, with an accuracy of about a tenth of magnitude.

The magnitude alert project on may 15,2002

The MAP is managed jointly by the ALPO and by AUDE.
Together, Lawrence and myself share ideas on improving, publication, and promotion of the MAP.
While Lawrence issues MAP alerts and reviews, I handle the data received from each observer in the MAP Database and furnish each month the MAP Observation Program.

The map members

Table 2: "distribution of the 49 map members"

NATIONALITY	MEMBER TYPES	OBSERVER TYPES	VISUAL OBSERVERS	CCD USERS
19 Americans	32 Observers	8 visual Observers	6 Americans	10 Frenchmen
17 Frenchmen	17 Readers	24 CCD Observers	1 Frenchman	5 Americans
7 Swisses			1 Australian	5 Swisses
2 Italians	5 Professionals			2 Italians
2 Brazilians	44 Amateurs			1 Canadian
1 Australian				1 British
1 Canadian	46 Individuals			
1 British				
1 Spanish	3 Groups			
1 Hindu				
1 Czech				

The 5 more active Observers, on May 15,2002

René ROY	744	CCD measures
Gérard FAURE	415	visual measures
Brian WARNER	>291	CCD measures (lightcurves)
Andrew SALTHOUSE	296	visual measures
Roger HARVEY	255	visual measures

The Most active visual Observers and their total of asteroids seen

Observer	Total	Date
Roger HARVEY	4037	02/05/15
Frederick PILCHER	1801	01/03/24
Gérard FAURE	1586	02/05/15
Andrew SALTHOUSE	1420	02/01/13
Ben HUDGENS	1170	01/12/31
Tom LASKOWSKI	1148	01/03/10
Lawrence GARRETT	1073	02/05/13

Map targets: the asteroids with discrepancies of magnitude

MAIN TARGETS = Numbered Asteroids and only Unnumbered Asteroids of particular Families
MAP OBJECTS = Asteroids with discrepancies of 0.3 Magnitude and more between Predicted and Observed magnitudes
TOTAL MEASURES ON MAY 15,2002 = 3204 Measures
TOTAL OBJECTS INCLUDED IN THE MAP = 319 Asteroids

The 12 MAP Asteroids with the greatest magnitude discrepancies :

Minor Planets	Mag. Discrepancy	Number of measures	Number of Observers
1166 Sakuntala	1.1 F	16 measures	4 Observers
1612 Hirose	1.1 B ?	5 measures	2 Observers
5641 Mc Cleese (Mars-crosser)	1.1 F	15 measures	5 Observers
1384 Kniertje	1.2 F	19 measures	6 Observers
4440 Tchantches (Hungaria)	1.2 F	8 measures	3 Observers
881 Athene	1.3 F ?	4 measures	2 Observers
921 Jovita	1.3 B	9measures	4 Observers
5749 1991 FV	1.3 F ?	3 measures	2 Observers
6911 Nancygreen (Hungaria)	1.3 F ?	3 measures	2 Observers
9162 1987 OA (Apollo 1)	1.3 B ?	6 measures	1 Observer
1388 Aphrodite	1.4 F	9 measures	4 Observers
1444 Pannonia	2.2 F ?	5 measures	2 Observers

(B or F = brighter or fainter than predicted // "?" = Put on asteroids observed less than three times and by three observers)
NB: the high error of mag H for 1444 Pannonia has been confirmed by three Australian Observers, in the last MPB (April 2002)
Most of the MAP suspects having been found by the visual Observers, the MAP Objects are mainly minor planets brighter than V16.0. Then, most of the MAP objects are in the ten first thousands numbered asteroids.

TABLE 3 : "DISTRIBUTION OF THE 275 FIRST MAP OBJECTS ON MARCH 10,2001"

Distribution by Number		**Distrib.by 0.10 Mag. of the average diff.of mag.V**				**Distribution by Absolute Mag. H**	
		Brighter than predicted		Fainter than predicted			
1 to 999	**32**	Mag	Total	Mag	Total	Mag. H	Total
1000 to 1999	**67**	0.1	**9**	0.1	**13**	3 to 7	**0**
2000 to 2999	**23**	0.2	**11**	0.2	**22**	8	**7**
3000 to 3999	**13**	0.3	**16**	0.3	**19**	9	**14**
4000 to 4999	**24**	0.4	**17**	0.4	**29**	10	**37**
5000 to 5999	**24**	0.5	**11**	0.5	**39**	11	**71**
6000 to 6999	**27**	0.6	**5**	0.6	**15**	12	**71**
7000 to 7999	**18**	0.7	**4**	0.7	**12**	13	**38**
8000 to 8999	**2**	0.8	**1**	0.8	**7**	14	**9**
9000 to 9999	**5**	0.9	**2**	0.9	**7**	15	**1**
10000 to 10999	**2**	1.0	**0**	1.0	**5**	16	**7**
11000 to 11999	**3**	1.1	**1**	1.1	**2**	17	**4**
12000 to 12999	**4**	1.2	**0**	1.2	**2**	18	**8**
13000 to 13999	**2**	1.3	**2**	1.3	**3**	19	**2**
14000 to 14999	**1**		**79**	1.4	**1**	20	**3**
15000 to 15999	**1**			1.5 to 2.1	**0**	21	**2**
16000 to 16999				2.2	**1**	22	**1**
17000 to 17999					**177**		
18000 to 18999		Diff. = 0.0	**16**				
19000 to 19999	**1**						
20000 to 20999	**1**	Indefinite	**3**				
Unnumbered	**25**						
	275		**275**		**275**		

Remarks on Table 3:
On March 10,2001 only 42 MAP objects had a known lightcurve (15% of the MAP Objects)
With an average variability of 0.4 magnitude for the asteroids, the discrepancies due to the variability may often concern the H magnitudes for about 0.2 magnitude (half-amplitude of the variability) , than less the lower MAP limit of 0.3 mag

The tools of the map

THE MAP ALERTS

The messages "MAP Alerts" are sent by par Lawrence Garrett to the MAP Members and have been put on the Website of the ALPO Minor Planet Section at the address: http://www.lpl.arizona.edu/~rhill/alpo/minplan.html
In these messages, Lawrence announces the discovery of new discrepancies of asteroid magnitudes, the new Members and various other news.

THE MAP OBSERVATION PROGRAM

Made each month by Gérard Faure, it contains all the MAP Numbered Asteroids which are :
- Observable during the actual lunation
- Distant from more than 4 hours of Right Ascension from the Sun
- Brighter than the predicted magnitude V 16.5

They are classified by Right Ascension for the Date of the New Moon.
There also are bright "standard" asteroids with very small light variability which perhaps will permit to find standard discrepancies between the various types of measures collected by the MAP.

TABLE 4 : "ABSTRACT OF THE "MAP OBSERVATION PROGRAM"

NUM.	*	NAME	H	G	FAMILY	P	# H	MPB	PER.Hrs	VAR.	QUA.	Origin	M-MPC	Mopp	01	Vop	V.NL	RA+DEC 25.5/01	CNS
1731		Smuts	10.0	0.15		M	F/0.2?						69,7	-		-	16,1	4 h 17 +16 14'	Tau
31		Euphrosyne	6.74	0.15		S			5.531	0.09-0.13	4	EMP 2000	4,0	-		-	11,9	4 h 21 +44 04'	Per
862		Franzia	10.6	0.15		M	B/0.9?		> 24	>0.15		WARNER	25,7	-		-	16,0	4 h 22 +28 15'	Tau
840		Zenobia	9.3	0.15		M	F/0.4?						160,6	-		-	15,7	4 h 29 +23 12'	Tau
1384		Kniertje	9.7	0.15		M	F/1.2	O4/99					18,7	-		-	14,5	4 h 36 +12 42'	Tau
324		Bamberga	6.82	0.09		S			29.43	0.07	3	EMP 2000	50,2	-		-	11,9	4 h 49 +30 29'	Aur
3731		Hancock	10.3	0.15		M	F/0.5?						312,4	-		-	16,2	4 h 59 +19 11'	Tau
2204		Lyyli	12.7	0.15	MARS-CR.	P			8.	0.5	2	EMP 2000	12,5	-		-	16,3	5 h 1 + 7 09'	Ori
100		Hekate	7.67	0.15		S			13.333	0.11	3	EMP 2000	128,1	-		-	14,1	5 h 6 +19 24'	Tau
1166		Sakuntala	8.8	0.15		M	F/1.1						154,1	-		-	14,7	5 h 14 +20 04'	Tau
491		Carina	8.5	0.15		S			14.87	0.12	3	EMP 2001	41,5	-		-	14,3	5 h 29 + 5 19'	Ori
1243		Pamela	9.68	0.15		M	B/0.3?		26.017	0.49	2	EMP 2001	153,8	-		-	15,7	5 h 40 +15 13'	Ori
33		Polyhymnia	8.55	0.33		S			18.601	0.14	3	EMP 2000	82,0	-		-	14,2	5 h 44 +25 15'	Tau
6249		Jennifer	12.4	0.15	MARS-CR.	M	F/0.3	O4/99					100,2	-		-	16,5	6 h 3 - 8 20'	Mon
737		Arequipa	8.81	0.15		S			14.13	0.15	3	EMP 2000	142,1	-		-	14,6	6 h 19 +10 57'	Ori
128		Nemesis	7.49	0.15		S			39.	0.10	3	EMP 2000	86,4	1	1.2	10.9	12,8	6 h 34 +27 50'	Gem
57		Mnemosyne	7.03	0.15		S			12.463	0.12	3	EMP 2000	57,0	1	3.1	11.3	12,6	6 h 42 + 6 32'	Mon
982		Franklina	9.9	0.15		M	B/0.4	O4/99					189,8	1	8.7	15.3	16,4	6 h 50 +23 36'	Gem
1122		Neith	11.1	0.15		M	F/0.5?						65,1	1	3.4	13.6	15,9	6 h 52 +27 45'	Gem
4440		Tchantches	12.3	0.15	HUNGARIA	M	F/1.0?						359,8	1	13.2	13.6	15,5	7 h 10 + 2 21'	CMi
85		Io	7.61	0.15		S			6.875	0.15	4	EMP 2000	155,9	1	14.9	12.1	13,2	7 h 19 + 8 39'	CMi
1656		Suomi	12.4	0.15	MARS-CR.	M	F/0.2?		2.42	0.09-0.11	2	EMP 2000	36,3	1	7.8	14.4	15,2	7 h 27 + 2 34'	CMi
779		Nina	8.3	0.15		P			11.186	0.25	3	EMP 2000	155,8	1	24.9	12.8	13,9	7 h 56 +11 18'	Cnc
91		Aegina	8.84	0.15		S			6.025	0.15	3	EMP 2000	48,2	1	22.9	11.6	13,2	7 h 57 +22 53'	Gem
552		Sigelinde	9.4	0.15		M	0.0						246,4	1	24.2	14.1	15,1	7 h 58 +13 40'	Cnc
1423		Jose	10.5	0.15		M	F/0.1?						111,6	1	25.8	14.5	15,7	8 h 5 +23 53'	Cnc
1365		Henyey	11.7	0.15		M	F/0.4						284,8	1	27.4	14.6	15,6	8 h 7 +13 34'	Cnc
1178		Irmela	11.81	0.15		M	B/0.4	O4/99	19.17	0.34	2	EMP 2000	346,0	1	25.8	14.6	15,7	8 h 12 +15 43'	Cnc
1469		Attila	11.1	0.15		M	?						334,8	1	28.6	15.1	16,1	8 h 19 +18 46'	Cnc
4181		Kivi	12.0	0.15		M	F/0.5?						12,9	1	27.3	14.9	16,0	8 h 20 +17 13'	Cnc
378		Holmia	9.80	0.15		S			4.450	0.13	3	EMP 2000	100,7	1	29.4	13.8	14,8	8 h 20 +10 14'	Cnc
11548		Jerrylewis	13.1	0.15		M	F/0.5?						18,3	2	3.4	15.0	16,1	8 h 27 - 9 28'	Hya
19164		1991 AU1	13.5	0.15	HUNGARIA	M	F/0.5?						41,2				16,1	8 h 39 +17 49'	Cnc
5749		1991 FV	10.7	0.15		M	F/1.3						205,1	2	4.4	15.4	16,1	8 h 44 + 7 01'	Cnc
4060		Deipylos	8.9	0.15	TROYEN-E	M	B/0.4?						20,0	2	2.3	15.2	15,8	8 h 45 + 9 00'	Cnc
1403		Idelsonia	10.6	0.15		M	F/0.5?						137,6	2	4.8	15.3	16,2	8 h 45 +14 54'	Cnc
4483		Petofi	11.9	0.15	HUNGARIA	M	F/1.0		4.28	0.98	3	EMP 2000	141,9	2	5.7	14.7	15,1	8 h 50 - 3 37'	Hya
847		Agnia	10.29	0.15		M	B/0.2?						101,6	2	8.8	14.2	15,1	9 h 3 +13 50'	Cnc
1067		Lunaria	10.99	0.15		M	B/0.3		7.74	0.13	2	EMP 2000	89,3	2	11.4	15.0	15,9	9 h 12 + 5 51'	Hya
4628		Laplace	11.0	0.15		M	F/0.2		9.011	0.48	3	EMP 2000	0,4	2	17.3	14.2	14,8	9 h 36 - 4 06'	Hya
4063		Euforbo	8.6	0.15	TROYEN-E	M	F/0.3						65,1	2	16.5	15.3	15,8	9 h 43 +27 11'	Leo
6009		1990 FQ1	12.3	0.15		M	F/0.3	O4/99					247,1	2	18.6	16.5	16,5	9 h 43 -14 00'	Hya
1130		Skuld	12.1	0.15		M	B/0.1						196,5	2	20.9	15.6	16,3	9 h 49 +10 17'	Leo
20790		2000 SE45	16.6	0.15	AMOR-3	M	B/0.6?										17,5	9 h 53 - 4 47'	Sex
927		Ratisbona	9.54	0.15		M	B/0.4						348,1	2	21.9	13.8	14,4	9 h 56 +24 09'	Leo
1687		Glarona	10.25	0.15		M	0.0?		6.3	0.75	3	EMP 2000	86,5	2	21.5	14.6	15,4	9 h 58 +15 45'	Leo

Data included in the Monthly Observation MAP Program

This MAP Program has many columns with interesting indications on each asteroid.

Num. The Asteroid number
Name/Nom The name or the provisory designation of the asteroid
H The H magnitude actually used by the MPC

G The G slope parameter
Family/Famille The eventual family of the asteroid
P The state of the asteroid in the MAP Program:
M = MAP Object
P = Potential MAP asteroid with a H discrepancy discovered before the MAP and yet not observed again
S = Standard asteroid with an accurate H magnitude and a small variability < 0.15 magnitude.
A = Astéraude (Asteroid discovered by the AUDE Members)
# H Average discrepancy of magnitude observed by the MAP Members (B/x.x et F/x.x = x.x mag. brighter or fainter)
The magnitudes followed by a "?" define the priority MAP objects with an average discrepancy not sure.
MPB Indication of the year and the month publication in the Minor Planet Bulletin
These objects are not priority objects for the obtaining of new MAP Measures

Period.Hrs Rotation period of the asteroid in hours
Variab. Amplitude of light variability
Q Quality of the lightcurve parameters (Origin: CALL and EMP)
Origin/Origin Main Origins of the data lightcurves:

Raoul Behrend Website	http://obswww.unige.ch/~behrend/page_cou.html
CALL Website from Brian Warner	http://www.MinorPlanetObserver.com/astlc/default.htm
Harris Catalog of March 31,2001	http://cfa-www.harvard.edu/iau/mpc.html
Icarus review	http://astrosun.tn.cornell.edu/Icarus/Icarus.html
Minor Planet Section of the ALPO	The Minor Planet Bulletin
Petr Pravec et al	http://sunkl.asu.cas.cz/~ppravec/

The following reliability codes (Origin EMP and CALL) are used:
1: Result based on fragmentary lightcurve(s), may be completely wrong.
2: Result based on less than full coverage, so that the period may be wrong by 30 percent or so.
Also used to indicate cases where an ambiguity exists as to the number of extrema between lightcurves
Hence the result may be wrong by an integer ratio.
3: Secure result with no ambiguity, full lightcurve coverage.
4: In addition to full coverage, denotes that a pole position is reported.

M-MPC MPC Mean anomaly "M" of the asteroid (for the last MPCORB file downloaded)
Opp Date+V Month of the eventual opposition in the year (Origin EMP)
Day of the eventual opposition in the year (Origin EMP)
V magnitude at the opposition (Origin EMP)
V.NL V magnitude for the day of the New Moon (Origin GUIDE 8)
RA Hour of 2000.0 Right Ascension for the day of the New Moon at 00H UT (Origin GUIDE 8)
Minutes of 2000.0 Right Ascension for the moon day at 00H UT (Origin GUIDE 8)
+ DEC Degree of 2000.0 Declination for the day of the New Moon at 00H UT (Origin GUIDE 8)
Minutes of 2000.0 Declination for the day of the New Moon at 00H UT (Origin GUIDE 8)
CNS Constellation which contains the asteroid on the day of the New Moon (Origin GUIDE 8)

THE MAP DATABASE

Kept by Gérard Faure on an Excel File, it is updated about 3 times by year and contains:

- For each asteroid all the measures made by the MAP Members and some old measures of the MPB.
- For each asteroid, there are also the chronological account of its H magnitudes since 1985 and the averaged discrepancy of magnitude.
- The description of all the magnitude types used by the MAP
- A Recapitulative LIST of MAP asteroids with their actual H magnitude discrepancy

Table 5: "abstract of the map database"

		Year/Année	M.	Day/Jour	N	Mag:	Obs.	#.Mu	Pred.	# O-P	Uncert.	Observer/Observateur	Avr/night - Moy/nuit
921 a		921 Jovita											
921 d	1	1998	10	03.10392		UMu	13,9		15,5	-1,6	B	Dennis CHESNEY	-1,70
921 d	2	1998	10	03.13022		UMu	13,7		15,5	-1,8	B	Dennis CHESNEY	
921 d	3	1998	10	19.75139		GMu	15,9		15,8	0,1	F	Pierre ANTONINI	N
921 d	4	1998	10	19.77821		GMu	15,9		15,8	0,1	F	Pierre ANTONINI	N
921 d	5	1998	10	19.80288		GMu	15,8		15,8	0,0		Pierre ANTONINI	N
921 d	6	1998	10	19.83010		GMu	16,0		15,8	0,2	F	Pierre ANTONINI	N
921 d	7	1998	10	24.01311		AMv	14,4		15,9	-1,5	B	Lawrence GARRETT	-1,50
921 d	8	1998	10	24.12501		AMv	14,4		15,9	-1,5	B	Lawrence GARRETT	
921 d	9	2000	12	27.01944	+	AMv	15,6		16,1	-0,5	B	Gérard FAURE	-0,87
921 d	10	2000	12	27.04097	+	AMv	15,3		16,1	-0,8	B	Gérard FAURE	
921 d	11	2000	12	27.05486	+	AMv	14,8		16,1	-1,3	B	Gérard FAURE	
921 d	12	2001	02	19.87986	+	UMu	16,1		16,8	-0,7	B	Jean-Gabriel BOSCH	-1,35
921 d	13	2001	02	19.88854	+	UMu	14,8		16,8	-2,0	B	Jean-Gabriel BOSCH	
921 h	1												
921 h	2	H = 10.03 (EMP 1988 => 1991); H= 10.6 (EMP1992 => 2001)											Diff/ H -1,35
921 n	e	Possible great variability											
921 n	f	Grande variabilité possible											
921 r		921 Jovita			+	H =	10.6		EMP2001		9	<= Measures // Observers =>	4 Diff.H = 1.3 B ?
921 z													
921 z													
1166 d		Year/Année	M.	Day/Jour	N	Mag:	Obs.	#.Mu	Pred.	# O-P	Uncert.	Observer/Observateur	Avr/night - Moy/nuit
1166 a		1166 Sakuntala											
1166 d	1	1998	02	26.2326.	+	AMv	14,0		13,1	0,9	F	Andrew SALTHOUSE	0,97
1166 d	2	1998	02	26.2361.	+	AMv	14,1		13,1	1,0	F	Andrew SALTHOUSE	
1166 d	3	1998	02	26.2604.	+	AMv	14,1		13,1	1,0	F	Andrew SALTHOUSE	
1166 d	4	1998	02	26.95486		AMv	14,5		13,1	1,4	F	Gérard FAURE	1,30
1166 d	5	1998	02	26.99236		AMv	14,6		13,1	1,5	F	Gérard FAURE	
1166 d	6	1998	02	27.1528.	+	AMv	14,1		13,1	1,0	F	Andrew SALTHOUSE	
1166 d	7	1998	03	01.02415		AMv	14,2		13,1	1,1	F	Lawrence GARRETT	1,10
1166 d	8	1998	03	06.1389.	+	AMv	14,0		13,1	0,9	F	Andrew SALTHOUSE	0,90
1166 d	9	1998	05	18.88120		UMu	14,9		14,0	0,9	F	René ROY	0,95
1166 d	10	1998	05	18.90383		UMu	15,0		14,0	1,0	F	René ROY	
1166 d	11	1999	07	08.1493.	+	AMv	12,1		11,1	1,0	F	Andrew SALTHOUSE	1,00
1166 d	12	1999	07	12.1528.		AMv	12,5		11,0	1,5	F	Andrew SALTHOUSE	1,50
1166 d	13	1999	07	15.1389.		AMv	12,5		10,9	1,6	F	Andrew SALTHOUSE	1,60
1166 d	14	2000	11	24.1667.	+	AMv	14,1		13,2	0,9	F	Andrew SALTHOUSE	0,90
1166 d	15	2000	11	29.2049.	+	AMv	14,0		13,1	0,9	F	Andrew SALTHOUSE	0,90
1166 d	16	2000	12	03.1840.	+	AMv	14,0		13,0	1,0	F	Andrew SALTHOUSE	1,00
1166 h	1												
1166 h	2	H = 11.5 (EMP 1988 => 1991); H = 11.3 (EMP 1992 => 1997); H = 8.8 (EMP 1998 => 2001)											Diff/ H 1,10
1166 r		1166 Sakuntala			+	H =	8.8		EMP2001		16	<= Measures // Observers =>	4 Diff.H = 1.1 F
1166 z													

Content of the MAP Database:

I - DATA of observed MAP objects

II - Recapitulative LIST of MAP asteroids with their actual H magnitude discrepancy

I - Data of observed MAP objects

Database columns and indications:

Year/Année = Year of the measure

M. = Month of the measure

Day/Jour = Day and fraction of day of the measure

N = New measure since the last Database update, noted by a N or a M (if the measure was modified)

Mag: = MAP Magnitude type:

- AMv Visual magnitude with asteroid comparison
- GMv Visual magnitude with GSC comparison [Not used for H revision]
- UMv Visual magnitude with USNO comparison
- UMr Unfiltered CCD magnitude with USNO-A2 mag.R comparison [Not used for H revision]
- GMu Unfiltered CCD magnitude with GSC comparison [Not used for H revision]
- LMu Unfiltered CCD magnitude with LONEOS or LANDOLT comparison
- PMu Unfiltered CCD magnitude with PGSC comparison
- UMu Unfiltered CCD magnitude with USNO-A2 mag V comparison
- TMu Unfiltered CCD magnitude with TYCHO 2 mag V comparison
- UMB CCD magnitude with Blue filter and USNO comparison [Not used for H revision]
- UMR CCD magnitude with Red filter and USNO-A2 comparison [Not used for H revision]
- GMR CCD magnitude with Red filter and GSC comparison [Not used for H revision]
- LMV CCD magnitude with V filter and LONEOS or LANDOLT comparison
- PMV CCD magnitude with V filter and PGSC comparison
- TMV CCD magnitude with V filter and TYCHO 2 comparison
- UMV CCD magnitude with V filter and USNO-A2 comparison

Obs. = Observed magnitude

.Mu = Standard discrepancy of unfiltered CCD measures and visual measures
(some UMr and UMR measures with solar stars comparison are taken in account with V=R+0.4)
(a "?" designates a possible erroneous measure)
Pred. = Predicted V MPC Magnitude
# O-P = Difference of magnitude between Observed and Predicted magnitudes
- Magnitude differences:
x.x F x.x magnitude fainter than predicted
x.x B x.x magnitude brighter than predicted
Uncert. = Magnitude Uncertainty of the measure
Observer/Observateur = Observer first name and name
Avr/night - Moy/nuit = average magnitude discrepancy for a same night, put in the line of the first measure of the night
- Various indications:
"Diff.H = x.x" with a "?" Uncertain average H magnitude which requires other measures
H = …. (EMP 1988 =>…. = History of the evolution of H magnitude since 1988
Nota: The GMv,GMu,GMR, UMr, UMR and UMB are not used for the revision of MAP Asteroid H magnitudes.
Lightcurve parameters:
Rotation period of the asteroid in hours (Main Origins: Websites Behrend, CALL-Warner and IAU-Cat.Harris)
Amplitude of light variability (Main Origins: Websites Behrend, CALL-Warner and IAU-Cat.Harris)
http://obswww.unige.ch/~behrend/page_cou.html
http://www.MinorPlanetObserver.com/astlc/default.htm
http://cfa-www.harvard.edu/iau/mpc.html

THE PUBLICATIONS OF THE MAP ON THE MINOR PLANET BULLETIN

Two articles already have been published in "The Minor Planet Bulletin" of April 1999 (Volume 26, Number 2, A.D.1999 April-June) and October 2001 (Volume 28, Number 4, A.D.2001 October-December).

The first of them contains 18 objects measured at least by two observers who found fairly similar magnitude discrepancies. The second article gave the results for 23 other asteroids at least observed by three observers, often during two or more oppositions, with nearly similar results for each of them.

The range of the discrepancies of the individual measures (Article N°1), or the list of the measures and the Observers was furnished (Article N°2). A revision of the H absolute Magnitude also was proposed.

Table 6: "Results of the second article of october 2001" (See the table on the next page)

The asteroid magnitudes and their problems

All the asteroid magnitudes must be based on the V Band. It is not always the case…
The stellar magnitudes used for the measures of the asteroid magnitudes must be in the V Band, rather than in the R Band frequently used by the CCD Observers.

ACTUAL FORMULA FOR THE PREDICTION OF THE APPARENT ASTEROID MAGNITUDES
(Origin: "Ephemerides of Minor Planets" from the IAA of St Petersburg - Russia)

This formula was adopted by IAU Commission 20 (New Delhi, November 1985, the Minor Planet Circulars 10193-10194
It is based on the Absolute magnitude of an Asteroid located at 1 astronomical Unit from the Sun and the Earth.

magnitude H = + 5 * log(r*delta) - 2.5 * log [(1-G)*phi1 + G*phi2]

r and delta respectively are the heliocentric and geocentric distances at solar phase angle Phase=0
H is the absolute magnitude in the V band
G is termed the slope parameter (= 0.15 si G unknown)
phi1 and phi2 are two phase functions given by the expressions : phi1 = exp[-3.33*(tan (beta/2))0.63]
phi2 = exp[-1.87*(tan (beta/2))1.22]
The formula predicts the observed opposition surge and the non-linear drop off in brightness at large phase angles, and is valid for 0°< Phase <120°.
H and G are fundamental photometric parameters for each minor planet.

Table 6: "results of the second article of october 2001"

Minor Planet	MPC H Value	Revised H Value	Change (magnitude)	Total of Measures	Total of Observers	Total of Oppositions
457 Alleghania	11.0	10.7	**-0.3**	22	6	1
921 Jovita	10.6	9.3	**-1.3**	9	4	2
942 Romilda	10.3	10.8	**-0.5**	12	3	1
1002 Olbersia	11.1	10.5	**-0.6**	14	4	2
1067 Lunaria	10.99	10.7	**-0.3**	11	3	1
1166 Sakuntala	8.8	9.9	**1.1**	13	4	3
1239 Queteleta	12.5	11.8	**-0.7**	13	4	3
1296 Andree	10.9	11.3	**0.4**	5	3	3
1330 Spiridonia	10.17	9.8	**-0.4**	8	3	1
1388 Aphrodite	8.89	10.3	**1.4**	9	4	1
1444 Pannonia	9.1	11.3	**2.2**	5	4	2
4063 Euforbo	8.6	8.9	**0.3**	7	3	2
4339 Almamater	13.6	14.0	**0.4**	17	7	1
4483 Petofi	11.9	12.9	**1.0**	7	4	2
4497 Taguchi	11.5	12.3	**0.8**	11	4	1
4766 Malin	12.2	12.7	**0.5**	14	4	1
5092 Manara	11.0	11.5	**0.5**	8	3	1
5153 1940 GO	11.2	11.7	**0.5**	10	3	1
5231 Verne	11.1	11.8	**0.7**	12	4	2
5738 Billpickering	14.1	15.0	**0.9**	7	4	1
5785 Fulton	11.8	12.7	**0.9**	9	4	1
7776 Takeishi	12.8	13.3	**0.5**	7	4	1
9262 Bordovitsyna	13.0	13.7	**0.7**	14	5	1

Main causes of h magnitude errors :

In the Past, during the Photographic period discoveries, B photographic magnitudes were often roughly estimated.

The conversion from the B band of the old system to the V band of the new system was carried out using the approximate relationship : H = B(1,0) - 1 magnitude

The magnitudes reported with the astrometric measures to the MPC often are incorrect and sometimes furnished without the concerned light band concerned light band.

The inaccuracy of the great stellar catalogues actually used yet is an important cause of the errors of magnitude.

Some modifications of H Magnitudes have been made in 1991 and 1997 by the MPC, but since the last date, no other change appeared.

The MPC actually is too busy with the huge amount of data given by the Automatic Observatories to do the new modifications.

Table 7: "catalogs of stellar magnitudes actually used"

Catalog Name of Star mags	Year of Issue	Total Stars	Range of Magnitudes	Photometric Inaccuracy	Remarks
LANDOLT	1982	526	11,5 to 16,0	**BVRI references**	V 11,5 to 16,0 (Ecliptic zone)
GSPC	1988 and +	~8900	V 9 to 15	**0,05 to 0,1 mag**	0.1mag only for faintest stars
GSC 1.1	1989	19 M.	V 14 to 16	**>0,5 mag. to > 1 mag.**	
USNO-A	1996 + 1998	488 M.	B and R < 20	**>0,25 mag. Up to -20°**	**>0.5 magnitude south of -20°**
USNO-SA	1996 + 1998	55 M.	B and R < 20	**<0,25 magnitude**	Selection on Solar type stars

GUIDE+USNO	1996 and +	55 a 488 M.	B,**V**,R < 20	**<0,25 to > 0,5 mag.**	
LONEOS	1998 and +	~32400	11 to 22	BVRI references	
UCAC 1	2000	27 M.	R < 17	**> 0,3 mag.**	Southern stars
TYCHO 2	2000	2,5 M.	up to V 11,5	**0,013 to 0,1 mag**	0.1mag only for faintest stars

The methods of the map for the obtaining of the revised h magnitudes

An asteroid may be included in the MAP if it is at least three-tenths of a magnitude in error from its predicted value in the Ephemerides, during the first night of its observation by a MAP Member.

Sometimes, the later measures may show a light variability of the object. Then, if there is not also a slight discrepancy of H magnitude, the average difference of the magnitude statistically decreases towards 0.0

With the lack of accurate stellar catalogues, the best method to measure the magnitude discrepancies :
- for the visual Observers is to compare Asteroids with similar predicted magnitudes.
- for the CCD Observers, is to use the best stellar magnitudes, actually the Tycho 2 catalogue.

The stellar magnitudes used for the measures of the asteroid magnitudes must be in the V Band.

As soon as possible, the asteroid magnitudes also must be based on the V Band.

As we have various types of observers (visual and CCD) and even various uses of the CCD cameras (Unfiltered or filtered measures and various types of light band), it's not easy to join all the measures made for the MAP… Then, we only use those which are in the V Band or near it.

Of course, it is necessary to have numerous isolated measures to be sure of the accuracy of H magnitude.
In this case, the numerous measures often may statistically reduce the eventual errors of the few inaccurate measures.

The time passed by the Asteroid at the maximum or at the minima of light is short. Then, the measures are often concerned only by a fraction of the half-amplitude of light.

Individual measures are normally divided up along the asteroid lightcurve and the effect of the half-amplitude is statistically diminished.

For each measure, a difference of magnitude between the predicted and the observed magnitudes is calculated.
Then for each asteroid, the average of the differences of magnitudes is calculated, night by night.
Finally, the difference of H magnitude is the average of all the averages calculated for the same asteroid.

All the measures received by the MAP are included in the MAP Database, but only some of them are used to calculate the average difference of the H magnitudes.

MAP Magnitude types
(See the Content of the MAP Database already given)

The goals of the map

THE PAST AND FUTURE EVOLUTION OF THE MAP METHODS

In first, we took all the measures given by the Observers to estimate if it was possible to obtain similar results with various Observation methods.
In second, we made analyses to discover the magnitude differences between these various Observation Methods (visual and CCD observers and between various types of CCD images and light bands used).
The third phase will be the use of standard deviations and the search of methods to permit the obtaining of good results for the unfiltered measures, because it is generally difficult to amateurs to obtain V filter measures for asteroids fainter than V14.
The MAP Database now contains a column for the future standard deviations. Up to now, only some R magnitudes of solar-type stars, with a deviation of + 0.4 magnitude have been used after rectification, in a few cases of lack of data.
the MAP doesn't pretend to obtain the most accurate magnitude measures, but an accuracy of about 0.1 magnitude, better than the actual inaccuracy of numerous numbered Asteroids, is often possible, notably with the future use of standard deviations

between different light bands.

The analyses of the map measures

The Basis of the Analyses : Our 2834 first measures.

Table 8: "the analysis of the 2834 first measures"

Distribution of Magnitude Types for the 2834 MAP measures made up to March 10,2001		
Visual measures :		
AMv	**776**	
UMv	**54**	
GMv	22	***Not used for the H revisions***
Unfiltered CCD measures :		
UMu	**1209**	
GMu	431	***Not used for the H revisions***
UMr	39	***Not used for the H revisions***
LMu	**1**	
Filtered CCD measures :		
TMV	**43**	
UMV	**17**	
GMV	20	***Not used for the H revisions***
UMB	3	***Not used for the H revisions***
UMR	8	***Not used for the H revisions***
LMV	**0**	
Indefinite magnitudes :	211	***Not used for the H revisions***
	2834	

Remarks :
With the delivery of new big star catalogues, the use of them in the MAP evolved:
- At first, the GSC was used by the CCD Observers.
- Then the less inaccurate USNO and notably the USNO-SA (Solar type stars) were recommended.
- Actually, the best big stellar Catalogue is the Tycho 2.

The distribution of the MAP measures shows that there is a small use of filters and of the Landolt or Loneos stars.
They are not easy to use (cost of the filters, decrease of the limit magnitude, no accurate star near the asteroids then double work and lack of time)

Up to the availability of the Tycho 2 for the CCD V measures, the visual ones were used as reference, to estimate the validity of the CCD measures received by the MAP.

Three different analyses of the map database of march 2001

1) AVERAGE OF THE MEASURE DISCREPANCIES OF THE MAIN TYPES :

The average of all the discrepancies of the individual measures has been calculated for each type of the 5 main types of obtained measures.
This average has been after ajusted on the average standard deviation obtained for the Tycho 2 measures (TMV).

Magnitude types	Total of measures		Average of the Discrepancies	Adjusting on Tycho 2
AMv	776	measures	0.2 mag fainter	**0.0**
UMu	**1209**	measures	**0.0**	**0.2 mag brighter**
TMV	43	measures	**0.2 mag fainter**	**0.0**
GMu	431	measures	0.3 mag fainter	**0.1 mag brighter**
UMr	39	measures	0.1 mag brighter	**0.3 mag brighter**

2) COMPARISON BETWEEN VISUAL AND UNFILTERED DIFFERENCES , BY ASTEROID, ON MARCH 10,2001

The comparison between the visual measures and the unfiltered CCD measures obtained with the USNO, according to the individual differences noted for the asteroids for which we had the two types of measures.

Selected Objects = The ones followed by at least 2 visual Observers and if possible 2 CCD Observers

Result : Global Average Difference "Visual - Unfiltered CCD" = 0,10 magnitude brighter for the unfiltered CCD measures

A previous other analysis type in 1999 gave a result of 0.17. Then the average discrepancy is about 0.1 to 0.2 magnitude.

3) GLOBAL AVERAGE DIFFERENCE OF EACH MAGNITUDE TYPE, based on the difference of the average difference by each asteroid measure type by comparison to the actual average difference of H magnitude of each Asteroid

The calculations will be made with the better measures included in the MAP Database

.

Each average has been after adjusted on the average standard deviation obtained for the Tycho 2 measures.

Magnitude Type	Average of differences	Average Diff - Global Diff.	Adjusting on Tycho 2
AMv	0.25 mag fainter	0.04 mag fainter	**0.22 mag fainter**
TMV	0.03 mag fainter	0.18 mag brighter	**0.0**
GMu	0.41 mag fainter	0.20 mag fainter	**0.38 mag fainter**
UMr	0.17 mag brighter	0.38 mag brighter	**0.20 mag brighter**
UMu	0.12 mag fainter	0.07 mag brighter	**0.11 mag fainter**
UMv	0.15 mag fainter	0.06 mag brighter	**0.12 mag fainter**
UMV	0.34 mag fainter	0.13 mag fainter	**0.31 mag fainter**
UMR	0.36 mag brighter	0.62 mag brighter	**0.44 mag brighter**

Conclusions

All the Visual, Unfiltered USNO-SA2 and TMV measures are included in a maximum range of 0.2 magnitude, despite the effect of the light variability of the asteroids and the slight inaccuracy of the measures.

The R and B measures are the most unsuited light bands among those received by the MAP. We have the confirmation that the GSC is the most inaccurate star catalogue. We always have a deviation of 0,1 to 0,2 magnitude between the visual measures

and the unfiltered CCD measures made with the USNO and the Tycho 2. The visual magnitudes seem less good than CCD Tycho filtered measures, but we not have yet a great number of Tycho measures to be sure. It is now necessary to use the Tycho 2 and the V star magnitudes rather than R magnitudes and the USNO-SA. With a standard deviation, the unfiltered V magnitudes would be with an accuracy of a tenth of magnitude. The magnitude discrepancies found by the MAP often are greater than the magnitude inaccuracies found in the MAP analyses.

The future of the map

TWO MAIN GOALS: The better accuracy and the simplification of the MEASURE Methods by :

- The use of the best accurate star catalogues and V filters if the asteroid is not too faint.
- The use of Monthly Lists of conjunctions between the MAP asteroids and the Loneos, PSGC or Tycho 2 stars, even for the visual observers.
- The search and the use of "standard deviations" for each CCD camera to permit the accuracy of his unfiltered measures.
- Some tests on "standard asteroids" with small variability (< 0.16 magnitude) and sure H magnitude to try the confirmation of the standard deviations of various types of CCD measures.
- The new measure of the old CCD images with the future best star Catalogues.

Final conclusion

The MAP work is useful :
- To detect the asteroids with errors of H magnitude and to suggest the revision of false H magnitudes, even with a slight residual inaccuracy.
- To permit best future ephemerides and statistical works on diameters.
- To detect sometimes asteroids with a great light amplitude, as (7505) 1992 AM2.
- To obtain a rough estimate of the magnitude deviations.
- To permit a scientific work, without important means and without long observations for each target (Useful for bad climates or short times of observing).

Bienvenue in the MAP if you wish !

References

AUDE Website http://www.ccdaude.com/

Raoul Behrend Website of Lightcurves (http://obswww.unige.ch/~behrend/page_cou.html)

CALL http://www.MinorPlanetObserver.com/astlc/default.htm

Alan Harris Lightcurve Asteroid Catalogue (http://cfa-www.harvard.edu/iau/lists/LightcurveDat.html)

IAA – Russia "Ephemerides of Minor Planets" from 1985 to 2002

Minor Planet Center Various Data on Asteroids (http://cfa-www.harvard.edu/iau/lists/MPLists.html)
Files of Orbital elements of Asteroids (http://cfa-www.harvard.edu/pub/MPCORB/)

Minor Planet Section of the ALPO "The Minor Planet Bulletin", from 1983 to 2002
http://www.lpl.arizona.edu/~rhill/alpo/minplan.html

ON THE DISCOVERY OF NEW FAINT JUPITER TROJANS

Eric W. Elst

Holbach-Foundation, Kapellenboslei 7, B-2950 Kapellenbos (Belgium), ericelst@holbach-foundation.com

Reflections are made about the discovery of new faint Trojans. It seems indeed that we are approaching the end in discovering new Jupiter Trojans, as far as a limiting magnitude of V=19.5 is envisaged. What could be the reason for this ? Are we really approaching an end, as the consequence that there should be a kind of gap between faint and faintest Trojans -assuming anyway the presence of « faintest » Trojans in L4 and L5- or is it just the consequence of the fact that present instruments are not reaching beyond the limiting magnitude, from whereon we may expect to discover again new Trojans?

Introduction

Trojans are for many reasons important objects to investigate, after their discovery. They may be related with comets captured by the gravitational field of Jupiter; but they can also be remnant material from the time of the formation of the solar system. The question why Jupiter Trojans are accumulating at two particular places in the solar system, roughly 60 degrees ahead and 60 degrees behind on the orbit of Jupiter, has been mathematically demonstrated by Lagrange (1772), reason why these particular positions have been called *Lagrange libration points L4 and L5.*

New investigations

Present observational data shows a rapid decline in absolute magnitude (towards fainter values) when considering newly discovered Trojan-asteroids. This tendency is also clearly shown in the *cumulative distribution curves of Jupiter Trojans*, which are monthly provided by the Minor Planet Center in Massachusetts (U.S.). Let us therefore look at a typical example of such a cumulative distribution curve (Fig. 1) :

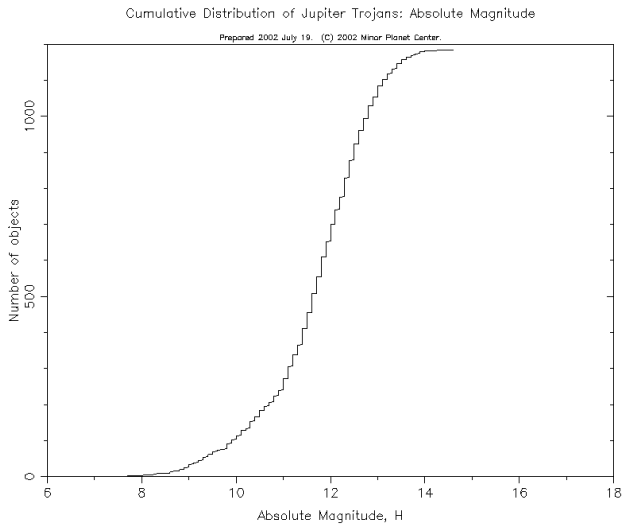

Fig. 1: Jupiter Trojans, distribution curve (MPC)

We may asssume that, during the last three years, effectiv sky covering has been neatly accomplished by the larger asteroid-search-programs (LINEAR, LONEOS, Spacewatch, Catalina and NEAT) :

LINEAR is covering the sky from quadrature to quadrature and from 60 deg north to 38 deg south quite beautifully down to mag 19 or so. There are some gaps, notably in the July-August rainy season, but there is excellent night to night and month to month and opposition to opposition linkage, and the strong effect of this on the numbering of minor planets is becoming evident (Brian Marsden, 2000, private communication).

From Fig.1 we may therefore infer that during 1999-2001 all Trojans with absolute magnitudes less than H=12.0 have been discovered, since the location of the *inflection point* from the distribution curve is a measure for completeness (Elst, 2001).

However, Trojans with high inclinations tend to be discovered much later during the searches. Since they may have only a small influence upon the aspect of the distribution curve, they should thererefore not have to be taken into account. Fig. 2, which shows the number of Jupiter Trojans versus Absolute Magnitude, is quite interesting, since it has almost Gaussian shape, confirming our findings from the cumulative distributing curves.

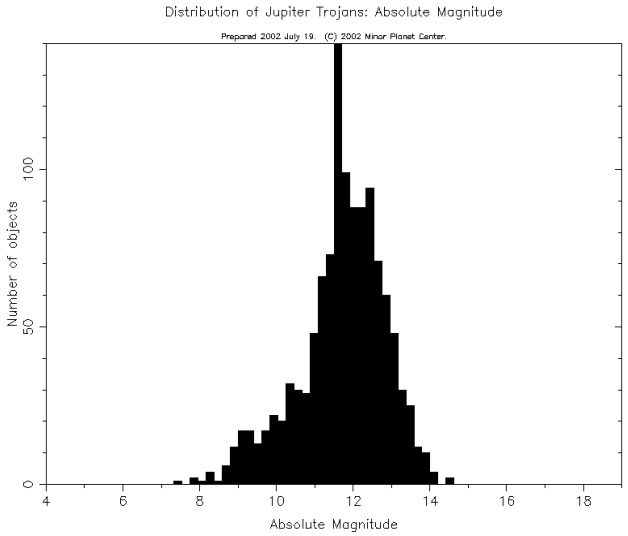

Fig. 2: Number of Trojans / Absolute Magnitude (MPC)

Interesting also is the *unexpected* peak at H=11.8, the result from intensive searches by LINEAR during last February and March 2002, indicating probably the presence of a casual or real *cluster* of L4-Trojans (40 objects) at H= 11.8. In proportion with increasing limiting magnitude the summit of this plot will move to higher values, while moving at the same time to fainter absolute magnitudes. It will be necessary to wait for the following opposition of L4-Trojans, in order to interprete this *artifact* more appropriately.

It follows further from fig.1 -by linear extrapolation- that about 250 more Trojans may be discovered (if they should be present) in the range of H=12.5–13.5, remembering that Trojans are located at nearly the same distance (5.2 A. U.). Enhancing the limiting magnitude of the search programs may therefore result in the discovery of new faint Trojans.

References

Lagrange J. P., Le probleme des trois corps, Prix de l'Académie Royale des Sciences de Paris, tome IX, 1772
Elst E W., Are we approaching the end of asteroid-discovery ?, Planetary and Space Science, 49, 781-786, 2001

Acknowledgements

It is a pleasure to thank the Minor Planet Center, Massachusetts , US, for allowing us to use some of their figures.

PHOTOELECTIRC PHOTOMETRY OF MINOR PLANET 1998 WT_{24}

Sergio Foglia

Serafino Zani Astronomical Observatory, UAI Minor Planets Section, F. Bisleri 11, I-20148 Milano, Italy
e-mail: s.foglia@libero.it

Photoelectric observations of Near Earth Asteroid 1998 WT_{24} were made on December 15/16, 2001 from Serafino Zani Astronomical Observatory located in Lumezzane (Italy, MPC Code 130) using a 40-cm Ritchey-Chretien telescope with a 1P21 single-channel photometer. A DCF-77.5 kHz radio signal receiver was used to determine Universal Time. During this night the geocentric distance of 1998 WT_{24} was only 0.013 A.U. and it was very difficult to find comparison's stars due to the fast motion of the minor planet. Observational's period cover 5 hours (from december 15, 21:00 U.T. to december 16, 02:00 U.T.); spectrum analisys of the obtained data gives a probable period of rotation of 4.558 hours. Observed amplitude in the V band was enlarged by the brightness of the comparison's star used.
The following is the obtained light curve reduced to the V(1,0) magnitude using the relation:

$$V(1,0) = V - 5 \cdot \log(r \cdot \Delta) + 2.5 \cdot \log[(1-g) \cdot F_1 + g \cdot F_2]$$
$$F_1 = \exp\left\{3.33 \cdot [\tan(\beta/2)]^{0.63}\right\}$$
$$F_2 = \exp\left\{1.87 \cdot [\tan(\beta/2)]^{1.22}\right\}$$

where:

V	*observed V magnitude*
r	*heliocentric distance*
Δ	*geocentric distance*
g	*slope parameter (0.15)*
β	*phase angle*

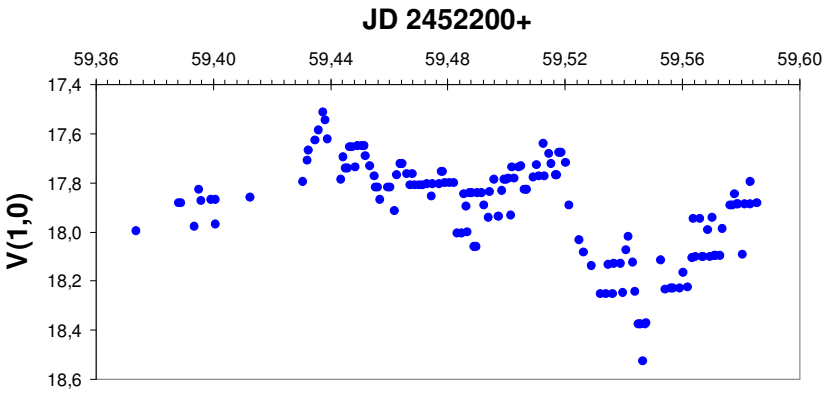

CORRECTORS FOR WIDE-FIELD CCD IMAGING: how to design, manufacture and use them

Željko Andreić

Ruđer Bošković Institute, division of Materials physics, Thin Films Laboratory, Bijenička 54, POB 180, Zagreb, Croatia
andreic@rudjer.irb.hr

In recent time, many advanced amateurs and small astronomical facilities, have access to 1 m-class telescopes. Most of these telescopes are Newtonians or classical Cassegrains, both types having parabolic primary mirrors. These instruments are either self-made, or are old instruments that are not primary research instruments anymore. To adapt them for CCD photography, one usually needs a field corrector which corrects the of-axis coma of the primary mirror and, at the same time, flattens the image plane so that the whole CCD sees a sharp image. If this lens system also shortens the focal length, it is usually called a telecompressor.

It is supposed that such telescopes will be equipped with 1" CCDs, with a possible upgrade up to 2" in the years to come, as the prices of such cameras fall with time. Also, a point source (star!) image of about 30 μm is taken as the upper limit of the acceptable image blur. Larger instruments (focal length of abut 3 m upwards, will have larger seeing blurs, so 50 μm blur can be tolerated in such a case. A review of suitable corrector designs is presented, starting from a single lens field-flattener, up to a 5-lens multiple-glass focal corrector.
It is found that single-lens correctors have no sense in such an arrangement, as the image improvement is marginal or non-existent. At telescopes around 0.5 m in diameter, field-flatteners do improve the image sharpness a little, but this effect is completely hidden by the of-axis coma. The first usable corrector design is a two lens Ross corrector, which is usable at focal ratios of about F/4 or larger. For faster mirrors, it fails to produce small enough point images, although coma is still greatly reduced.

The great advantage of a Ross corrector is that it is one-glass design with relaxed tolerances, so it can be produced by a skilled amateur optician. Many amateur telescope builder are skilled enough to attempt such a work.

The first really good corrector is the three lens Wyne corrector, which is often used on larger telescopes. It is still one-glass design, but the tolerances of individual lens surfaces are very tight. A skilled optician is needed to produce such a corrector successfully.

Last, but not least, an example of modern multiple-glass, 5 lens focal reducer for an F/3 parabolic mirror is presented. Its tolerances are not so tight as the ones of the Wyne corrector, but it requires 3 different glasses, at least one of which is difficult to grind and polish. Again, a skilled optician is the best choice for manufacturing of such a corrector.

Introduction

Telescopes with apertures between 0.5 and 1.5 m are not considered primary research instruments anymore and are often being closed or access is granted to serious amateur groups. At the same time, more and more amateurs are building instruments in this size range. This article is targeted to them, assuming that the telescopes will be used for CCD imaging. In such a case, the telescope optics alone is not capable of covering the CCD chip (even it is by modern measures a small one, say 1/2" to 1" one). That means that some sort of field corrector, constructed from one or several lenses is needed to flatten the field and to reduce the off-axis aberations of the telescope optics. In the analysis pesented below, a 1 m telescope with a parabolic mirror with a focal ratio of 3 is assumed. The reason for this choice is that for slower mirrors, the same correctors can be used, and they will produce a better image quality than at focal ratio of 3. Another reason was more practical: most of these designs were studied in connection to the new Visnjan Observatory telescope, which is a 1m F3 instrument. Now, for the case of a parablic mirror, a corector designed for one focal ratio will perform better as the focal ratio is increased. Of course, the distance between the last corrector surface and the focal plane has to be kept at the same value as in the original design. RC hiperbolic primaries are not studied in detail, as they are relatively rare, but the few trials done indicate that same corrector designs work with them also, but they have to be optimised for the particular RC mirror, as each RC mirror has unique shape.

If the telescope aperture is changed, the scalling rules can be used to predict the corrector performance. The most important scalling rules for our case are as follows:

1. if all dimensions of an optical system are multiplied (scaled) by a fixed factor, spot diagrams will also be multiplied by the same factor.
2. in such a procedure, field angles are preserved

The first rule implies that it is quite safe to reduce the size of an optical system, as then all spots will be reduced by the same factor. However, as rule 2 stresses, the field angles will not be changed by such a scalling. Thus, the linear field of view of the original design will also be reduced by the scalling factor. In this fact lies the only danger hidden in the scalling procedure: if after the scalling

the linear field of view has to be increased, the off-axis aberrations may explode! Otherways, if the optical system is enlarged in size, the aberations will also be magnified by the same factor. But, if the same linear field of view is required, the resulting decrease in the angular fied of view

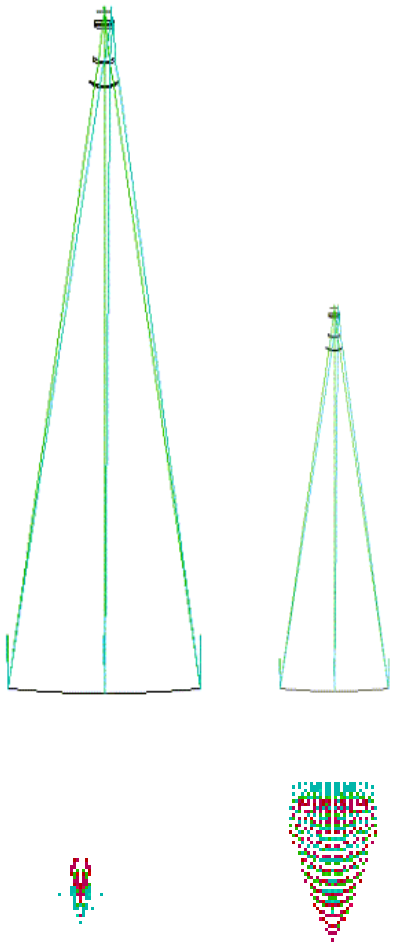

may still produce satisfactory results.

Figure 1: An 1m F3 telescope with a Wyne corrector has been scaled down to 40 cm of aperture, and afterwards, the linear field of view has been forced to stay the same. The resulting 2.5-fold increase in angular field resulted in huge off-axis aberrations, as is illustrated with the spot diagrams for the edge of the filed of view below the corresponding telescope sketches. In such a case, the scaling rules fail to deliver the required performance.

Before we start analyzing possible corrector configurations, we need to determine some basic parameters of the complete imaging system, from seeing, through the telescope optics and up to the CCD surface. The typical seeing experienced at sites used by amateurs and older observatories in populated areas of Europe is not as good as at the best observatory sites. We can safely assume that it will be about 1" at best, values around 2" being much more probable. Combining this with focal lengths of several meters that we encounter in the 1m class telescopes, we arrive to seeing discs several tens of micrometers in diameter (Fig. 2).

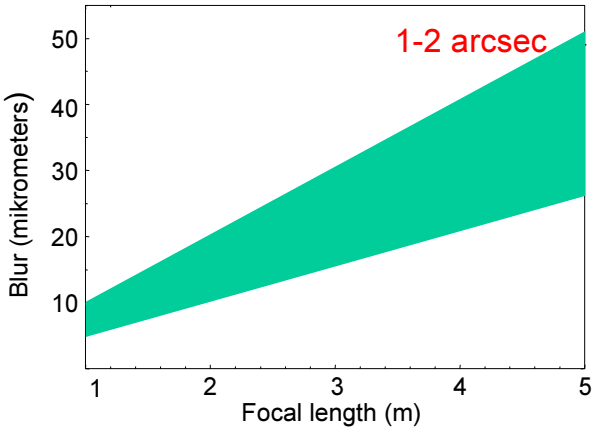

Figure 2: Blur disk size caused by seeing between 1" (lover line) and 2" (upper line) as function of the telescope focal length.

The required complexity of a field corrector depends mostly on the required field of view, which on its own is clearly defined by the size of the CCD chip we want to use. The relation between the chip size and the required

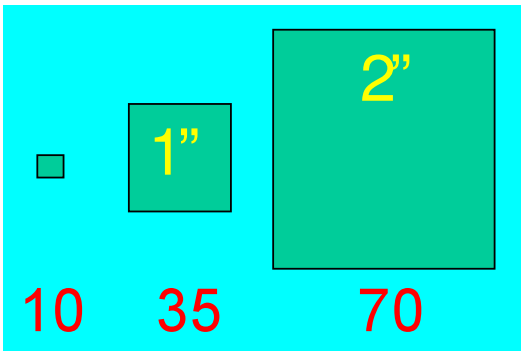

diameter of the field of view is illustrated on the Fig. 3.

Figure 3: relative size of CCD chips used for amateur and semi-rofessional astronomical work (drawn proximately to scale). The left one is typical for good amateur CCD cameras, a 1" chip is used by serious amateurs and proffesionals with a low budget alike, and 2" may be within their grasp in next five to ten years. The red numbers give the required diameter of the well-corrected field of view of the telescope (in millimetres).

The CCD chips have quite different pixel sizes, somewhere between 7 and 25 µm, with the trend going towards smaller pixels, the average being currently around 10 µm. Combining this with the fact that the star image has to be at least two pixels in diameter, to allow precise astrometry and photometry, and with the size of the seeing disc discussed before, it is obvious that the blur circle of the corrector needs not to be much smaller than about twenty micrometers. So, in the following analysis, the acceptable

spot diagram diameter was taken to be about 20 µm in the center of the filed, and about twice of it at the extreme edge.

Last but not least, the broad spectral sensitivity of CCD that ranges from near UV (400 nm can be set as a practical limit for low altitude observatories) to about 1 µm in near IR requires more attention to be put on cromatic aberrations as in the case of visual or photographic lenses. As most CCDs have their peak sensitivity near 700 nm, this is set to be the central wavelength for the raytracing and optimization analysis of the correctors discussed below. The other two wavelengths were set to 400 and 1000 nm, at the practical limits of the range in which CCDs are sensitive.

Spot diagram was chosen as the analytical tool for assessing the corrector performance. Although the spot diagram lacks precise qualification of aberrations involved in creating it, it has a great advantage of being a visual, easy to understand tool for demonstrating the performance of an optical system. In generating a spot diagram, the entrance aperture of the optical system is divided into a large number of equal parts, and a light ray from the object (in our case a point source which we can imagine as a star at desired place in the field of view) is sent through each of these parts. The path of each ray, usually for three colors, is calculated and the point where it crosses through the image plane is marked on the image plane. The crossing points for of rays give the blur circle that such an optical system would produce by the laws of geometrical optics alone (i.e. the diffraction is neglected).

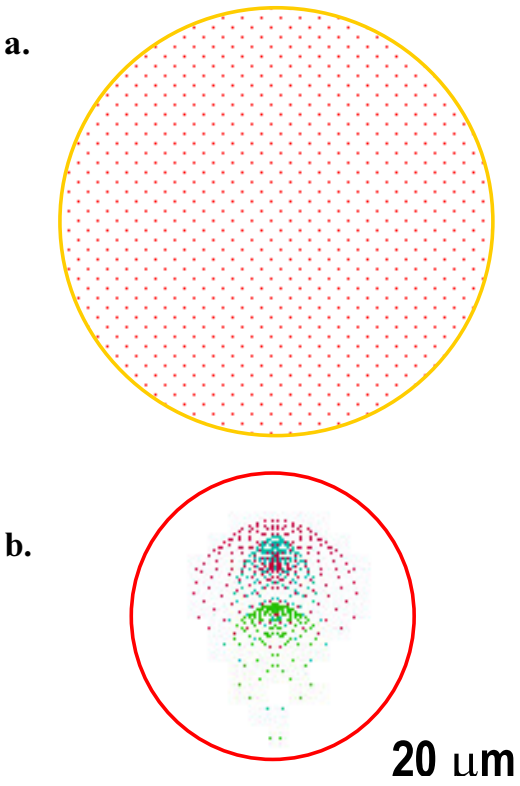

Figure 4: a. An example of ray distribution over the entrance aperture used to calculate a spot diagram. In general, several hundred to several thousand rays are distributed evenly over the entrance aperture.
b. the resulting spot diagram, with a tolerance circle plotted around it. Note that the rays of three different wavelengths used in the calculations are coded by different colors. Blue is used for the shortest, red for the longest and green for the middle wavelength, regardless of their actual colors.

All results presented in this article were obtained by the free version of the optical design program OSLO LT (V5.4) which can be downloaded at the following address:

http://www.sinopt.com/

The performance of the parabolic mirror alone

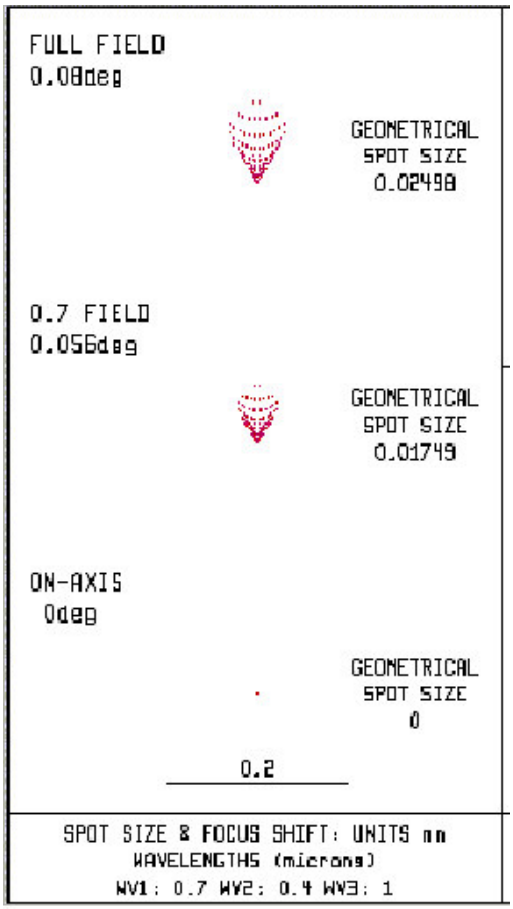

EFL=2942 mm, FOV= 8 mm dia.

Figure 5: Parabolic mirror (1m F/3 in this case) exhibits a very strong coma which limits the usable field of view to a few milimetres around the axis.

The parabolic mirror alone is totally unsuitable for primary focus imaging. The field of view is limited by severe coma to a circle less than 1 cm in diameter. The situation is a little better at F/4, but still far from satisfactory one.

Single lens field flattener

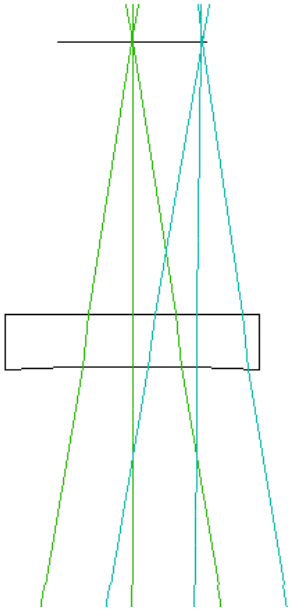

Figure 6: A sketch of the optimized solution for a single lens field flattener.

A single lens field flattener is put in front of the focal plane to correct the curvature of the field. The possibility to influence the other aberrations with such a lens is minimal. The minimal increase in usable field of view can be attributed to a slight increase in effective focal length of the complete system, and in my opinion it is not worth using in this class of telescopes. Its effect is more pronounced with smaller mirrors as then the field curvature is larger and its correction brings more than with such large mirrors.

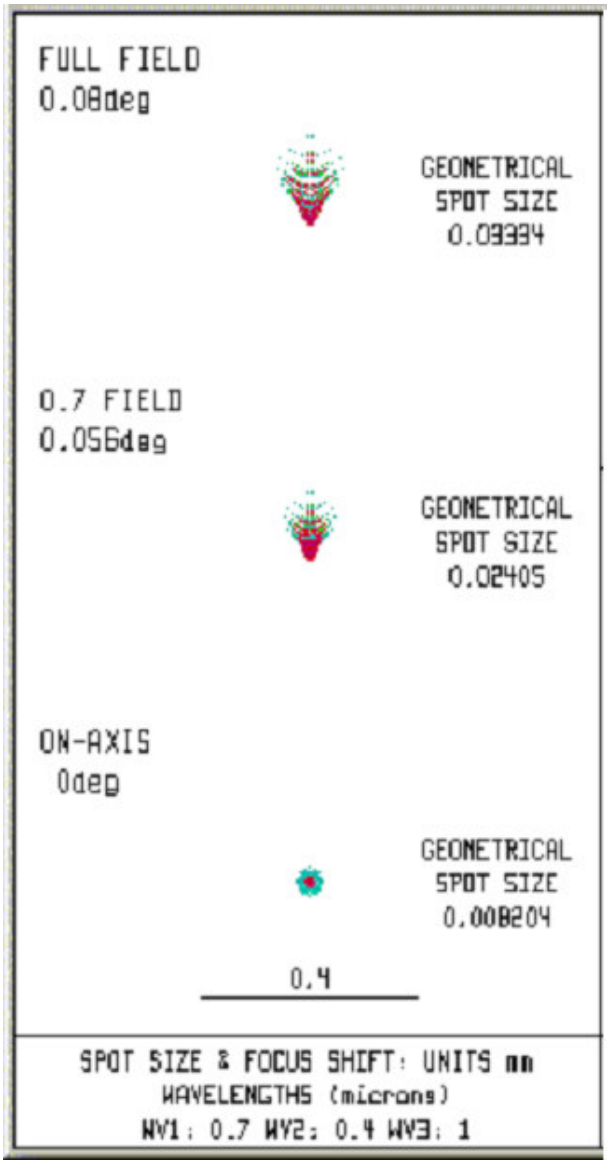

EFL=3120 mm, FOV= 10 mm dia.

Figure 7: the spot diagrams for a single lens field flattener.

Single lens meniscus corrector

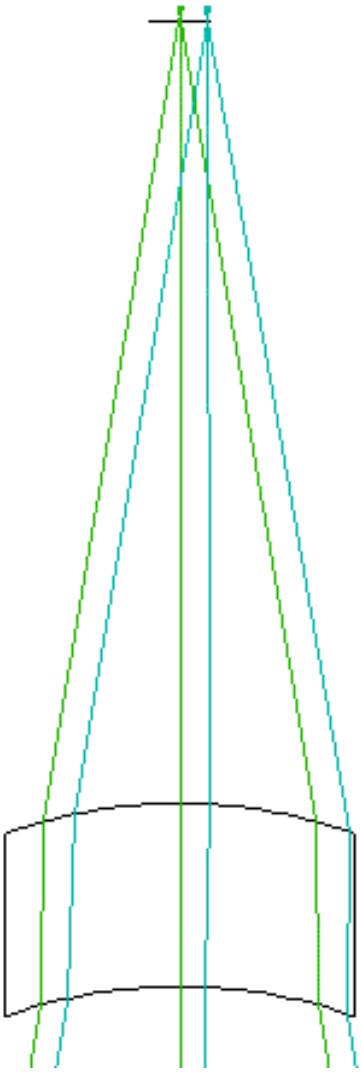

Figure 8: A sketch of the optimized solution for a single lens filed flattener.

A single lens meniscus corrector can compensate coma quite well over a limited flied of view. Although the increase in usable filed is not as large as one would like, the resulting spot diagrams are almost round, which is very desirable for astrometric and photometric work, so this design is preferred to the single lens field flattener discussed above, and makes sense if one has a small CCD chip.

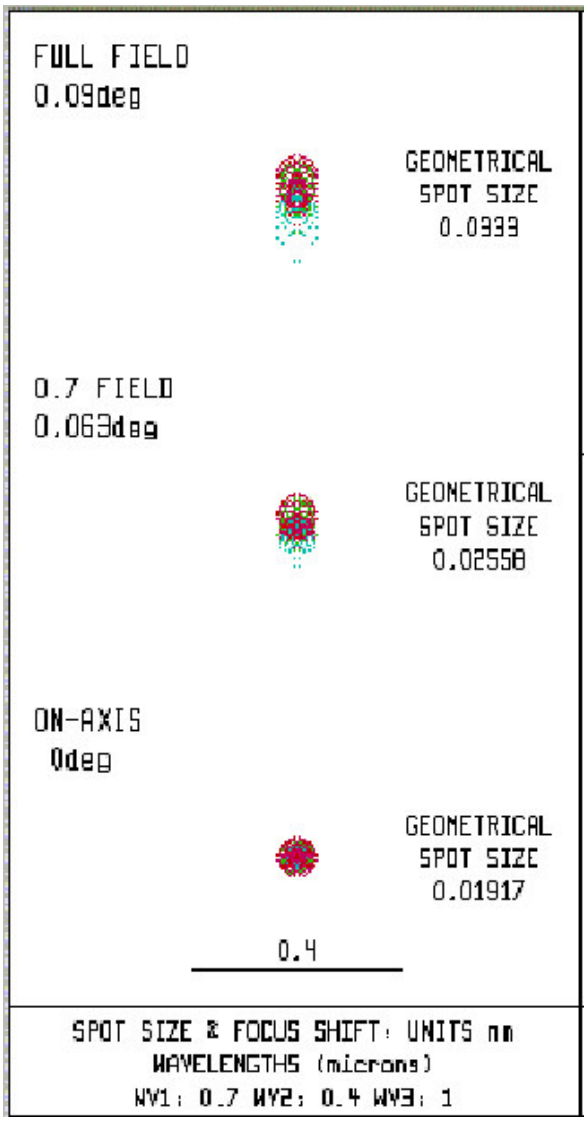

EFL=2979 mm, FOV= 10 mm dia.

Figure 9: the spot diagrams for a single lens meniscus corrector. Note that the spot diagrams are almost round, a very desirable feature. Some color spreading (the so called lateral color) is present at the edge of the field.

Ross corrector

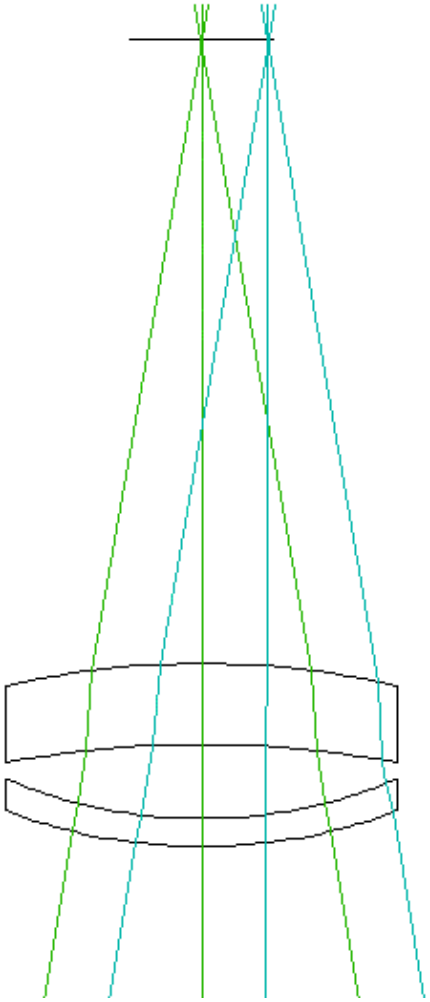

Figure 10: A sketch of the optimized solution for a two lens Ross corrector.

A two lens Ross corrector provides better correction over much larger field. However, at F/3 its performance is limited by higher order aberrations. At F/4 it gives much better performance over filed of view of 40 mm in diameter. One advantage of the Ross corrector design is that both lenses are made of the same optical glass, and its type is not critical. Usually the standard BK7 glass is used, but semi-optical glasses can also be used without any problem. Also, the surface tolerances are not too tight, so this type of corrector can be easily produced by a skilled amateur optician.

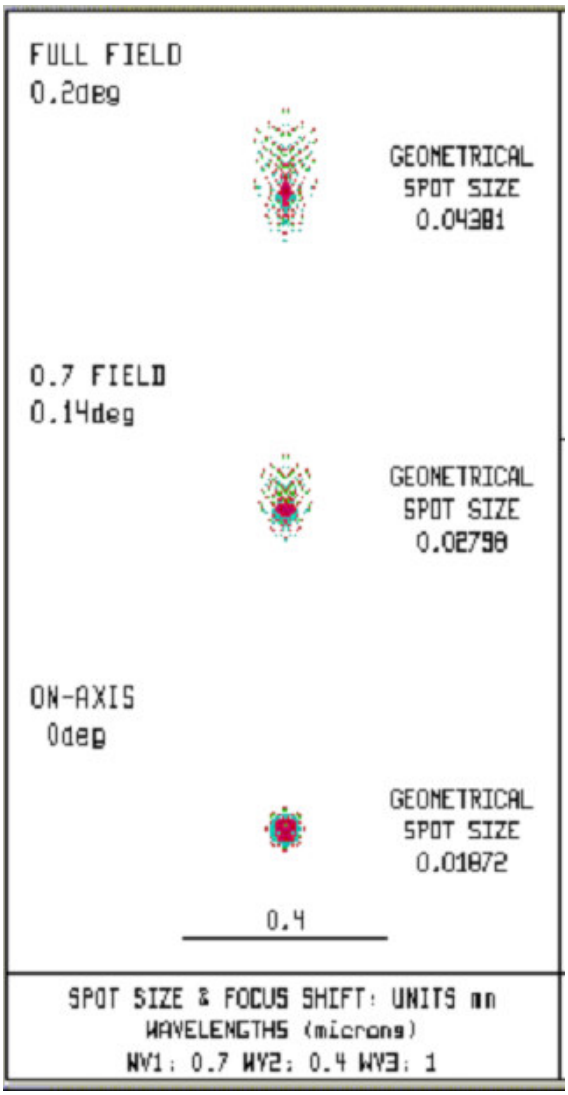

EFL=2925 mm, FOV= 20 mm dia.

Figure 11: the spot diagrams for the Ross corrector. The residual aberrations can not be compensated at F/3, but at F/4 the correction is much better.

Two lens focal reducer

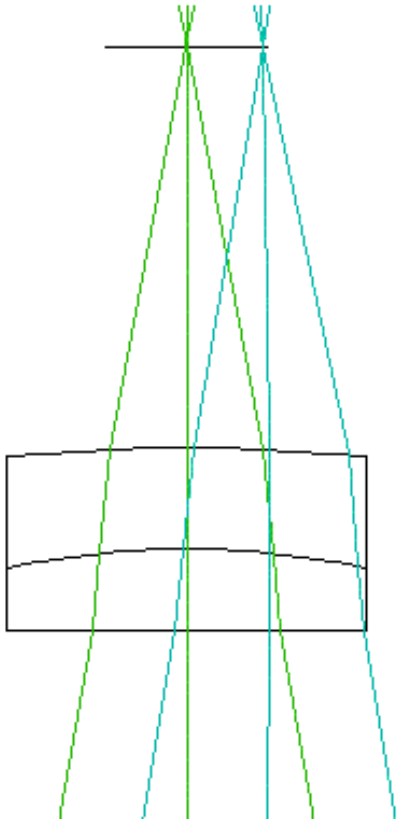

Figure 12: A sketch of the optimized solution for a two lens (cemented) focal reducer.

The focal reducer attempts to reduce the focal length and to correct the aberrations of the telescope optics at the same time. To deal with chromatic aberration, two different glasses must be used. In the example above good performance is achieved over a 20 mm field of view. The lens is still easy to make and tolerances are quite relaxed.

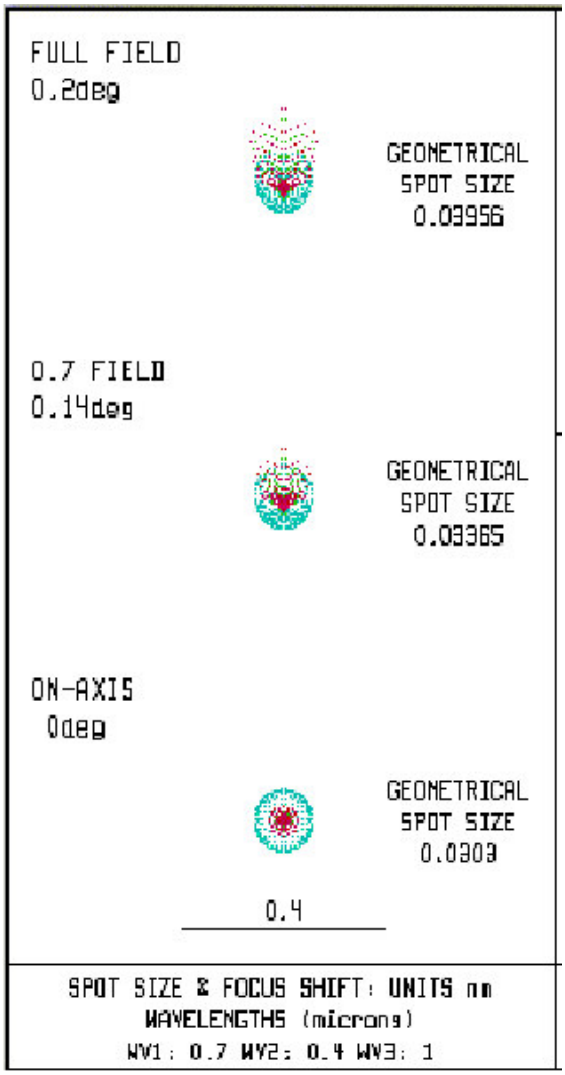

EFL=2646 mm, FOV= 20 mm dia.

Figure 13: the spot diagrams for the two lens focal reducer.

.

Wyne corrector

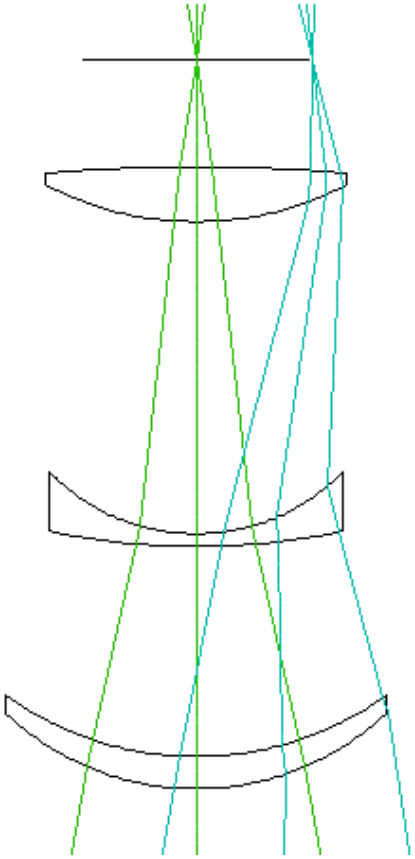

Figure 14: A sketch of the optimized solution for a three lens Wyne corrector.

Wyne corrector is used on many larger telescopes with both parabolic and hyperbolic primary mirrors. It is a three lens design, usually using the same glass for all lenses, although more complex designs with different glasses also exist. It achieves very large fields of view, and its main drawback is that surface tolerances of corrector lenses are very tight, so a well equipped professional optical facility is needed to produce such a corrector.

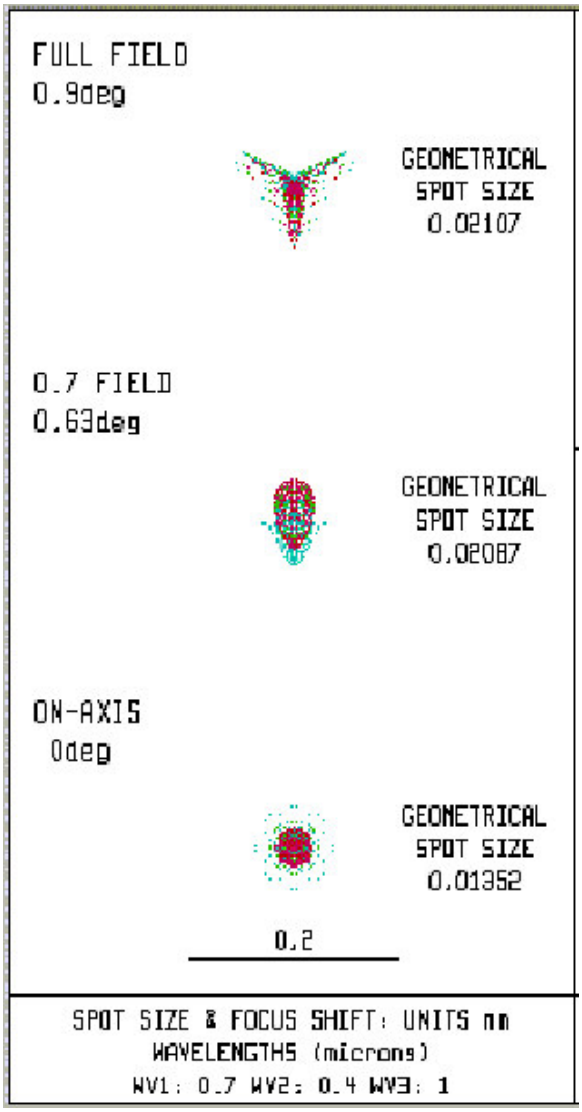

EFL=3320 mm, FOV= 105 mm dia.

Figure 15: the spot diagrams for the Wyne corrector. Note the huge field of view and quite small spot diagrams.

A complex focal reducer

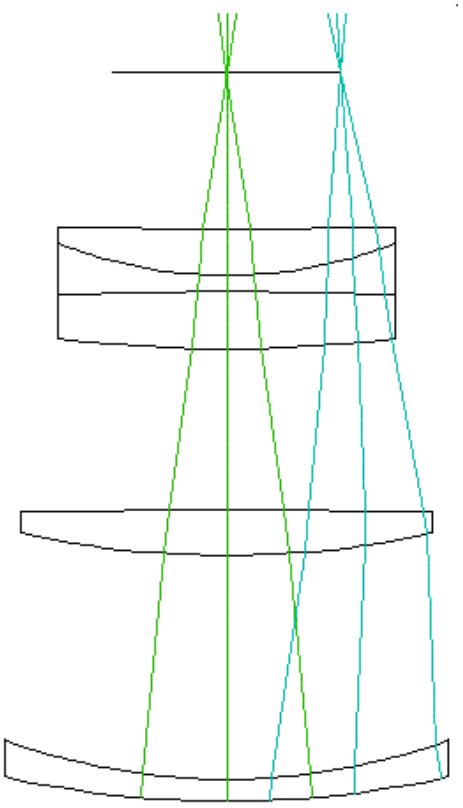

Figure 16: A sketch of the optimized solution for a five lens focal reducer with a large FOV.

A complex focal reducer is a new design developed for the Višnjan observatory 1m telescope. It is capable of covering a 2" CCD at F/2.4 effective focal ratio. Again, several optical glasses and many lens surfaces with tight tolerances require a well equipped professional optical facility to produce such a corrector.

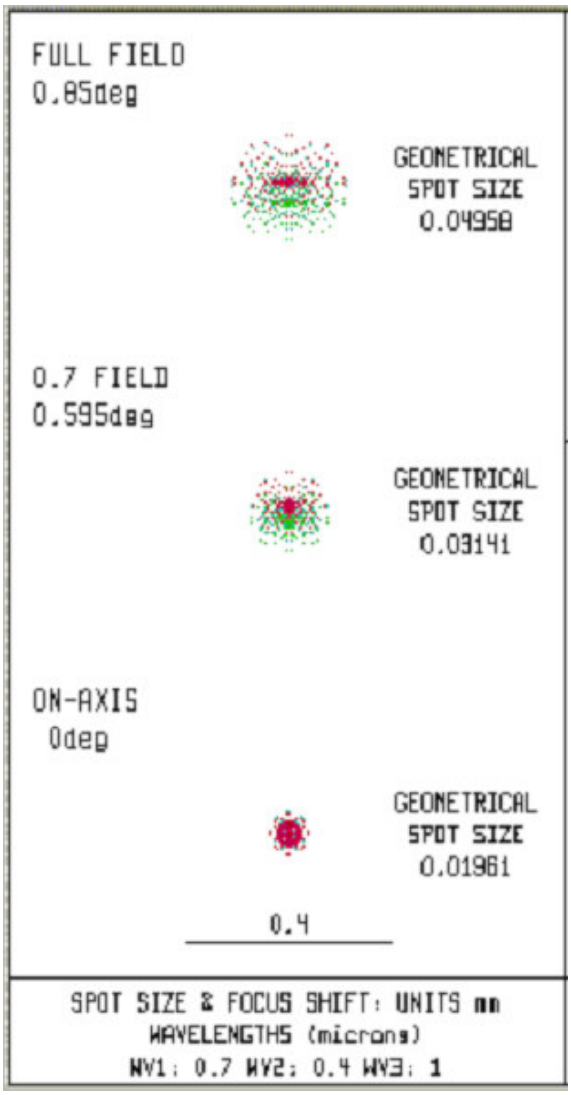

EFL=2404 mm, FOV= 72 mm dia.

Figure 17: the spot diagrams for the novel five lens focal reducer.

Conclusions

The main problem of 1m class telescopes is off-axis coma, combined with a relatively large angular field of view required to cover 1" or 2" CCD. At F/3, which we assume is the lower practical limit for the primary mirrors, single lens correctors are unusable, and a 2 lens Ross corrector produces marginal performance over 20 mm diameter field of view. For such a telescope, more complex 3 lens Wyne corrector or even more complicated focal reducer designs must be used.

Increasing the F/number allows better image quality and simpler correctors, usually over larger field of view. A jump from F/3 to F/4 produces drastic improvements in performance of corrector systems.

Ritchey-Cretien primaries were not studied in detail for this article, but some general comments can be given: such mirrors have overcorrected spherical aberration in addition to coma, and usable field of view of correctors is reduced by 25-50%. Also, as each RC primary is unique, the corrector design must be optimized specifically for it and is not usable on other RC mirrors.

Simple and two-lens correctors can be home-made by a skilled amateur optician with modest equipment. However, the more complicated Wyne and multi-lens correctors have strict tolerances and require dedicated measuring equipment and highly skilled opticians to make.

References

1. Better but bigger prime focus corrector lenses for Ritchey-Creiten telescopes, Richardson E H, Harmer C F W and Grundmann W A, Mon. Not. R. Astr. Soc. **206**, 47-54 (1984)

this article is the source for the initial Wyne corrector data.

2. Telescope optics, Rutten H and Van Venrooij M, Willmann-Bell, Richmond, USA, 1988

very usable introduction into astronomical optics and optical design, with many examples. Initial data for single lens correctors were taken from it.

3. Lens design fundamentals, Kingslake R, Academic, Orlando, USA 1978

a very good textbook on optical design in general. Initial data for the Ross corrector were taken from this book.

Appendix

Design parameters of correctors discussed in the article (Oslo LT format). In all designs, the first surface is parabolic with this entry parameters:

```
*CONIC AND POLYNOMIAL ASPHERIC DATA
 SRF        CC          AD          AE          AF          AG
  1      -1.000000      --          --          --          --
```

All optical glass data are taken from Schott catalogue.

a. single lens field flattener

SRF	RADIUS	THICKNESS	APERTURE RADIUS		GLASS	SPE	NOTE
OBJ	--	1.0000e+20	1.3963e+17		AIR		
AST	-5.8830e+03	-2.8900e+03	500.000000	A	REFLECT	*	
2	--	--	12.789241	S	BK7	C	
3	--	-24.000000	12.789241	S	AIR		
4	247.209782	V -5.000000	12.000000		BK7	C	
5	--	-25.950000	12.000000		AIR		
6	--	--	7.000000		BK7	C	
7	--	--	7.000000		AIR		
IMS	--	-0.003385	4.371599	S			

b. single lens meniscus corrector

SRF	RADIUS	THICKNESS	APERTURE RADIUS		GLASS	SPE	NOTE
OBJ	--	1.0000e+20	1.5708e+17		AIR		
AST	-5.8830e+03	-2.7000e+03	500.000000	A	REFLECT	*	
2	--	--	53.000000		BK7	C	
3	--	-24.000000	53.000000		AIR		
4	143.327096	V -50.000000	48.000000		BK7	C	
5	140.762250	V -213.490000	48.000000		AIR		
6	--	--	8.000000		BK7	C	
7	--	--	8.000000		AIR		
IMS	--	0.004404	4.786813	S			

c. Ross corrector

SRF	RADIUS	THICKNESS	APERTURE RADIUS	GLASS	SPE	NOTE
OBJ	--	1.0000e+20	3.4907e+17	AIR		
AST	-5.8830e+03	-2.8000e+03	500.000000 A	REFLECT	*	
2	--	--	33.826238 S	BK7	C	
3	--	-23.800000	33.826238 S	AIR		
4	-84.861952 V	-4.300000	30.000000	BK7	C	
5	-76.789679 V	-11.400000	30.000000	AIR		
6	163.842358 V	-12.400000	30.000000	BK7	C	
7	135.118568 V	-95.750000 V	30.000000	AIR		
8	--	--	11.000000	BK7	C	
9	--	--	11.000000	AIR		
IMS	--	-0.004144	10.275486 S			

d. achromatic focal reducer

SRF	RADIUS	THICKNESS	APERTURE RADIUS	GLASS	SPE	NOTE
OBJ	--	1.0000e+20	3.4907e+17	AIR		
AST	-5.8830e+03	-2.8500e+03	500.000000 A	REFLECT	*	
2	--	--	25.501706 S	BK7	C	
3	--	-23.800000	25.501706 S	AIR		
4	-1.4383e+04 V	-10.000000	22.000000	F6	C	
5	110.638687 V	-12.400000	22.000000	SF11	C	
6	225.616904 V	-49.178338 V	22.000000	AIR		
7	--	--	10.000000	FK52	C	
8	--	--	10.000000	AIR		
IMS	--	-0.187999	9.273804 S			

e. Wyne corrector

SRF	RADIUS		THICKNESS		APERTURE RADIUS		GLASS	SPE	NOTE
OBJ	--		7.8397e+19		1.2316e+18		AIR		
AST	-5.8830e+03		-2.6000e+03		500.000000	A	REFLECT	*	
2	--		--		98.889682	S	BK7	C	
3	--		-35.120000		98.889682	S	AIR		
4	-128.011535	V	-15.000000		88.000000		BK7	C	
5	-150.980362	V	-97.648702		88.000000		AIR		
6	-336.209170	V	-5.879760		68.000000		BK7	C	
7	-94.755529	V	-145.034080		68.000000		AIR		
8	-151.666181	V	-25.000000		70.000000		BK7	C	
9	1.0747e+03	V	-50.110000	V	70.000000		AIR		
10	--		--		52.000000		BK7	C	
11	--		--		52.000000		AIR		
IMS	--		-0.000708		52.174634	S			

f. five lens focal reducer

SRF	RADIUS		THICKNESS		APERTURE RADIUS		GLASS	SPE	NOTE
OBJ	--		5.6743e+19		8.4186e+17		AIR		
AST	-5.8830e+03		-2.7197e+03		361.897150	A	REFLECT	*	
2	-320.748335	V	-6.878973		70.000000		BK7	C	
3	-202.021812	V	-70.677574		70.000000		AIR		
4	-310.258760	V	-14.475886		65.000000		F6	C	
5	4.3789e+03	V	-50.665601		65.000000		AIR		
6	-443.950052	V	-18.094858		53.000000		BK7	C	
7	1.7508e+03	V	-5.066560		53.000000		SF11	C	
8	-144.758860		-14.475886		53.000000		LAFN28	C	
9	-2.8344e+03	V	-49.830000		53.000000		AIR		
10	--		--		36.000000		BK7	C	
11	--		--		36.000000		AIR		
IMS	--		-0.001395		35.780712	S			

SPECTROSCOPIC OBSERVATIONS OF COMETS WITH AMATEUR MEANS

Mike Kretlow [a], Matthias Jung [b]

[a] Michael Adrian Observatory, Fichtenstrasse 7, D-65468 Trebur, Germany, e-mail: mkretlow@gmx.de

[b] University of Siegen Observatory, Adolf-Reichwein-Strasse, D-57068 Siegen, Germany, e-mail: matt.jung@gmx.de

Even today, where high sophisticated CCD cameras and telescopes with 0.4m-0.8m aperture are not unusual for amateur or public observatories, spectroscopic observations, particularly of comets, are not very common. One reason could be, that suitable spectrographs cannot be bought (or would be too expensive and/or too big and heavy). In most cases they have to be build. Details of our spectrographs will be given on our webpage (http://astro1.physik.uni-siegen.de/uastro/spektro/)

We present spectroscopic observations of comet C/1995 O1 (Hale-Bopp), C/1996 Q1 (Tabur) and C/2002 C1 (Ikeya-Zhang), carried out with self-made spectrographs attached to the 300/1440mm Newton reflector of the Siegen University observatory. For comet Hale-Bopp the sodium emission tail could be confirmed.

Introduction

In 1996 we started our first attempts in spectroscopic observations of comets. Therefore we built a slit spectrograph (YASSP1) using an Amici prism (Fig. 1).

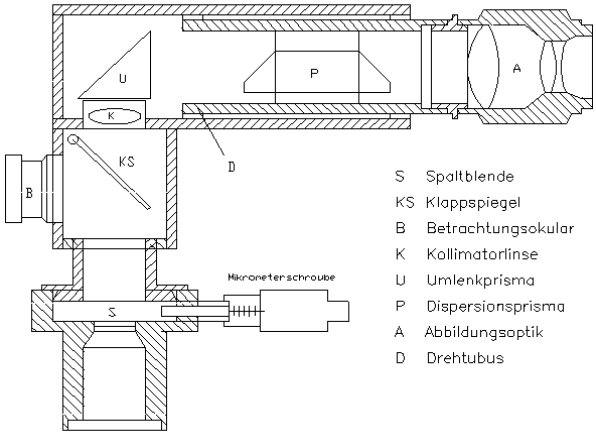

Figure 1: S Slit, KS Flip mirror, B control ocular, K collimator lens, P dispersion prism, A imaging lens (ordinary photo lens).

With this spectrograph we observed comet Tabur in October 1996. A couple of months later, we made a mechanical re-design of this spectrograph, but essentially (optical parts) it was the same. This spectrograph (YASSP2) was used for observations of comet Hale-Bopp in 1997. Because of different problems with this new concept and other tasks, we could not get very much data of reasonable quality. These spectrographs had a pixelscale of only about 1-2 nm / px.

In 2001/2002 a third spectrograph (YASSP3) was built by M.Jung. Now, a blaze grating (1200 lines/mm) was used and the optic was optimized for the f/4.8 focal ratio of our telescope. Wavelength calibration is possible using 2 or 3 background lines (Hg) because of the linear dispersion function. The linear dimension of the spectra is about 25mm. The pixelscale is about 5A / px. Now we use the KAF-0401E and 1602E devices (Audine cameras), which have a better response, especially in the blue part. On 2002-Apr-22 a first spectrum of comet Ikeya-Zhang was obtained.

Results and discussion

Figure 2 shows the final spectrum of comet Tabur, obtained on 1996-Oct-14 with YASSP1. It was taken with our 300mm Newton reflector and a CCD camera running the KAF-0400 device in 2x2 binning mode. For wavelength calibration we used spectra of streetlights, which could be easily taken, because the observatory is located in the city and the dome is surrounded by streetlights and buildings …
At the time of observation the comet had a visual total-magnitude of about 5.5mag. For the reduction a background image with the same integration time was subtracted. No flux calibration was made, thus the spectrum is folded with the CCD response function. The emission lines were identified by [1].

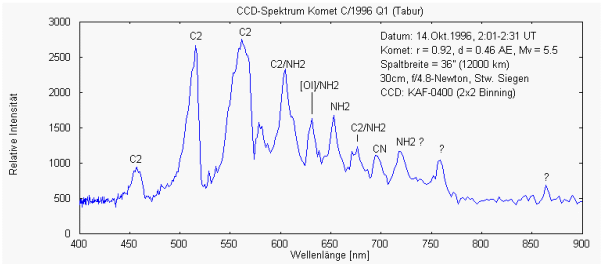

Figure 2: Reduced spectrum of comet Tabur in the range approx. 430 nm to 900 nm.

Some months later we observed comet Hale-Bopp on several nights with our second spectrograph. Figure 3 shows a sample of three nights. On 1997-Apr-20 we got the message, that a sodium tail was discovered at La Palma observatory (see IAUC 6631) and we could confirm this on the same night. Re-checking our previous taken spectra

we found a weak emission line at 589nm on an image of 1997-Apr-06, for which we believe that this is a Na-emission from the comet and not from the background (we should note, that subtraction of the background image does not always eliminate the background complete, because the imaging conditions like seeing, transparency etc. may change).

On 2002-Apr-22 a CCD spectrum of comet Ikeya-Zhang was taken with the new YASSP3 spectrograph (see Fig. 4). Again, this was made with the 300/1440mm Newton reflector at Siegen observatory and a self-made Audine CCD camera running the KAF-1602E device in 2x2 binning mode.

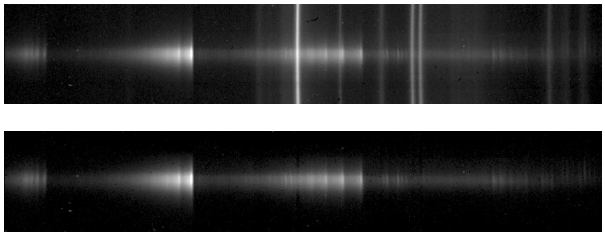

Figure 4: Raw CCD spectra of comet Ikeya-Zhang on 2002-Apr-22 in the range approx. 470 nm – 630 nm. Top: with background (the 546.1/577.0/579.1 nm Mercury lines are visible). Bottom: background subtracted.

A preliminary reduction of this spectrum is given in Figure 5. For the wavelength calibration, the three Mercury background lines at 546.1nm, 577.0nm and 579.1nm were fitted against a linear function, but no flux calibration has been done. Lines were yet not identified by wavelength, but the C_2 Swan bands and also some NH_2 emissions can be recognized. No Na emission is visible. But it should noted, that the sodium emission was detected by M. Fujii using a 0.28m and 1.01m telescope on March 3 (IAUC 7851).

Conclusions

We think, that it is possible for amateurs to make useful contributions to the exploration of comets, e.g. by investigating the spectral evolution over weeks, what in general cannot be done at professional observatories. Even with small instruments (D < 0.5m) comets of 6-8mag and brighter can be observed.

Acknowledgment

We thank the University of Siegen Observatory for assistance and access to their facilities.

References

[1] Brown, M.E. et al. (1996): A high-resolution catalog of cometary emission lines. Astron. Journal 112 (3), 1197-1202.

[2] http://astro1.physik.uni-siegen.de/uastro/spektro/index.html

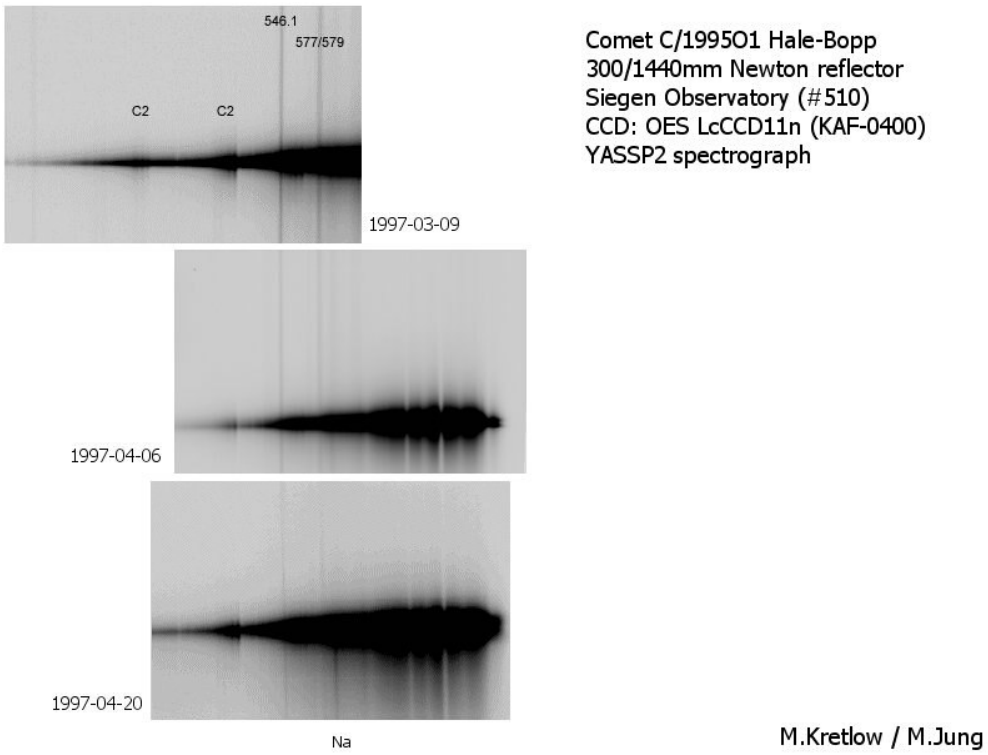

Figure 3: This composite image shows three raw CCD images. On April 20, the Na emission is visible. The image taken on Apr 06 shows also a very weak emission on the same position (probable not visible here in the paper; see [2]).

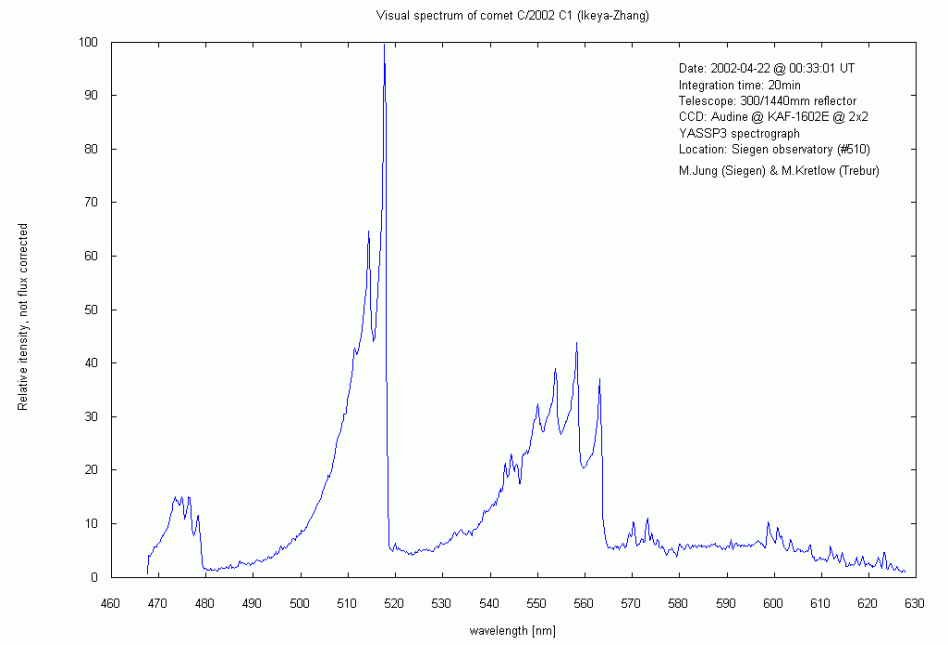

Figure 5: Preliminary reduced spectrum of comet C/2002 C1 (Ikeya-Zhang), taken on 2002-Apr-22 with the YASSP3 spectrograph on a 300/1440mm Newton reflector. The slit was centered on the head of the comet. The intensity is scaled to 100% for the strongest emission (C_2 at 515nm). Some of the smaller peaks between 570nm and 630nm should belong to NH_2 and probable to H_2O^+, but apparently no sodium emission is detectable.

A new 60-cm telescope for the Črni Vrh Observatory

H. Mikuž[a], B. Dintinjana[b], S. Matičič[c], J. Skvarč[d] , D. Žgavec[e]

[a]Predgriže 29a, SI-5274 Črni Vrh nad Idrijo, Slovenia, herman.mikuz@uni-lj.si, http://www.fiz.uni-lj.si/astro/comets/.

[b]Zemljemerska 11, SI-1000 Ljubljana, bojan.dintinjana@uni-lj.si.

[c]Cesta 5. maja 12, SI-1370 Logatec, stanislav.maticic@guest.arnes.si.

[d]Tovarniška c. 14, SI-1370 Logatec, jure.skvarc@ijs.si.

[e]Črni Vrh 48, SI-5274 Črni Vrh nad Idrijo, dusan.zgavec@imp-klima.si.

Design of a fully automatized 60-cm, f/3.3 telescope built for asteroid survey and follow-up is described. The telescope is replacing the previous 36-cm, f/6.7 telescope which was not capable of detection of fast and faint asteroids. Except for the optics, the complete plans for the telescope are made by the group members, and the telescope parts were built in local workshops. Complete computer control was achieved of all relevant parts: both telescope axis, filter wheel, focuser, and mirror flaps. The telescope is ready for fully automatic observations.

Introduction

The extensive sky coverage by professional robotic surveys is producing asteroid discoveries at ever-deeper magnitudes. Existing telescopes at Črni Vrh Observatory were not sufficient anymore to be competitive both for follow-up and asteroid discovery. To comply with increasing technical requirements for successful asteroid and comet observations, we built a 60-cm, f/3.3 Deltagraph telescope. The 60-cm Deltagraph is a custom made, advanced technology, wide-field imaging system, designed for sky survey applications. All functions (pointing, imaging, focusing, filter exchange) are controlled by a single computer program and the system can work unattended.

System Design

The telescope projects were made with a help of advanced computer programs that support 3-D design and structural analysis as well as various simulations (fig. 1) . This let us carefully design all telescope parts with final properties being well known in advance. In that way we avoided construction errors and reduced the manufacturing time and the overall costs.

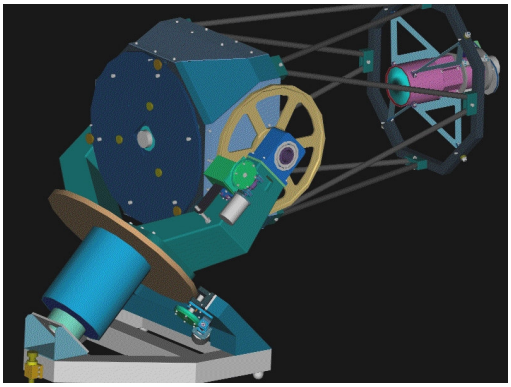

Figure 1: 3-D computer model of the 60-cm telescope.

The telescope design is compact and of low weight. We used a sheet metal to obtain the structure of a sufficient strength, free of flexure and vibrations, while keeping the overall weight to minimum. Stainless steel and aluminum were used for optical tube assembly and many other delicate parts for minimum maintenance and lower mass. The overall weight of a working telescope is only 500 kg. To achieve temperature stability of the tube assembly structure we used carbon tubes. This helps to keep the distance between the mirror and the coma corrector as constant as possible, in order to avoid focus changes due to nightly temperature variations. A motorized focusing device allows automatic refocusing of the system at any time during the observing session. The completed telescope is shown in fig. 2.

Figure 2: Final appearance of the 60-cm Deltagraph.

Optics

The Deltagraph is a wide field optical system and consists of a 600 mm, f/3 parabolic mirror and a 3-lens Wynne corrector which produce images free of coma and other aberrations over the wavelength range 400 nm to 700 nm. Optical components were designed by Astrooptik (1) and made by LOMO (St. Petersburg). According to spot diagrams (fig. 3), we obtain stellar images of less than 5 □m diameter inside the field radius of 20 mm and less than 20 □m diameter at the field radius of 50 mm. Stellar spots are thus much smaller than CCD pixels across the majority of 100 mm field diameter. The back focus is rather short (63.8 mm) what implies the usage of a very thin filter wheel.

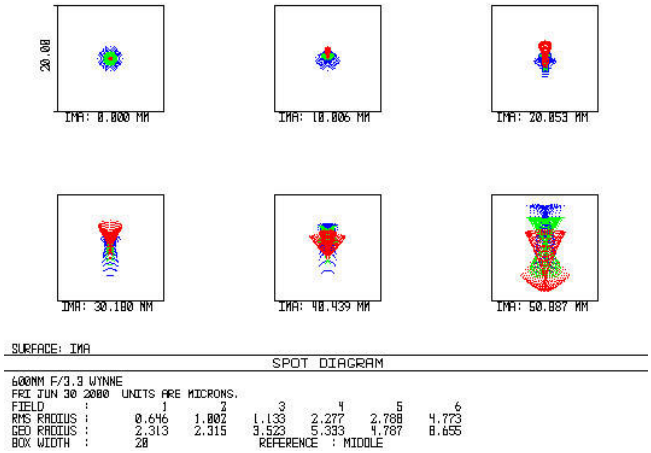

Figure 3: Spot diagram for the 60-cm, f/3.3 optical system. Box sizes are 20 µm x 20 µm. Our current CCD pixels are 24 µm x 24 µm what implies that the optical resolution of the 60-cm system is not fully exploited. Diagram courtesy P. Keller, Astrooptik Co.

Telescope Mount and Tube Assembly

Imaging of asteroids, comets, NEOs and other objects across the sky requires a mount design that is able to access any part of the visible sky with a minimum time delay. Another requirement was that the telescope tracking system should be able to follow the objects with the accuracy of +/- 1 arc sec over the period of 10 minutes. Otherwise we would need another system for precise telescope guiding which would increase the costs and make the system more difficult to use.

To meet these demands, we made a telescope mount with a fork-type friction drive system and with servo motors on both axes, enabling precise tracking as well as fast slewing with up to 5°/second. The polar and equatorial disks are driven by 1:24 and 1:32 rollers, respectively, through 1:180 worm gears and servo motors. Unguided exposures of up to 10 minutes duration are possible.

To protect the mirror from dust and moisture when the telescope is not in use, we added motorized flaps. The mount base, forks and lower part of OTA were made of thin sheet steel and shaped on a CNC machine for a maximum precision.

Extra care has been devoted to the perpendicularity of the polar and the equatorial axes which have been carefully adjusted to +/- 0.5 arc min, using laser technique.

The primary focus assembly contains an optical corrector housing, a motorized focusing device, a four-position filter wheel and a CCD camera. To achieve the desired degree of image correction the housing has been milled to high tolerances, assuring proper corrector lens distances. We use the standard Bessell BVR (W) 50 mm diameter filter set from the Omega Optical (2). A special focus carriage device is driven by a stepper motor and carries the filter wheel and the CCD camera. Also, the filter wheel control is fully motorized and computer controlled. The 1k x 1k Finger Lake Instruments (3) CCD camera has a thinned, back side illuminated sensor. Main telescope specifications are summarized in table 1.

Primary mirror	600 mm, f/3 paraboloid
Coma corrector	Wynne 3 lens with 1.1x optical power
Diameter of corrected field	100 mm
System focal length	1989 mm
System resolution	2.5 arcsec with 24 µm pixels
Field of view on 1k x 1k CCD	0.7° x 0.7°
Telescope mount	fork type, friction drive + servo motors
Limiting magnitude	in 1 min. exposure 20.0m with V filter

Table 1: Basic telescope characteristics.

Telescope Electronics

The main purpose of the electronics is to accept commands from the main computer and to control the servo motors and other motors. It consists of several units. The power stages of the servos are two Epsilon Eb Digital Servo Drives from Emerson Motion Control. The main feature from the constructor point of view is that they are controlled in the same way as simple stepping motor controllers - by a direction signal and a step pulse. So the rest of electronics does not need to worry about the details of servos and can be used for steppers without any change. The main processing unit is built around the Rabbit 2000 microcontroller, which has a command set based on the old Z80 processor. The program for it written in the Dynamic C language which is an extension of C and allows execution of seemingly parallel programs. The Rabbit processor communicates with the main computer using either RS-232 or RS-485 interface. On a separate board, on which the main unit is piggy-backed, there are further three Atmel AT90S2313 microcontrollers which are used as intelligent precision pulse givers - one for the sidereal clock and the other two for the right ascension and declination axis. Another circuit board using AT90S2313

only takes care of switching the telescope electronics on and off through a solid state relay. The telescope can be switched on and off either using push buttons on the front panel or remotely by computer. This board also has input for the Dallas DS18S20 temperature sensor to control the possible overheating of the electronics.

In a separate box close to the telescope there are another two Atmel microcontrollers which are responsible for the filter wheel, the focuser motor, the mirror flaps and for the mirror ventilator. They communicate directly with the main computer using the RS-485 interface.

All in all, there are 7 microcontrollers in the system, which control all together 6 motors and hold the internal state of the telescope so that the control program running on the main computer actually does not need to keep track of any current parameters of the system. The schematic diagram showing the communication paths between different devices is presented in fig. 4.

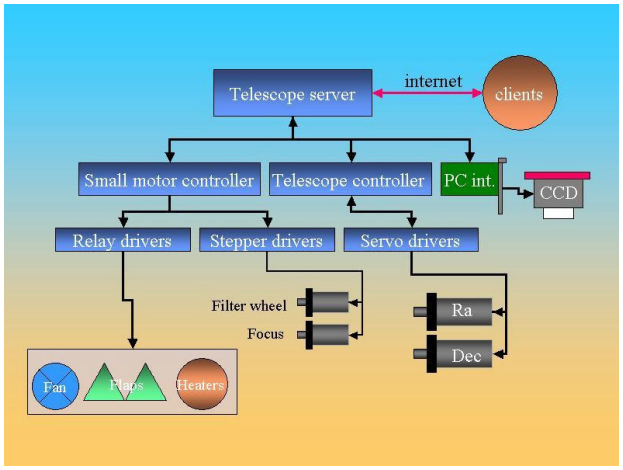

Figure 4: Schematic diagram of the telescope electronics and the computer-electronics communication paths.

System Operation and Software

For the computer control of the telescope we use a concept of servers which communicate with the hardware through drivers, written specifically to communicate with external devices. The programs which actually send commands are clients which do not need to know anything about the hardware details. The telescope server accepts commands from the TCP/IP network and executes them. When we want to move the telescope to a desired position, we simply send "point" command with RA and Dec coordinates and the telescope slews to the desired position. In the same way we send commands to a CCD camera to obtain images. The FITS header of each image contains various data such as the date-time of acquisition, the exposure time, the filter used, the WCS field coordinates and other information about the observation which are aquired from the telescope control server.

These commands can be used in a program script to perform specific tasks, such as automatic image calibration acquisition, (flat, dark, bias), focusing, filter exchange, field scanning for searching asteroids and comets. The operation of an imaging system is controlled by a "watchdog" program which alerts the operator in case of any hardware and software malfunctions, or a sudden cloud cover.

Telescope Performance

Due to the extended period of bad weather after the completion of the telescope we could not make all tests of the telescope yet. Here we only present preliminary results of the limiting magnitude determination. We took an image of a stellar field centered at RA=02:21:16 Dec=+45:56:46 on November 10, 2002 with 1k x 1k CCD and V filter. Exposure time was 60 seconds. Camera cooling was set to -20° C. After the calibration with Tycho-2 catalogue, we obtained the frame V limiting magnitude close to 20 m. The graph in fig. 5 shows experimental error estimates along with the theoretical curves for noise formation due to different sources.

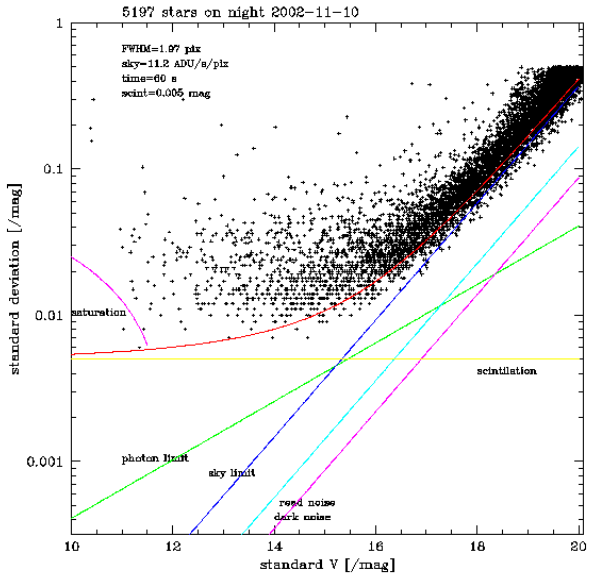

Figure 5: CCD photometry statistics for a stellar field at RA=02:21:16, Dec=+45:56:46. The standard deviation magnitude error is plotted against the V Johnson standard magnitude. The theoretically predicted curves for photon, sky and camera noises are plotted in the same diagram. The red curve represents all theoretical noises summed together. The measured data conform well to the theoretical curve.

Acknowledgment

The authors gratefully thank the Planetary Society for the Shoemaker grant 2000 awarded to H. M. which greatly helped the successful conclusion of the telescope building project.

References

1. Astrooptik Company (2002), www.astrooptik.com.
2. Omega Optical Inc. (2002), www.omegafilters.com.
3.Finger Lakes Instrumentation (2002), www.fli-cam.com

BUILDING THREE COMPACT-LOW COST 61-CM KLEVTSOV TELESCOPES FOR NEO FOLLOW-UP

J. Nomen, S. Sanchez, J. Guarro, J. Rodriguez, A. Garcia, M. Blasco

Observatorio Astronomico of Mallorca
Cami de l'observatori s/n, 07144 Costitx, Mallorca, Spain astroam@bitel.es

In the latest years, the increment and efficiency of the big surveys are facilitating the discovery of a greater number of NEO asteroids, in general, with fainter magnitudes. The traditional follow-up task made by observatories with medium aperture telescopes is resulting more and more difficult and, in many cases, is getting impossible.

We are in front of a paradox in which many of the new discoveries of NEOs cannot be confirmed neither carry out the correct follow-up the next days by these observatories usually dedicated to such task, and is frustrating, therefore the improve in the equipment in many of those observatories with medium size telescopes is, commonly, costly and not easy to finance.

The present project is born on the interest of the members of the observatory of Mallorca in arranging some telescopes of greater aperture to continue with the work of NEO follow-up that traditionally has come carrying out the last years. For that, after a first experimental phase along 3 years, in which 3 Schmidt cameras of 40 cms were already built, practically only with their own means, the construction of 3 new telescopes of 61 cms has been initiated, also mostly undertaken with the optical, technical, mechanical, electronic and data processing resources of the team and the collaborators of the observatory.

The new telescopes have some very characteristic premises, that could turn out the project interesting and attractive also for other observatories with medium apertures and limited economic resources. Those goals are: Very economical total cost, automated observation, low weight, very reduced size to fit in small domes, among others. It's described and justified the design and construction, on the basis on the previous experience.

Introduction

In the present work, we will justify the design and construction of our new project: Three compact, 61-cm Klevtsov telescopes based on the last three year experience working in astrometry with three 40-cm Schmidt cameras, also build practically by our means. Knowing that other observatories have similar projects or are already working on that, the observatory of Mallorca has also the need of improving the tools to be able to continue with the astrometric work, especially refered to the NEO confirmation, follow-up and recovery. There is an evident fact: The efficiency and increase of the big surveys is producing an every time more number of NEO discoveries and, at the same time, of fainter magnitudes. Also, the Medium Aperture Observatories are having an every time greater difficulty confirming and following-up them , producing generally, a less quality astrometry, due to the weak signal obtained when observing the faintest and the fastest objects. Given that situation, a number of alternatives have been often discussed in different forums, such as the Minor Planet Mailing List. Being the most common: A preferential dedication to the photometry. The recovery of under-used "old dinosaures" telescopes by groups of observers working in shifts. The purchase of commercial telescopes, a really costly option, if apertures are over 50-cm. And finally the construction of greater telescopes mainly by means of own resources, meaning an important cost reduction. In our case, we have choosen this last option.

Materials and methods: our previous project

Althought during many years we have built several telescopes, it was in 1999 when we finished the construction of three, 40 cm Schmidt cameras, mainly aimed at observing asteroids. Both the primary mirrors and front corrective plates where grinded and polished by Joan Guarro member of the Observatory of Mallorca, and we tested with them different mountings: Altazimuth, German, and Forks ones, and several electronic and clock driver mechanisms. Three Audine Kaf 1602E CCDs were acquired (1).
With all them we have carried out the majority of the astrometric observations during the last three years from 620-Mallorca, 946-Ametlla de Mar, and 165-Piera. In a moment our intention was even to establish a small jointed survey from the three stations, since the covered field (60 x 40 minutes) and the optical system speed, made us suppose the possibility to cover extensive areas of the sky per night.
(Figure 1)

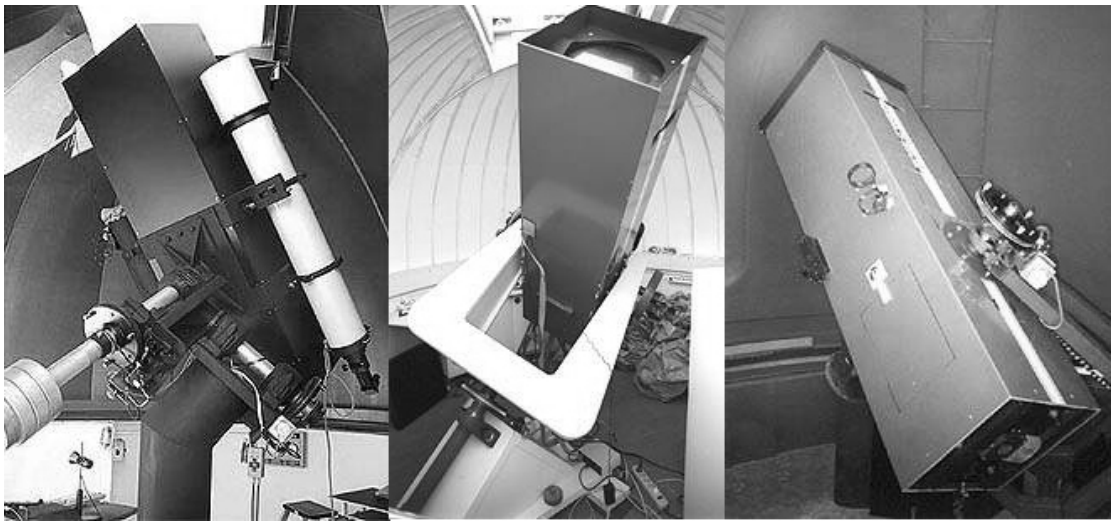

Figure 1: The three Schmidt cameras of 946-Ametlla de Mar, 165-Piera and 620-Mallorca

Results and discussion : after last 3 years

After these last three years we have obtained some experience and results of great importance for us before begining the construction of the new 61-cm telescopes. Some of the most important points are discussed:
CCDs: Perhaps one of our main errors was thinking, at that moment, that a considerable sized chip could never be affordable.

The need of obtaining a wide field made us consider a very short focal lenght, centered on F2 / 40-cm Schmidt cameras, that is, only 80-cm of focal lenght. Some negative consequences refering to the low contrast and to the high arcsec/pixel ratio appeared, or in other words, not allowing to reach faint magnitudes and the astrometry quality not being the most accurate.

Tecnology develops, and for the cost of our Audines Kaf 1602E CCDs, we can obtain presently cameras with more extensive and sensitive chips, and therefore, the need of very short focal lenghts remain in great part discarted.

Refering to the MOUNTINGS, we installed our 3 Schmidt cameras over the different kinds of mountings built by ourselves or by some collaborators of the Observatory of Mallorca. They were automated by means of the free hard-soft project of Mel Bartels (2), and controlled by programs developed by us through LX200 commands. Our experience made us decide towards the election of fork mountings for our new project, because they are, in our opinion, the easiest to automatize, without GEM flips or field rotations, and we think that they are the ones presenting, in general, better accurate tracking and the easiest to neutralize their errors by PEC. These graphs (Figure 2) show the Periodic Error Corrections produced by two of our mountings carrying similar 40-cm Schmidt tubes. The PEC curves are the average for three different azimuth, 135º, 155ºand 175º. The period of the X axis is eight minutes, although the numbers show correction steps. In the Y axis the periodic error is represented in tenths of arcseconds.

It is important to point out that the closer we get to the meridian, the more regular and expected the PEC is becoming, however, the farther we get, the more the curve is altered and changed. Also the curves appear completely horizontally inverted after making a meridian Flip on German ones. We believe these effects are produced especially due to small deficiencies in the counterbalancing, depending on the tube orientation, in our opinion this is more critical in German mountings. Is important to point out that they only show some results testing our own mountings.

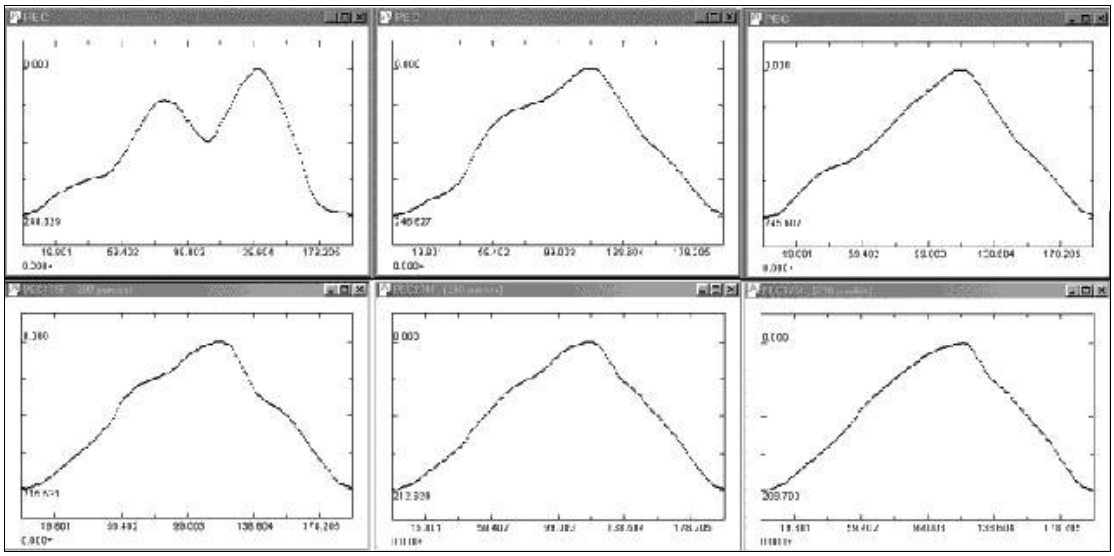

Figure 2: Periodic Error Corrections at three azimuth. Left to right: 135o, 155oand 175oof two different mountings with similar drive mechanism and optical tubes: The Ametlla de mar German mounting on the upper part and the Mallorca fork mounting on the bottom.

Relating to the OPTICAL DESIGN, Despite considering that our Schmidt cameras, did not have too large tubes, we believe that a more compact optical scheme should be one of the main objectives
to achieve, because this involves small and light mountings, (easy to be installed in small domes, or not provided with special foundations), and mountings with less flexions and finally, reasonably priced.
Another disadvantage, refering to the optical scheme, we have been using during these three years, is that such a short focal ratio reduces in great measure the contrast, especially considering that our sky doesn´t have the best clearness. Our Schmidt cameras are very fast and in a bit more than 15 seconds reach 17 mag, however, in longer exposures, of several minutes, they don´t overpass the 18.5 mag aproximately.
With reference to our experience concerning the OPTICAL TUBE, we have been very lucky to benefit from the advantages of having a close telescopes, with the CCD cameras inside. In our mediterranean humid weather the opticals suffer in general great environmental degradation.

Given that the close tubes represent a great advantage, in bigger telescopes, due to high technical complexity and high cost, the front correcting plates shall be discarted. To solve this problem, we have successfully tested Turbofilm ™ sheets, a plastic polimer which gets perfect homogeneity and performs equal to one tenth (1/10) wave plane parallel optical window. Turbofilm ™ protects the optical equipment, closing the telescope tube against dust and humidity and greatly reduces air currents, all without lost the optical quality of the telescope image (3).

For the before mentioned reasons we prefer close structure tubes, although they may be heavier.
The TELESCOPE CONTROL hard-soft developed by Mel Bartels has proved to be very successful in
the last three years. This is a very economical system, easy to perform, and can be controlled from our own program in a second computer, at the same time, through a serial port by LX200 commands. (Figure 3).

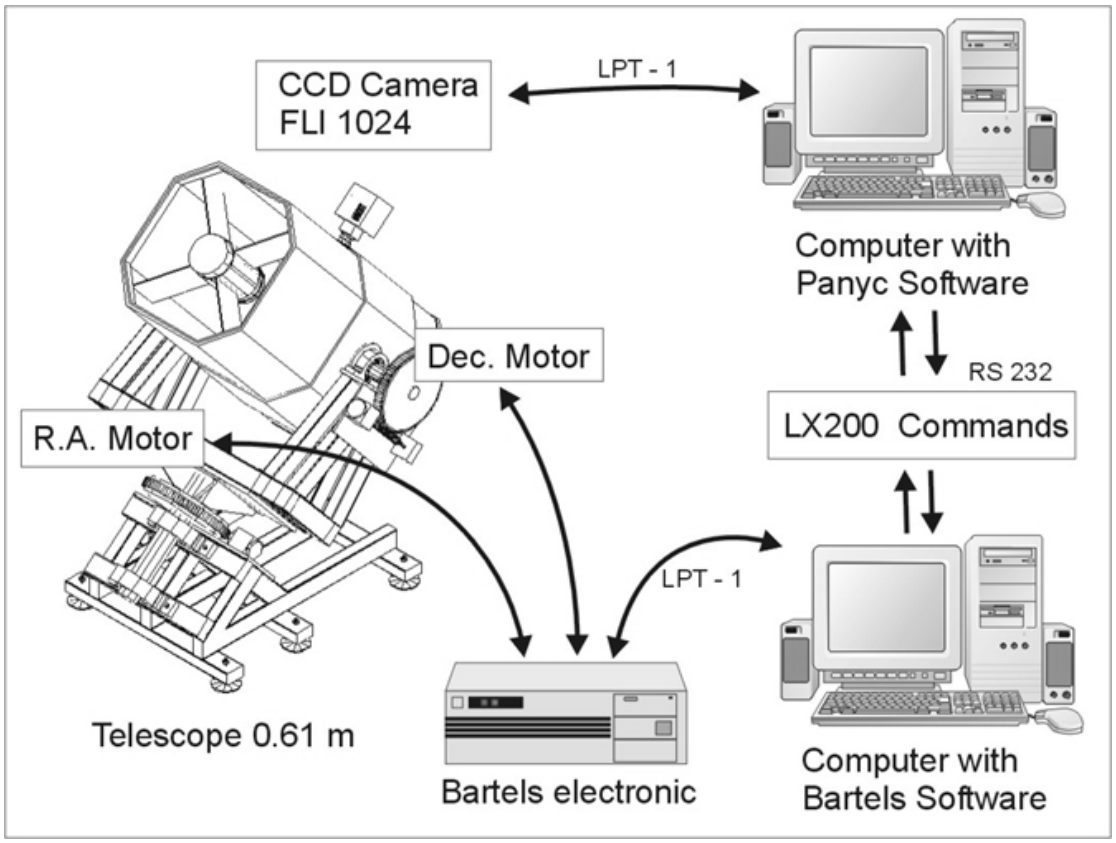

Figure 3: Telescope control scheme

Due mainly to the lack of contrast and the lack of the most suitable arcsec/pixel ratio, we shall sumarize saying that those three 40-cm F2 Schmidt telescopes built, are basically exceptional for the survey of bright objects, and this can only be achieved, nowadays, before the sunrise and after the sunset and polar regions, searching for bright comets. This will be probably the only main task of those telescopes once we have the new 61-cm working.

In some ocasions, they have been really useful with fast and bright NEOs, as it happened with 2001 DZ76, an Apollo discovered by LINEAR and confirmed from 946-Ametlla de Mar, when it moved at 158 arcseg/minutes and 16.3 V magnitud (4). With only 4 seconds exposition, it was fixed on the images (Figure 4).

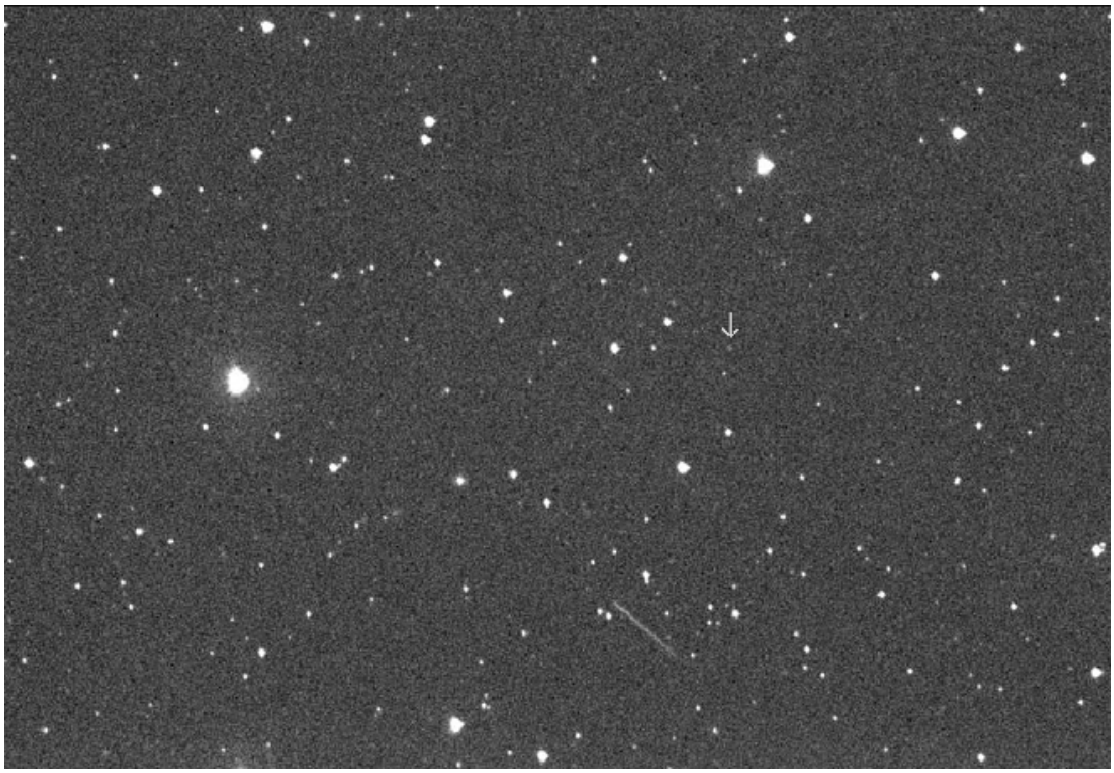

Figure 4: 2001 DZ76, Apollo, mag 16.3 and moving 158 arcsec/min. Was fixed only with a 4 seconds exposure. The stripe on the bottom belongs to a satellite.

Furthermore, they are very good telescopes taking images such as the one shown in the following figure (Figure 5). However we consider that nowadays they are not the most apropriate for our work in asteroids follow-up.

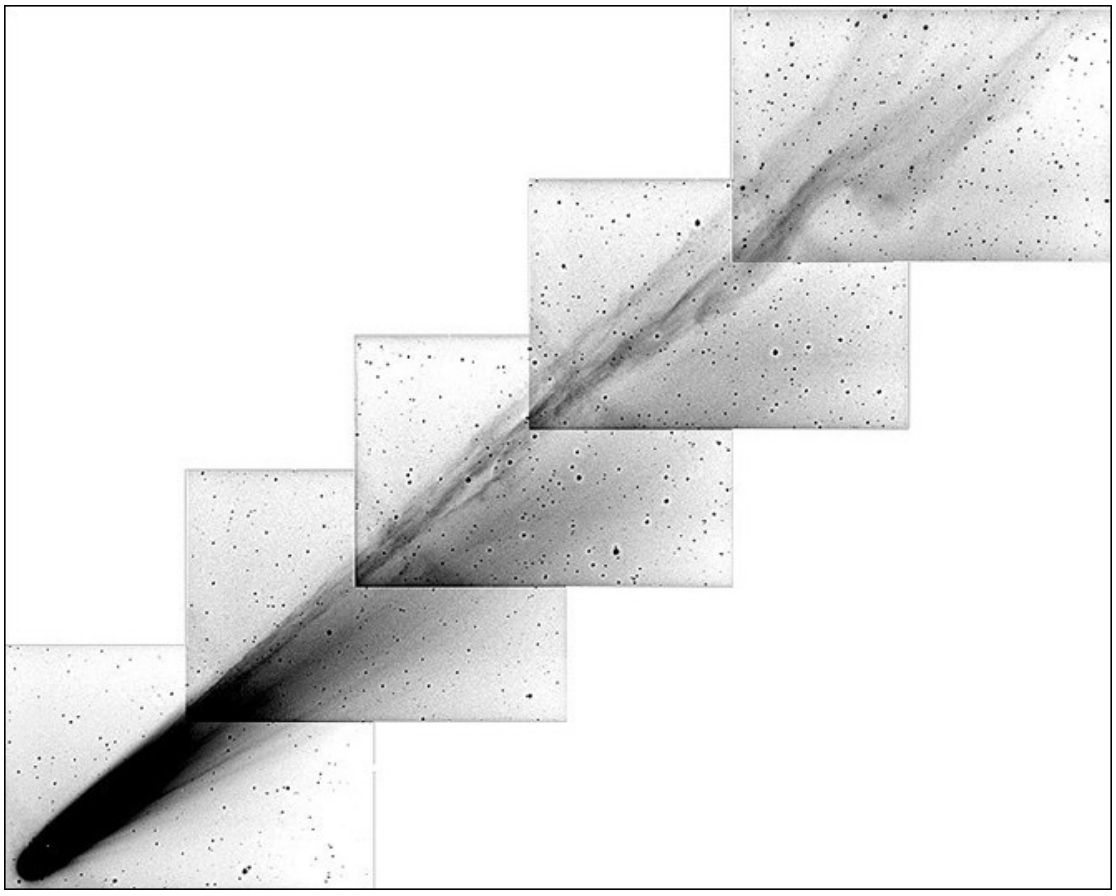

Figure 5: Comet Ikeya-Zhang on March 20, 2002. Mosaic of 5 images of 60'x40' taken with one of the 40-cm f2 Schmidt cameras. Exposure times between 30 and 60 seconds. (946-Ametlla de Mar). Great part of its resolution was lost after reducing the scale.

Conclusions: applied to the building of the new 61-cm telescopes

Which are the conclusions reached when starting the construction of the new 61-cm telescopes?
If we found a very compact optical design, relatively easy to perform, with focal ratios between 3.5 and 4.5, this would offer all the advantages already mentioned, such as, small mountings, fewer structure flexions, lower weigh, and smaller economic cost. One posible solution choosen by some other projects is deltagraph designs (5), however, another possible solution, the one that we have finally opted is the Klevtsov design (6), (7).

In 1974 Yuri Klevtsov designed an original telescope based on all spherical surfaces: A primary mirror, A quasi afocal meniscus, and a secondary negative lens aluminized on the opposite side. He achieved a simple and very compact system (8). Besides the already mentioned features, such us the very compact design and the low production cost given the spherical surfaces, It provides excellent optical performance, due partly to the reduced correcting lens diameter, lower than one third (1/3) of the primary diameter. (Figure 6)

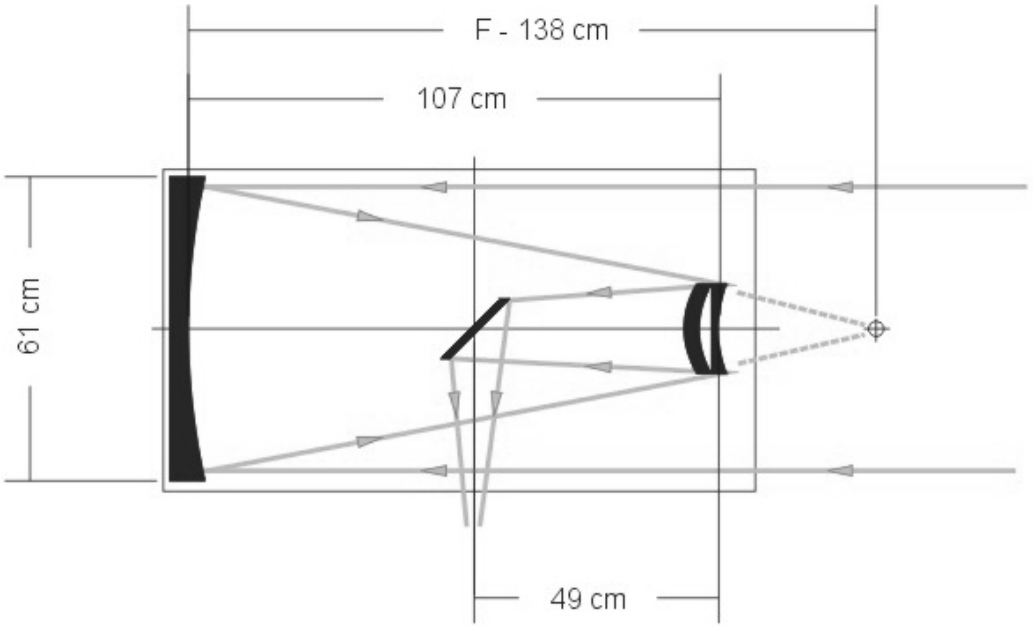

Figure 6: The Klevtsov optical design of the 61-cm new telescopes

It is important to stress the fact that for our primary 61-cm mirrors, in only 107-cm distance between glasses, all the optical system can be included.

Contrarily, we are faced with an open front tube design, exposed to our humid mediterranean weather. In order to prevent that, we are going to use the before mentioned Turbofilm ™ sheets.

We have been working for aproximately one year, first in the design and later in the setting up of the new 61-cm Klevtsov. Presently, on 2002 May, the three new mountings are very advanced, and the three primary mirrors, BVC (Vitrified Ceramic), blanks acquired roughly precurved (9) are already finished by members of the observatory of Mallorca (10). The fact of their spheric shape has permited an easier and faster elaboration. (Figure 7)

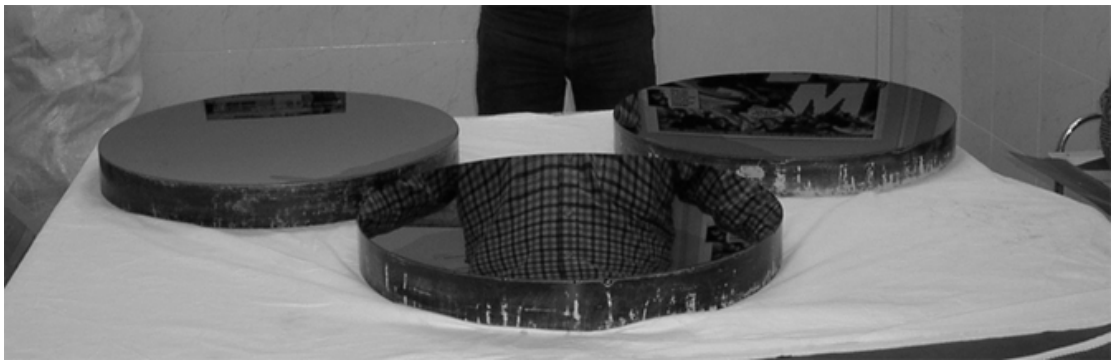

Figure 7: The three primary f 2.3 spherical mirrors already finished

The corrector Klevtsov lens have been ordered to an alien French company: VALMECA SARL (11), following the previous raytracing design by Mr.Gerardo Avila, from the Optical Instrument Group of the European Southern Observatory.

Three CCD Thinned Site 1024x1024, 24 microns, Finger Lakes (12) were already acquired for them
These telescopes will be installed in the 620-Mallorca, 946-Ametlla de Mar, and 165-Piera observatories.
We expect them to be operative at the end of 2002.

Appendix

In the following images, the different steps of such construction are shown. (Figures 8-9)

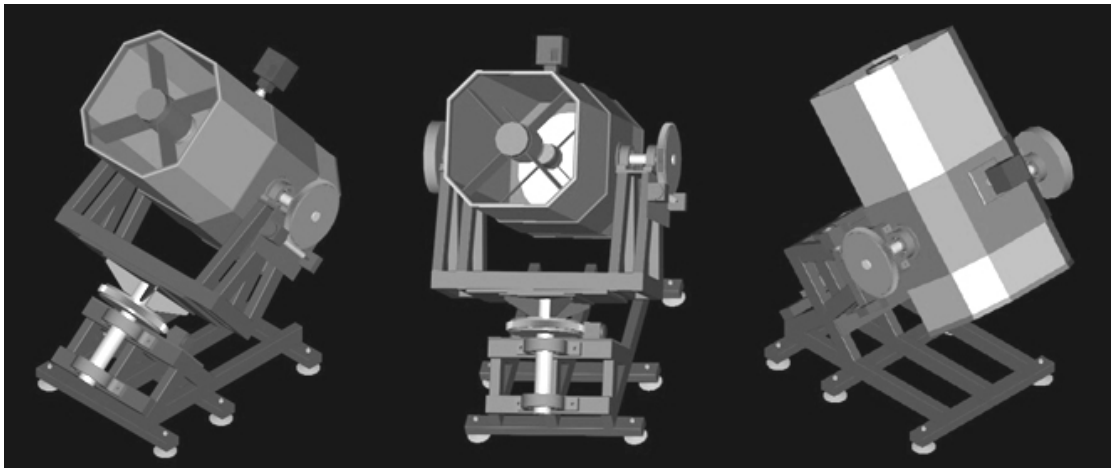

Figure 8: 3D-CAD drafts of the new 61-cm telescopes. A very simple and light design.

Figure 9: Bulding the new mountings: All tubular structure: simple, easy, light and low cost

References

1. Audine CCD cameras http://www.astrosurf.com/audine/index0.htm
2. Mel Bartels soft-electronic http://www.bbastrodesigns.com/cot/cot.html
3. Turbofilm http://www.kendrick-ai.com/baader_tech.html
4. Minor Planet Electronic Circular 2001-D33: 2001 DZ76 http://cfawww.harvard.edu/mpec/K01/K01D33.html
5. http://www.apm-us.com/professional/deltagraph.htm
6. Yu.A. Klevtsov, USSR Inventor's Certificate No. 605189, Byull. Izobret., No. 16 (1978).
7. Yu.A. Klevtsov, "Telescope of novel design," Zemlya Vselen., No. 5, 92 (1991).
8. Yu. A. Klevtsov, Description of the novel catadioptric telescope design by Klevtsov and it's comparison with other compound systems Opticheskij Zhurnal 67, 104-109 (February 2000) Design-Engineering Institute of Applied Microelectronics, Russian Academy of Sciences. Siberian Branch, Novosibirsk http://www.telescopes.ru/articles/article1.phtml
9. ASM Products, 754 Chemin de la Montagne, Mont St. Hilaire, Quebec, Canada, J3G 4S6. http://pages.infinit.net/asmprod/glass.html , Sieva@videotron.ca
10. http://www.oam.es/oam/unicorn/ninstrumental_en.htm
11. VALMECA SARL (Serge Deconihout), Lantelme 04700 PUIMICHEL (France).
12. Finger Lakes Cameras http://www.fli-cam.com/

ACCURACY OF THE WORLD ASTEROID CCD OBSERVATIONS OBTAINED BY AMATEUR AND PROFESSIONAL OBSERVATORIES IN 1998-2001 YRS"

O.P.Bykov, V.N.L'vov, I.S.Izmailov (1) and N.K.Sumzina (2)

(1) Pulkovo Astronomical Observatory, St.-Petersburg, Russia
(2) Institute of Applied Astronomy, St.-Petersburg, Russia

e-mail: oleg@OB3876.spb.edu

Positions of the Numbered Minor Planets (NMPs) which have been sent by observers to the Minor Planet Center in 1999 – 2001 yrs were automatically analysed by means of calculation of (O--C) values with the help of the EPOS Software Package created in Pulkovo Astronomical Observatory. More then 2 millions individual positions of the Numbered Minor Planets obtained by professional and amateur observatories were taken into consideration. Internet accessible version of Bowell's Orbital Catalogue containing more 40 thousand orbits of NMPs was used for calculations of their theoretical positions and comparisons with the observed ones. The values of "Mean error of a single observation" were calculated for the most of considered observatories during this period. These errors show the accuracy of observations and processing for each telescope in the assumption that the accuracy of the theory of motion of each Numbered Minor Planet is higher than that of its observations. When we analyse the (O--C) residuals for one night asteroid positions we obtaine an "internal" estimation of an accuracy of observations (marked by symbol "int." in the Table). If our (O--C) residuals are calculated for asteroid positions obtained during several close nights of obsevations we can derive an "external" estimation of their accuracy (marked by symbol "ext." in the Table). Of course, we must have a lot of observations of various NMPs in the set for each observatory under consideration. An example of our analysis is given in the Table which represents the European observatories observing the Near Earth Objects and - as "by product" - the Number Minor Planets also. Table contains the number of observed Minor Planets, the number of analysed positions, the instrumental and accuracy parameters and star catalog used for astrometriŁ reductions. These Tables were obtained by authors for each of 310 working observatories as professional, as amateurs. Astronomical community includes now a lot of amateur stations carring out positional CCD asteroid and comet observations with advanced technique and high quality. Their job may be used for a decision of several scientific problems.
Our investigation seems to be the first of that kind for the MPC data. It could be continued in future and be expanced to the Unnumbered Minor Planets.

CALCULATED with EPOS SOFTWARE (Pulkovo Observatory)

Accuracy of the World NMP observations in 1999, 2000 and 2001 yrs for European observatories

MPC code	Country Observatory	Diam. Focus (m)	FOV	CCD scale, Catal.	Number of pla- nets	posi- tions	Mean error of a single observation RA	DEC	
Year									
		"	"						
12	Belgium,	0.85	30 x 45'	0.9"	15	69	0.23	0.13	
	int								
999	Uccle	2.1		GSC					
12					16	111	0.38	0.28	int
2000					8	73	0.39	0.24	ext
12					43	282	0.40	0.29	int
2001					22	185	0.69	0.72	ext
46	Czech Rep.,	0.57	16 x 10'	1.8"	48	173	0.24	0.18	
	int								
1999	Klet	3.0		USNO	6	37	0.28	0.25	
ext									
46					35	142	0.22	0.19	int
2000					5	25	0.16	0.09	ext
46					62	252	0.19	0.34	int
2001					4	27	0.14	0.15	ext
49	Sweden,	1.0	35 x 35'	1.0"	49	172	0.24	0.19	
	int								
1999	Kvistaberg			USNO	15	78	0.32	0.20	
ext									
49					191	866	0.20	0.22	int
2000					53	368	0.47	0.29	ext
49					521	1817	0.29	0.31	int
2001					132	635	0.43	0.39	ext
71	Bulgaria,	0.50	17 x 20'	3.7"	6	28	0.36	0.50	
	int								

```
1999  National Obs.   1.7             GSC      3     19   0.39   0.42
ext
  71                                     12     78   0.74   0.74   int
2000                                      3     32   0.98   0.54   ext

 104  Italy, San      0.40  21 x 21'  2.5"    14     63   0.39   0.32
 int
1999  Marccello       2.0             GSC      6     42   1.73   0.82
ext
 104  Italy, San                              15     63   0.54   0.27
 int
2000  Marccello                                4     26   0.66   0.47
ext
 104  Italy, San                              78    296   0.50   0.36
 int
2001  Marccello                               22    118   0.39   0.50
ext

 106  Slovenia,       0.36  36 x 36'  2.0"   305   1003   0.48   0.45
 int
1999  Crni vrh        2.4            USNO     52    231   0.53   0.48
ext
 106                                     531   2118   0.40   0.35   int
2000                                     129    717   0.37   0.38   ext
 106                                     568   2087   0.41   0.34   int
2001                                     164    923   0.42   0.34   ext

 108  Italy,          0.30                    21     76   0.89   0.84
 int
1999  Montelupo       1.7             GSC      9     39   0.74   0.68
ext
 108                                       8     33   0.45   0.51   int
2000

 113  Germany,        0.50  13 x 10'    2"    12     47   0.17   0.24
 int
1999  Schonbrunn      2.3            USNO      5     25   0.47   0.52
ext
 113                                     20    136   0.53   0.28   int
2000                                      7     59   0.31   0.28   ext
 113                                     25    167   0.34   0.26   int
2001

 117  Germany,        0.20  15 x 11'  2.5"    26    322   1.37   0.85
 int
2000  Sendling        2.0             GSC     19    331   1.67   1.18
ext
 117                                     16    162   0.37   0.52   int
2001                                     14    161   0.92   1.36   ext

 118  Slovakia,       0.57  14 x 10'  0.6"    26    130   0.22   0.16
 int
1999  Modra           3.3            USNO     42    262   0.37   0.30
ext
 118                                     14     54   0.20   0.18   int
2000                                     20    122   0.31   0.28   ext
 118                                     20     77   0.18   0.21   int
2001                                     11     60   0.29   0.33   ext

 120  Croatia,        0.41  51 x 51'  2.8"   340   1399   0.51   0.35
 int
1999  Visnjan         1.8            USNO    314   2008   0.58   0.40
ext
 120                                     257   1133   0.64   0.40   int
2000                                     188   1306   0.62   0.39   ext
 120                                     83    297   0.80   0.45   int
2001                                     34    149   0.75   0.47   ext

 121  Ukraine,        0.70  10 x 8'     2"    11     86   0.46   0.57
 int
1999  Kharkov Univ.   2.8             GSC      4     69   0.61   0.72
ext
 121                                      9    106   0.36   0.39   int
2000                                      7    115   0.62   0.59   ext
 121                                      3     21   0.53   0.48   int
2001                                      3     23   0.38   0.41   ext

 122  France,         0.40                    4     19   0.40   0.43
 int
2001  Pises Obs.      1.9            USNO
```

127	Germany,	0.19	20 x 30'	2.4"	8	36	0.14	0.08	int
1999	Bornheim	0.8		GSC	12	61	0.37	0.48	ext
127					7	38	0.08	0.15	int
2000					6	34	0.37	0.41	ext
127					19	106	0.16	0.15	int
2001					21	147	0.40	0.35	ext
130	Italy,	0.4	15 x 10'	1.2"	10	40	0.35	0.27	int
1999	Lumezzane	2.6		USNO					
130					19	69	0.24	0.22	int
2000					4	13	0.46	0.33	ext
130					14	54	0.37	0.19	int
2001									
133	France,	0.20	33 x 22'	2.6"	16	51	0.27	0.27	int
1999	Les Tardieux	0.7		USNO					
133					5	15	0.42	0.44	int
2000									
133					11	36	0.47	0.30	int
2001									
138	France,	0.20	36 x 24'	2.8"	4	12	0.48	0.43	int
1999	Village-Neuf	0.8		GSC					
143	Switzerland,	0.40	20 x 20'	2.4"	12	57	0.49	0.30	int
1999	Gnosca	1.64		GSC	5	40	0.56	0.56	ext
143					14	100	0.37	0.19	int
2000					3	21	0.96	0.39	ext
143					19	184	0.36	0.32	int
2001					6	76	0.87	0.78	ext
145	Belgium,Gra-	0.20	24 x 18'	2.2"	13	54	0.64	0.40	int
1999	venwezel Obs.	0.7		ACT	5	25	0.48	0.54	ext
145					4	18	0.37	0.26	int
2000									
145					8	71	0.28	0.26	int
2001					2	15	0.15	0.34	ext
147	Italy, Osser.	0.40	16 x 16'	1.9"	5	36	0.52	0.54	int
1999	Astr. di Suno	1.6		USNO					
151	Switzerland,	0.25	16 x 24	0.9"	41	299	0.61	0.44	int
1999	Eschenberg	2.0		USNO	22	214	0.62	0.52	ext
151					39	361	0.34	0.51	int
2000					10	177	0.41	0.40	ext
151					43	560	0.31	0.35	int
2001					17	404	0.36	0.36	ext
152	Lithuania	0.35			2	6	0.37	0.49	int
2000	Moletai AO	1.2		GSC					
152					3	12	0.16	0.26	int
2001					2	11	0.54	0.26	ext
153	Germany,	0.25	16 x 12'	2.8"	4	23	0.18	0.14	int
1999	Stuttgart	1.8		GSC	4	26	0.21	0.34	ext
153					4	42	0.55	0.54	int
2001					4	44	0.58	0.63	ext
159	Italy,	0.51	13 x 10'	2.2"	14	66	0.76	0.40	int
1999	Monte Agliale	2.3		USNO					
161	Italy, Cerri-	0.13			3	11	0.70	0.43	ext

```
2000  ni Tololo       0.8             GSC

 162  Italy,          0.20  13 x 10'  1.1"     3      9   0.25   0.45
 int
2000  Potenza         1.3             GSC     14     50   0.68   0.80
ext
 162
2001                                     6     20   1.00   0.58   ext

 163  Luxembourg,     0.46  17 x 17'  2.0"     2      8   0.34   0.35
 ext
2000  Roeser Obs.     2.1             ACT
 163                                     5     25   0.20   0.15   int
2001

 164  France,         0.21                    28    170   0.62   0.67
 int
1999  St.Michel       0.8            USNO     16    137   0.64   0.72
ext
 164                                     8     24   0.53   0.41   int
2000

 165  Spain,          0.40                     2     10   0.32   0.15
 int
1999  Piera Obs.      0.8             GSC      4     19   0.54   0.26
ext
 165
2000                                     4     12   0.48   0.22   ext

 166  Czech Rep.,     0.3                      2      6   0.08   0.08
 int
1999  Upice           1.0             GSC      6     24   0.24   0.09
ext

 169  Italy,          0.25  29 x 19'  2.3"     4     23   0.31   0.31
 int
1999  Rosignano       1.6             GSC
 169                                     6     25   0.97   1.06   int
2000
 169                                     7     28   0.39   0.40   int
2001

 170  Spain, Obs.     0.28                     4     12   0.89   1.35
 int
2000  de Begues       1.8             GSC      9     36   0.83   1.23
ext
 170                                     6     28   0.74   0.43   int
2001                                     5     27   2.15   0.48   ext

 171  Malta,          0.25  23 x 18'  2.3"     3     12   0.64   0.31
 int
1999  Flarestar       0.66            ACT      3     15   0.90   0.80
ext
 171                                     3     11   0.17   0.07   int
2001

 172  Switzerland,    0.18  11 x 7'   0.9"     3     13   0.59   0.74
 int
1999  Onnens          2.2            USNO      3     24   0.58   0.64
ext

 176  Spain,          0.2                      8     26   0.49   0.27
 int
2001  Mallorca        0.7            USNO      3     13   0.66   0.38
ext

 179  Switzerland,    0.6                      8     47   0.16   0.08
 int
2000  Monte Generoso  4.9            USNO      7     44   0.28   0.23
ext

 184  France,         0.6   28 x 28'  0.8"     9     43   0.33   0.26
 int
2000  Valmeca Obs.    3.6            USNO      2     18   0.46   0.33
ext

 185  Switzerland,    0.61  23 x 15'  0.9"     5     16   0.32   0.30
 int
2000  Jur.-Vicques    2.1            USNO      2      7   0.52   0.29
ext
```

185					61	439	0.35	0.31	int
2001					25	291	0.40	0.34	ext
195	Germany,	0.20	17 x 13'	2.6"	3	15	0.44	0.22	
ext									
2000	Untermenz.Obs.	1.3		USNO					
195					8	51	0.43	0.26	int
2001					5	49	0.53	0.38	ext
196	Germany,	0.20			5	80	0.10	0.07	
int									
2000	Homburg-Erbach	1.3		GSC	6	104	0.25	0.16	
ext									
198	Germany,	0.24	12 x 9'	2.0	14	155	0.32	0.17	
int									
2001	Wildberg	2.4		USNO	11	156	0.36	0.21	
ext									
199	France	0.59	12 x 8'	1.0"	3	24	0.20	0.40	
int									
2000	Buthiers	2.0		USNO					
199					3	33	0.16	0.08	int
2001					2	30	0.14	0.12	ext
200	Belgium, Beer-	0.40	12 x 8'	2.0"					
2001	sel Hills Obs.	2.0		GSC	4	14	0.36	0.47	
ext									
201	Italy, Jonath-	0.30	12 x 12'	1.6"	21	75	0.49	0.45	
int									
2001	an B.Postel	3.0		USNO	8	41	0.42	0.35	
ext									
202	France,	0.25			5	22	0.24	0.20	
int									
2001	Tamaris Obs.	1.6		USNO					
203	Italy,	0.13	28 x 19'	2.2"	10	39	0.26	0.27	
int									
2001	GiaGa Obs.	0.8		GSC	26	131	0.37	0.28	
ext									
205	Italy, Casa-	0.25	14 x 11'	1.4"	14	73	0.73	0.44	
int									
2001	lecchio di Reno	1.7		GSC	3	27	0.56	0.45	
ext									
209	Italy, Asiago	0.67	50 x 50'	1.4"	372	1561	0.29	0.25	
int									
2001	Obs., Cima Ekar	2.15		GSC	148	896	0.29	0.23	
ext									
215	Germany,	var.			5	23	0.12	0.29	
int									
2001	Buchloe			USNO					
221	Germany, IAS	0.35			5	129	0.42	0.54	
int									
2001	Obs., Hakos			USNO	2	58	0.13	0.08	
ext									
222	France, Yerres	0.10			4	18	1.25	1.08	
int									
2001	-Canotiers	1.10		USNO					
224	France,	0.30	29 x 19'	1.1"	5	24	0.26	0.20	
int									
2001	Ridge Observ.	0.53		Tycho2	5	31	0.59	0.44	
ext									
233	Italy, Sauro	0.25	15 x 10'	2.3"	21	126	0.95	0.37	
int									
2001	Donati Ast.Obs.	1.6		USNO					
239	Germany,Michael	1.2	22 x 22'	1.0"					
2001	Adrian Observ.	4.1		USNO	3	14	0.47	0.42	
ext									
240	Germany, Her-	0.40	15 x 10'	2.4"	7	22	0.34	0.23	

```
 int
2001  renberg Sternw. 2.0            USNO      7     45   0.22   0.21
ext

 461  Hungary, JATE   0.60  19 x 28'  1.1"     3     12   0.12   0.12
 int
1999  Asteroid Surv.  1.8             USNO
 461                                    10     35   0.21   0.22   int
2000
 461                                    27    122   0.74   0.30   int
2001                                    7     48   0.81   0.29   ext

 468  Italy,          0.80                     2      6   0.97   0.78
 int
1999   Campo Catino   3.2              GSC

 469  Switzerland,    0.20                     2      6   0.46   0.10
 int
2000  Courroux        1.3              GSC
 469                                    9     46   0.79   0.51   int
2001

 491  Spain,          0.40                     4     19   0.56   0.86
 int
1999  Yebes           2.0              GSC      2     12   0.99   0.73
ext

 504  France,         0.40  12 x 8'   1.9"     4     15   0.43   0.49
 int
2000  Le Creusot      2.0              GSC
 504                                    9     39   0.77   0.67   int
2001                                    6     32   0.89   1.25   ext

 517  Switzerland,    0.20  46 x 46'  2.2"    17    113   0.22   0.13
 int
2000  Genewa          2.0            Tycho
 517                                   12     68   0.07   0.08   int
2001                                    4     29   0.07   0.07   ext

 540  Austria,        0.30  15 x 20'  3.5"     5     28   0.29   0.27
 int
1999  Linz            1.5              GSC      3     19   0.33   0.33
ext
 540                                    3     13   0.95   0.69   int
2000
 540                                    4     17   0.97   0.45   int
2001

 544  Germany,        0.15 & 0.75 tel.         4     21   0.35   0.35
 int
1999  W.Foer.Obs.     2.2             HIP.     2     11   0.40   0.58
ext
 544                                    6     33   0.57   0.46   int
2000
 544                                    6     49   0.56   0.65   int
2001

 552  Italy,          0.45  15 x 20'  3.4"     5     23   0.33   0.42
 int
1999  San Vittore     1.5              GSC      2     14   0.34   0.42
ext
 552                                    2      6   0.26   0.60   int
2000
 552                                    2      7   0.32   0.30   int
2001

 557  Czech Rep.,     0.65  13 x 20'  1.6"    35    165   0.18   0.20
 int
1999  Ondrejov        2.3             USNO     13    100   0.19   0.18
ext
 557                                   31    190   0.23   0.20   int
2000                                   13    136   0.25   0.26   ext
 557                                   82    511   0.28   0.17   int
2001                                   38    378   0.24   0.21   ext

 560  Italy, Madon-   0.40  10 x 17   2.6"     9     45   0.58   0.32
 int
1999  na di Dossob.   2.0              GSC      6     38   0.69   0.51
ext
 560                                    2     12   0.25   0.04   int
```

2000					2	12	0.34	0.30	ext
560					5	25	0.68	0.60	int
2001					3	18	0.71	0.62	ext
561	Hungary,	0.60	19 x 28'	1.1"	13	68	0.30	0.27	int
1999	Piszkesteto	1.8		USNO	3	22	0.47	0.40	ext
561					11	60	0.21	0.24	int
2000									
561					11	49	0.21	0.19	int
2001					4	26	0.17	0.19	ext
563	Austria,	0.25			2	13	1.14	0.65	int
1999	Seewalchen	1.6		USNO	2	13	1.11	0.69	ext
563					4	23	0.63	0.40	int
2000					2	15	0.74	0.52	ext
586	France,	1.05			19	93	0.11	0.07	int
2001	Pic du Midi	6.3		USNO	2	29	0.16	0.10	ext
587	Italy,	0.50	17 x 13'	3.0"	3	12	0.31	0.32	int
2000	Sormano	1.7		GSC					
587					4	12	0.36	0.46	int
2001									
596	Italy, Colle-	0.40	24 x 18'	4.0"	14	62	0.26	0.53	int
1999	verde di Guid.	1.3		GSC	3	28	0.33	0.43	ext
596					11	36	0.36	0.43	int
2001									
599	Italy, Campo	0.60			73	268	0.56	0.59	int
2001	Imperatore	1.8		GSC	14	87	0.61	0.25	ext
610	Italy,	0.25	26 x 17'	2"	413	2676	0.44	0.33	int
1999	Pianoro	1.0		GSC	65	878	0.49	0.47	ext
610					40	536	0.44	0.30	int
2000					15	375	0.61	0.50	ext
610					21	1620	0.18	0.19	int
2001					16	1566	0.41	0.43	ext
611	Germany,	0.45	8 x 12'	2"	8	38	0.28	0.31	int
1999	Heppenheim	2.0		USNO	3	25	0.56	0.44	ext
611					5	19	0.31	0.33	int
2000									
611					15	52	0.50	0.37	int
2001									
615	France,	0.62			12	36	0.48	0.52	int
2001	St. V'eran	1.9		GSC	5	23	0.88	0.75	ext
619	Spain,	0.51	14 x 11'	2.8"	16	71	0.26	0.32	int
1999	Sabadell	2.0		GSC	10	57	0.37	0.38	ext
620	Spain, Obs.	0.30	16 x 24'	1.9"	5	16	0.73	0.87	int
1999	de Mallorca	1.0		GSC					
620					3	17	1.12	0.66	int
2000					3	12	2.09	0.78	ext
621	Germany, Ber-	0.60	11 x 10'	1.2"	17	125	0.21	0.15	int
1999	gisch Gladbach	3.1		USNO	17	134	0.22	0.21	

ext									
621					22	152	0.14	0.12	int
2000					19	156	0.22	0.15	ext
621					73	480	0.24	0.20	int
2001					55	455	0.28	0.21	ext
627	France,	0.26	19 x 12'	3"	29	119	0.54	0.50	
int									
1999	Blauvac	1.2		GSC	8	57	0.57	0.52	
ext									
627					17	72	0.38	0.36	int
2000									
627					5	16	0.25	0.23	int
2001									
628	Germany,	0.20	18 x 12'	2.4"	19	108	0.31	0.30	
int									
1999	Mulheim-Ruhr	1.2		GSC	5	48	0.46	0.48	
ext									
628					21	126	0.31	0.25	int
2000					4	26	0.42	0.23	ext
628					38	176	0.36	0.42	int
2001					7	52	0.31	0.31	ext
629	Hungary,JATE	0.28	10 x 15'	2.5"	4	14	0.77	0.85	
int									
1999	Obs., Szeged			GSC					
629					6	24	0.58	0.44	int
2001									
631	Germany,	0.15	18 x 14'	2.9"	5	20	0.32	0.54	
ext									
2000	Hamburg	1.2		GSC					
635	France,	0.28	17 x 25'	2.0"	3	12	0.25	0.14	
int									
1999	Perpignan	0.9		USNO					
635					3	49	0.40	0.33	int
2000					2	45	0.52	0.46	ext
636	Germany,	0.32	15 x 15'	1.7"	20	87	0.74	0.42	
int									
1999	Essen	1.8		USNO	24	126	0.72	0.47	
ext									
636					3	13	0.75	0.52	int
2000									
636					9	28	0.32	0.27	int
2001									
638	Germany,	0.25	15 x 10'	1.2"	7	24	0.92	0.71	
int									
1999	Detmold	1.6		GSC	3	12	1.31	0.72	
ext									
639	Germany,	0.25	14 x 11'	1.7"	4	21	1.92	1.68	
int									
2000	Dresden	1.5		GSC	2	10	1.29	0.42	
ext									
639					2	7	0.13	0.44	int
2001									
910	France,	0.90			176	930	0.19	0.16	
int									
1999	Caussols-ODAS			GSC	88	669	0.33	0.23	
ext									
938	Portugal,	0.25	9 x 14'		31	317	0.38	0.36	
int									
2001	Linhaceira	1.7		USNO	28	309	0.62	0.65	
ext									
939	Spain,	0.20			20	168	0.65	0.70	
int									
2001	Obs. Rodeno	2.0		GSC	14	150	1.07	0.89	
ext									
940	England, Wa-	0.25			6	30	0.92	0.95	
int									
2000	terlooville	1.6		GSC	6	35	0.87	1.03	
ext									

942	England,	0.20			3	12	0.45	0.58	
ext									
2000	Grantham	1.0		GSC					
944	Spain, Obs.	0.30	14 x 10'	2.2"	4	50	0.39	0.40	
int									
2000	Geminis	1.7		USNO	4	50	0.38	0.38	
ext									
945	Spain,	0.36	11 x 7'	0.6"	6	22	0.18	0.26	
int									
2000	Monte Deva	2.3		USNO					
945					8	30	0.38	0.48	int
2001									
946	Spain, Amet-	0.30			3	11	0.39	0.29	
int									
2001	lla de Mar	1.5		USNO					
947	France, Sa-	0.60			3	9	0.37	0.17	
int									
1999	int-Sulpice	3.4		USNO	11	43	0.67	0.63	
ext									
947					3	56	0.12	0.17	int
2000									
947					6	48	0.26	0.35	int
2001				USNO	8	49	0.83	0.58	
ext									
951	England,	0.25	15 x 15'	2.0"					
1999	Highworth	1.6		ACT	10	45	0.20	0.18	
ext									
951					13	81	0.57	0.28	int
2000					14	95	1.03	0.35	ext
951					46	201	0.63	0.44	int
2001					24	140	0.64	0.50	ext
952	Spain,	0.25	13 x 9'	1.8"	14	46	0.35	0.24	
int									
1999	Marxuquera	1.6		GSC					
952					4	17	0.13	0.19	int
2000					2	12	0.42	0.41	ext
952					32	116	0.41	0.41	int
2001					2	10	0.65	0.42	ext
955	Portugal,	0.25	4 x 4'	1.5"	12	159	0.66	0.60	
int									
1999	Sassoeiros	2.0		GSC	7	118	0.56	0.74	
ext									
955					3	15	0.73	0.98	int
2000									
958	France,	0.20	39 x 26'	3"	12	67	0.61	0.65	
int									
2000	Obs. de Dax	0.6		USNO	13	92	0.72	0.65	
ext									

ASTROMETRY AND PHOTOMETRY OF ASTEROIDS AT THE ASTRONOMICAL OBSERVATORY MODRA - RESULTS AND EXPERIENCES

Štefan Gajdoš, Adrián Galád, Leonard Kornoš, Juraj Tóth, Jozef Világi, Pavol Zigo

Astronomical Institute, Faculty of Mathematics, Physics and Informatics, Comenius University, Bratislava, Slovak Republic, e-mail: ago@fmph.uniba.sk

A summary of astrometry and photometry of asteroids performed at the Astronomical Observatory (AO) in Modra is presented. Brief results of astrometry, including the NEO follow-up and confirmation program are highlighted. Recently, an effort towards minor planets photometry is expended, with the aim of NEO investigation. Some preliminary results based on our new photometry software are presented. We plan to renew the aperture photometry of comets, too.

1. Introduction

The Astronomical Observatory (AO) at Modra belongs to the Astronomical Institute of the Faculty of Mathematics, Physics and Informatics, Comenius University Bratislava (Slovakia) and research made there is aimed at the interplanetary matter and the Sun.

The observations of asteroids and comets are performed with a 0.6-m f/5.5 Carl-Zeiss reflector. CCD SBIG ST-8 camera (up to July 1998 it was ST-6 camera) in its primary focus makes is used for astrometry and photometry of solar system bodies. Details about the telescope and camera configuration are described in Kalmančok *et al.* (1994, 1995), and in Kornoš and Zigo (1997).

2. Astrometry

The first tests of astrometric observations were performed at the end of 1994. From 1995 regular observations under the *Minor Planet Center* observatory code **118** have been conducted. The data processing is made using Astrometrica software (author H. Raab) and USNO star catalogue (previously GSC). The primary observation program started with the main-belt asteroids including ITA (*I*nstitute of *T*heoretical *A*stronomy, Petersburg, Russia) asteroids. It continued with recovery of several one-opposition main-belt asteroids, follow-up of the Near Earth Asteroids (NEAs) from the *Minor Planet Circulars*, and from its electronic version - M.P.E.C., with monthly lists of observable objects (critical and unusual list, and list of comets). For instance, in 1997 MPC received the largest amount of astrometric observations of comets from Modra. Objects from the *Obsplanner Service* of MPC were also included to the observations soon to speed up numbering rates. A nice "by-product" of the program was discovery of several dozens of new asteroids belonging mostly to the main belt. The discovery rate increased up to 1998. The decrease, which followed, was caused not only by changing the camera (ST8 with larger field of view was less sensitive than ST6), but also by the fact that powerful survey telescope LINEAR began its operation. Currently 43 numbered asteroids were discovered at Modra. From 1998 astrometric observations have been concentrated on new NEAs confirmation and follow-up.

3. NEO observation program

Owing to a progress in the field of minor bodies astrometry in 1995-1998 we decided to apply for The Planetary Society NEO Grant, in the category of the Near Earth Objects (NEOs) follow-up and confirmation observations. To support enhancement of our NEO activity we were awarded by receiving *The Gene Shoemaker NEO Grant for 1998*. The objective of our official program is to support and extend the orbital and physical characteristics of the known NEO population and contribute to the international activity in the field. This include:

a) confirmation of newly-discovered unusual objects (mostly NEAs and comets) from the NEO Confirmation Page (NEOCP),
b) follow-up of NEAs with poorly determined orbits (to lower uncertainty parameter),
c) bright NEAs photometry (a standard program for data processing is under preparation).

4. Results

As a research-educational observatory, the AO in Modra implemented the aimed NEO follow-up program soon and can utilize the advantages of a “small observatory” equiped with a low-/medium-sized device. According to Marsden and Steel (1996),

each active observatory with modest-sized instrumentation is needed - "…such (NEO) astrometry being absolutely necessary over an extended period so that the orbital parameters may be well determined - a battery of follow-up instruments will be needed". As the powerful NEO surveys produce a lot of NEO discoveries, the role of follow-up programs is still increasing.

		Positions of minor planets				NEOs from
Year	Disc.	MB	NEO	Other	Total	total sum
1995	10	449	78	47	574	13.59%
1996	18	673	474	125	1272	37.26%
1997	36	1237	597	250	2084	28.65%
1998	48	1409	1077	197	2683	40.14%
1999	24	1279	1497	294	3070	48.76%
2000	6	729	1935	94	2758	70.16%

Table :. The positions statistics of minor planets from 1995 until 2000 at Modra.

Figure 1:

Figure 2:

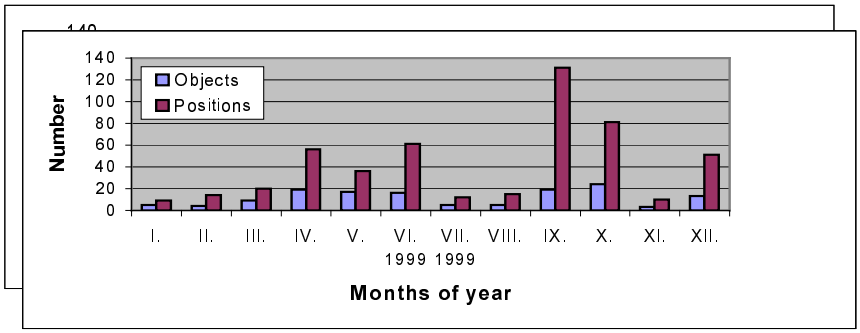

Figure 3:

Figures 1-3 show monthly rates of observations of NEOs from the NEO Confirmation Page of the IAU Minor Planet Center, as

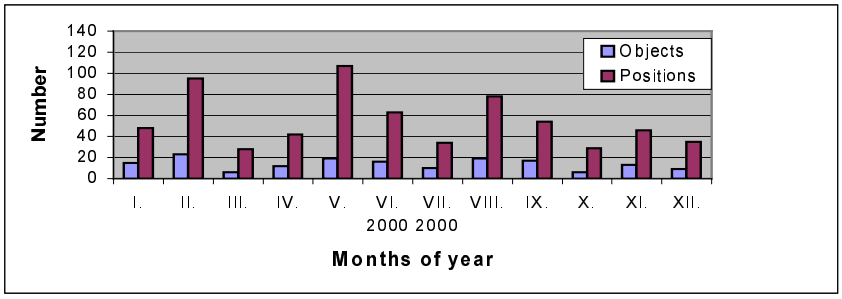

observed at the Astronomical Observatory in Modra. The rates refer to objects before preliminary designation, only. All the objects of cometary origin (after recognition) are excluded, as well as the main-belt asteroids. Designation *objects* denotes the number of individual objects. Legend *positions* denotes the number of precise positions of these objects. It covers repeated observations of the same object.

As a result of the NEO program, many minor planets precise positions were obtained, with a rising ratio of the NEOs among them (see Table 1). The number of observed objects from the NEOCP before they were given provisional designations, as well

as the number of reported precise positions in 1999, 2000 and 2001, are shown in Figs.1-3. The term „observed objects" denotes the number of different objects, not repeated observations of the same object that remained at NEOCP for several days. From 2000 the number of astrometric positions decreased due to photometric observations. The details of minor bodies astrometry at Modra can be found in Gajdoš *et al*. (1998), Galád *et al*. (2000) and Kornoš *et al*. (2001).

Along with the Modra NEO observations, several objects at NEOCP were identified with previously known asteroids. Three identifications were made after receiving provisional designation: 1998 RO1 = 1999 SN_5 (M.P.E.C. 1999-T10, MPC 36378), 1999 LS7 = 2000 LE2 (M.P.E.C. 2000-L20), 1990 TG1 = 2000 YP29 (M.P.E.C. 2001 A57).

5. Photometry

The CCD ST8 camera at Modra is equipped with standard BVRI photometric filters. Mainly R-filter is used for photometry of asteroids. Two bright main-belt objects with well known rotational and amplitude characteristics, namely (87) and (107) were chosen for tests. Their brightness allowed us to reach about 0.02 magnitude precision. The light curves were, however, relative, not absolute (e.g.using Landolt stars). Some tests were done even on a dimmer MB object (1807) with unknown period and several NEAs up to $V=15^m$. Their list is as follows: (5587), (31669), (33342), 1998 TU3, 2001 CB21, 2001 RB18, 2001 YB5, 2002 EQ9. All of them changed the star field quickly. Figure 4 contains light curves from two nights of (5587). Some of the other results will be available as soon as our Java software for data gathering and processing will be finnished. It uses differential aperture photometry to obtain the brightness of the object relative to a selected comparison star.

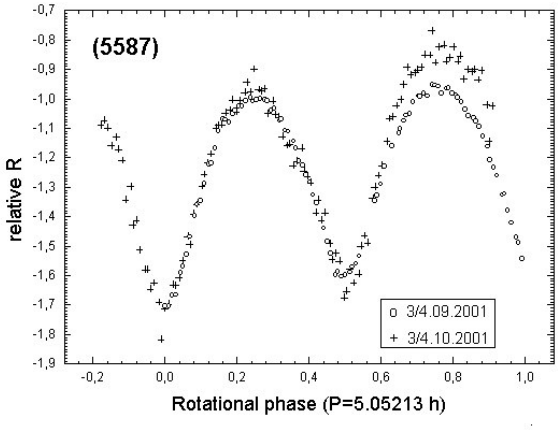

Figure 4: The light curves of (5587) observed at Modra.

Acknowledgements

This work was supported by the Slovak Scientific Grant Agency VEGA (No. 1/7157/20) and by The Planetary Society Gene Shoemaker NEO Grant.

References

Gajdoš, Š., Galád, A., Kornoš, L.: 1998, *Acta Astron. et Geoph.Universitatis Comenianae* **XX**, 18
Galád, A., Kornoš, L., Gajdoš, Š.: 2000, *Acta Astron. et Geoph.Universitatis Comenianae* **XXI-XXII**, 1
Kalmančok, D., Pittich, E., Zigo, P.: 1994, *Proceeding of the 3th International Workshop on Positional Astronomy and Celestial Mechanics*, (Garcia, A.L.eds.), 386
Kalmančok, D., Kornoš, L., Svoreň, J., Zigo, P.: 1995, *Meteor reports of the Slovak Astronomical Society* **16**, 57 (in Slovak)
Kornoš, L., Gajdoš, Š., Galád, A.: 2001, *Acta Astron. et Geoph.Universitatis Comenianae* **XXIII**, 31
Marsden, B.G., Steel, D.I.: 1996, *Earth, Moon and Planets* **74**, 85-92
Zigo, P., Kornoš, L.: 1997, *Acta Astron. et Geoph.Universitatis Comenianae* **XVIII**, 101

The Observing Campaign at the Davidschlag Observatory

Erich Meyer[a,b], Herbert Raab[a,c]

[a] Astronomical Society of Linz, Sternwarteweg 5, A-4020 Linz, Austria
[b] Erich Meyer, Ferd.-Markl-Str. 1/62, A-4040 Linz, Austria; erich.meyer@ooenet.at
[c] Herbert Raab, Schönbergstr. 23/21, A-4020 Linz, Austria; herbert.raab@utanet.at

The private Observatory in Davidschlag, near Linz, Austria (IAU Observatory Code 540), has been active in astrometry of minor planets and comets since 1979. After a short overview over the past work and the development of the observatory, we describe our current observing campaign, concentrating on late follow-up of NEOs. Follow-up observations of very fast moving asteroids, and recoveries of unusual objects in a second apparition are other activities. Two recent case studies (2002 AC_{29} and 2002 BG_{25}) as examples for our work, and the tables in the appenix list some objects observed during the recent years.

History of the observational program

The private observatory of Erich Meyer and Erwin Obermair is located in Davidschlag (48° 26' 33" N, 14° 16' 31" E, 815m above sea level), near Linz, Austria. Soon after construction works on the observatory were completed in 1978, we prepared for astrometric observations of minor planets. The first precise positions of a minor planet were accepted by the Minor Planet Center in 1979, and the observatory was rewarded with the observatory code 540.

Figure 1: The Davidschlag Observatory at dusk. The 0.6m f/3.3 reflector is visible inside the 4.5m plastic dome.

However, the optics of the 0.3m f/4.4 Newtonian badly suffered from coma, and getting precise positions was a difficult task. Therefore, the Newtonian reflector was replaced by a 0.3m f/5.2 Schmidt-Cassagrain telescope in 1982. In 1990, a computer with custom software replaced the programmable pocket calculator that was used for data reduction in astrometry. We concentrated on follow-up observations of new comets, and by the end of 1992, about 250 astrometric positions were obtained with a home-made measuring engine.

In early 1993, a CCD camera (SBIG ST-6) replaced photographic films. With the new detector, and the "Astrometrica" software that we have developed to carry out our astrometric campaign, we were able to participate in follow-up observations of NEOs. Within the first year, about 360 astrometric observations were obtained – more than the total observation in the 13 previous years using films!

Construction works on a new, larger telescope and a innovative fork mount began in early 1999. The mount, called "Austrian Mount" by its constructor R. Pressberger, features friction drives in both axes, which avoids any periodic error. Furthermore, there is neither a Right Ascension axis, nor a Declination axis, and no ball bearings are used. Instead, the fork rests on a steel ball, which is located inside the fork (Right Ascension), and two smaller steel balls hold the telescope in the fork (Declination). This design helps so save weight, and enabled to build a lightweight, compact and very stiff mount [1]. At the same time, the improved astrometric data reduction software "Astrometrica for Windows" was developed [2]. After only ten months, the 0.6m f/3.3 reflector and its innovative, computer controlled fork mount received "first light". Up to now, we still use the ST-6 CCD camera, which covers a field of 10' x 15', with the pixel size corresponding to 2.4" x 2.8".

Current Activity

The high rate of NEO discoveries in the past years require intensive follow-up observations [3] which are carried out by a small number of professional observatories as well as amateur astronomical sites. But while new discoveries, posted on the NEO Confirmation Page, receive high attention by the NEO community, later follow-up and arc-extending observations are frequently neglected. As a result, many NEOs are observed over a very short arc only, and the orbital elements are therefore highly uncertain, making a targeted recovery at a subsequent apparition very difficult, or even impossible. Currently (2002 May 15), there are 916 single-opposition NEOs in the MPCORB database [4]. Of these, 315 (34.4%) were observed over an

arc of 30 days or less, 242 (26.4%) were observed over 20 days or less, and for 183 NEOs (20.0%), the observed arc was 10 days or less. There are 116 objects (12.7%), which were observed for only five days or less.

Recognizing the need for late follow-up, our observing campaign concentrates on arc-extending observations of NEOs. A selection of objects successfully observed is listed in table 1 of the appendix. Many of these minor planets were are the range of 19^{mag} to 21^{mag}, with the faintest targets around 22^{mag}. Note that we were able to extend the observed arc significantly for all of the objects listed in that table. As the sky-plane uncertainty of a single-apparition asteroid at a later time is approximately inversely proportional to the square of the observed arc [5], increasing the arc by 100% (i.e., doubling the observed arc) reduces the uncertainty in the position of the minor planet at any later time approximately by a factor of four. With these arc extensions, the sky-plane uncertainty for further observations during the same apparition, at a future recovery opportunity, or for a precovery search in image archives, is therefore significantly reduced.

Other targets of high priority are NEOs at close approaches with high apparent motion. The computer control of the new 0.6m telescope is able to track moving objects, a feature that is unavailable at most amateur astronomical observatories. A selection of fast moving objects observed at our observatory is listed in table 2 of the appendix.

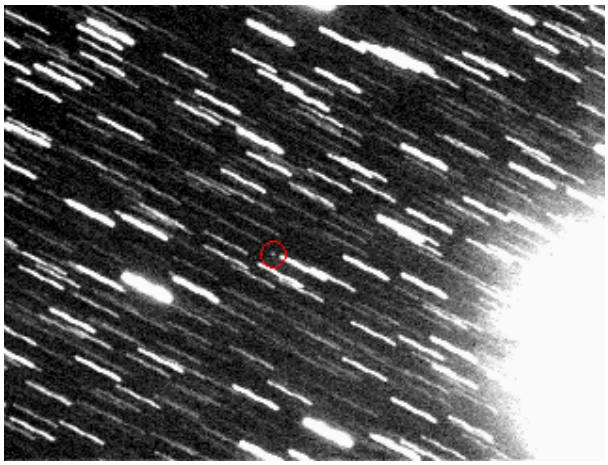

Figure 2: Asteroid 2000 UK_{11} in a 120 second CCD exposure, taken on 2000 November 2 with the 0.6m f/3.3 reflector at Davidschlag. This Aten asteroid, estimated to be less than 50m in size, passed only 0.01 A.U. from Earth at that time. Shining at 18.4mag, it moved about 0.6° per hour. A 5.7^{mag} star just enters the field at lower right.

Occasionally, we also performed recovery observations of faint NEOs. Successful recoveries of NEOs are listed in table 3 of the appendix.

Two recent case studies

The Apollo-type asteroid 2002 AC_{29} was discovered by the LINEAR project on January 13, 2002 at about 20.5^{mag}. The discovery was published on January 15 [4], with the orbital elements calculated from 20 observations over an arc of three days. Only three additional positions from January 21 from a single observatory were reported afterwards, extending the arc to eight days. We observed 2002 AC_{29} on February 2.7 UT at 20.5^{mag}, extending the arc by further 12 days. The formal sky-plane uncertainty at that time was only about ±30" (3σ), but our observations showed that the object was already 4' off track. About 24 hours later, we confirmed our previous positions with additional observations. With the additional positions, the orbit was significantly improved (e.g., the semimajor axis changed from 1.72 AU to 1.64 AU). Later, the January 21 positions were revised by the observer, now also fitting the improved orbit.

The PHA 2002 BG_{25} was discovered by the LINEAR project on January 25, 2002 at about 19.5^{mag}. The discovery was published on January 28, with the orbital elements calculated from 14 observations over an arc of slightly more than one day [5]. The ephemeris showed that a close approach to 0.05 AU would occur on February 6. Nevertheless, no additional observations were reported until February 1, when the sky plane uncertainty had already grown to ±3° (3σ). We were able to recover 2002 BG_{25} on February 1.9 UT about 35' from the ephemeris position. Subsequently, the improved ephemeris prompted a large number of additional observations by many amateur and professional astronomers, and finally even Radar observations at Arecibo on February 5.

References

1. Meyer, E.; Obermair, E.: Neues 60cm Teleskop der Sternwarte Davidschlag, Der Sternenbote, **42**, 222-227 (1999)

2. Raab, H.: Astrometrica Software http://www.astropmetrica.at

3. Tichá, J.; Tichý, M., Moravec, Z.: The importance of follow-up observations for newly discovered NEOs, Planetary and Space Science, **48**, No. 10, 955-959 (2000)

4. Minor Planet Center: MPCORB Database ftp://cfa-ftp.harvard.edu/pub/MPCORB

5. Muinonen, K; Bowell, E.; Wassermann, L.H.: Orbital uncertainties of single-apparation asteroids, Planetary and Space Science, **42**, No. 4, 307-313 (1994)

6. Spahr, T.: Minor Planet Electronic Circular MPEC 2002-A98 (2002 Jan. 15)

7. Spahr, T.: Minor Planet Electronic Circular MPEC 2002-B41 (2002 Jan. 28)

Appendix

Arc-Extensions of NEOs					
Designation	**Type**	**Magnitude at Observation**	**Observed arc, before Obs. (Days)**	**Observed arc, after Obs. (Days)**	**Extensin of arc (Percent)**
2000 RV_{37}	PHA	20.6	17	51	200
2000 SB_{25}	Amor	20.3	13	32	146
2000 SF_{8}	Amor	19.3	8	33	313
2000 SG_{8}	Apollo	19.5	15	47	213
2000 SJ_{8}	Amor	19.5	12	32	167
2000 SO_{10}	Apollo	20.9	3	27	800
2000 SR_{43}	Amor	19.5	2	26	1200
2000 SR_{43}	Amor	20.4	26	79	204
2000 TK_{1}	Apollo	18.5	3	28	833
2000 WQ_{19}	Apollo	21.0	22	55	150
2000 WL_{63}	Amor	18.9	28	149	432
2000 WM_{107}	Amor	19.4	6	27	450
2000 WO_{148}	PHA	19.7	8	29	263
2000 WO_{148}	PHA	19.2	30	74	147
2000 YM_{29}	Amor	19.2	19	51	168
2000 YN_{29}	PHA	20.0	4	12	200
2001 AO_{2}	Amor	19.2	46	76	65
2001 AO_{2}	Amor	19.1	78	116	49
2001 AU_{47}	Apollo	20.2	3	27	800
2001 DF_{47}	PHA	20.5	11	28	155
2001 EB_{16}	Amor	19.2	6	27	350
2001 FF_{7}	Amor	19.7	69	116	68
2001 FO_{32}	PHA	16.1	5	9	80
2001 FR_{85}	Aten	18.4	3	6	100
2001 FR_{128}	Apollo	19.7	2	26	1200
2001 HB	PHA	19.0	1	9	800
2001 HW_{7}	Amor	20.0	13	36	177
2001 HZ_{7}	PHA	18.4	6	12	100
2001 HZ_{7}	PHA	19.0	11	21	91
2001 JV_{2}	Apollo	20.5	13	40	208
2001 NZ_{1}	Amor	20.0	33	71	115
2001 OE_{3}	Amor	19.7	56	99	77
2001 PK_{9}	Amor	19.2	9	15	67
2001 PM_{9}	PHA	19.1	9	15	67
2001 QB_{34}	Amor	19.2	60	94	57
2001 RE_{8}	Amor	20.5	48	80	67
2001 RZ_{11}	Amor	18.5	36	69	92
2001 RY_{47}	Aten	17.6	18	31	72
2001 SA_{170}	Amor	17.8	6	14	133
2001 SA_{170}	Amor	18.5	16	24	50
2001 SJ_{262}	Amor	18.2	8	12	50
2001 SJ_{262}	Amor	17.5	19	24	26
2001 SJ_{267}	Amor	18.2	2	6	200
2001 SX_{269}	Amor	19.7	2	17	750
2001 SE_{286}	Amor	17.8	2	10	400
2001 SG_{286}	PHA	20.2	18	44	144
2001 SN_{289}	PHA	20.5	11	48	336
2001 TY_{44}	Amor	17.7	12	20	67
2001 TP_{103}	Amor	19.3	12	33	175
2001 UP_{16}	Amor	19.1	5	20	300
2001 UV_{16}	Amor	20.3	42	75	79
2001 UW_{16}	Amor	18.5	2	11	450
2001 UG_{18}	Amor	18.5	1	9	800
2001 WR_{5}	Amor	18.0	3	12	300

2001 XP	Apollo	19.5	1	4	300
(Continued from previous page)					

2001 XY_{10}	Aten	20.5	46	85	85
2001 XO_{88}	Apollo	20.3	5	21	320
2002 AO_{7}	Amor	20.0	10	28	180
2002 AC_{29}	PHA	20.5	8	21	163
2002 BG_{25}	PHA	17.0	1	7	600
2002 CE	PHA	17.1	4	14	250
2002 CP_{4}	Amor	19.7	5	11	120
2002 CU_{46}	Apollo	19.3	10	20	100
2002 CX_{58}	PHA	18.2	9	19	111
2002 CV_{46}	Amor	18.8	2	7	250
2002 DO_{3}	PHA	18.5	2	10	400
2002 EN_{7}	Apollo	19.7	2	7	250
2002 EN_{7}	Apollo	20.0	7	18	157
2002 EZ_{11}	PHA	20.3	8	15	88
2002 FB_{3}	PHA	18.3	3	11	267
2002 FQ_{4}	Amor	19.5	2	16	700
2002 FQ_{5}	PHA	18.3	2	12	500
2002 FU_{5}	PHA	17.9	3	9	200
2002 HE_{8}	Amor	19.4	11	17	55
2002 JC	Aten	18.8	3	7	133
2002 JD_{9}	Apollo	18.2	1	2	100
2002 JE_{9}	PHA	20.0	2	4	100

Table 1: A selection of arc-extending observations performed at 540 Linz. Besides some information on the objects observed, the table lists the arc covered by the observations published before our observations were made, the extended arc after our observations, and the extension of the arc in percent.

Fast moving NEOs				
Designation	Type	**Magnitude at Observation**	**Apparent Motion at Observation (“/min)**	**Distance from Earth (AU)**
2000 JF_{5}	PHA	18.0	16	0.061
2000 PH_{5}	Aten	15.2	32	0.015
2000 SM_{10}	Apollo	17.8	110	0.011
2000 UK_{11}	Aten	18.4	36	0.012
2001 EC_{16}	Apollo	15.1	52	0.014
2001 FO_{32}	PHA	16.1	13	0.17
2001 FR_{85}	Aten	17.7	13	0.014
2001 GQ_{2}	PHA	15.1	70	0.021
2001 KB_{67}	PHA	16.1	14	0.066
2001 OT	Aten	17.1	14	0.064
2001 UP	Aten	15.7	95	0.007
2001 UC_{5}	Amor	17.3	17	0.071
2001 UF_{5}	Apollo	16.5	25	0.033
2001 UU_{16}	Amor	18.1	25	0.031
2001 VB	PHA	17.9	15	0.17
2002 BG_{25}	PHA	15.5	36	0.056

Table 2: A selection of fast-moving NEOS observed at 540 Linz. Besides some information on the objects observed, the table lists the apparent motion and the distance of the object at the time of the observation.

Recoveries of NEOs		
Designation	Type	**Magnitude at Observation**
1994 LW	Amor	20.6
1998 SU_{27}	Apollo	20.0
1998 UL_1	Amor	20.5
1999 CT_3	Amor	18.5
1999 TL_{12}	Apollo	19.6
1999 YA	Apollo	19.5
2000 GX_{127}	Apollo	19.6
2000 JH_5	Apollo	19.6

Table 3: Successful recoveries of NEOs performed at 540 Linz.

Johann Palisa, the most successful visual discoverer of asteroids

Herbert Raab[a,b]

[a] Astronomical Society of Linz, Sternwarteweg 5, A-4020 Linz, Austria
[b] Herbert Raab, Schönbergstr. 23/21, A-4020 Linz, Austria; herbert.raab@utanet.at

Part of the Programme of MACE 2002 was a trip to the remnants of the old Pola observatory. Among minor planet observers, this observatory is mostly known for the work of Johann Palisa. This paper provides a short biography of Johann Palisa, as well as some information about his discoveries.
Palisa was director of the Pola observatory from 1872 until 1880. He discovered 28 minor planets and one comet during that time. In 1880, he took a position at the new Vienna observatory. Here, he discovered further 94 minor planets, all by visual observations. His most famous discovery is probably the Amor-type asteroid (719) Albert. Today, Palisa remains the most successful visual discoverer of asteroids.

A short biography of Johann Palisa

Johann Palisa was born on December 6, 1848 in Troppau, Silesia (now Czech Republic) [1,2]. From 1866 to 1870 he studied mathematics and astronomy at the University of Vienna, but did not graduate until 1884. Already in 1870, he became assistant at the University observatory in Vienna, and in the following year, he took a position at the observatory in Geneva.

Only 24 years old, Palisa became director of the Austrian Naval Observatory in Pola in 1872. Pola (now Pula) was harbor of the Austrian Navy from 1850 until the empire of Austria-Hungary collapsed at the end of World War I.

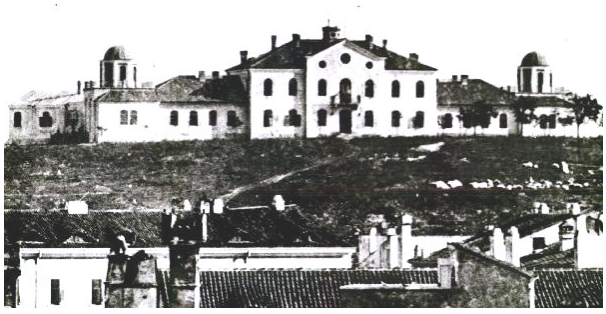

Figure 1: The Pola Observatory in the 19th century.

Palisa discovered his first asteroid, (136) Austria [3], at Pola on 1874 March 18, using a 6" refractor. He subsequently discovered further 27 minor planets and one comet at Pola with this small instrument.

When the new Vienna observatory was inaugurated in 1880 by emperor Franz Joseph I, he was offered a position as "Adjunkt", comparable to a modern night assistant. Palisa gave up his position as director of the Naval Observatory and accepted the subordinate employment, only because he was able to routinely use the large 27" refractor in Vienna, at that time the largest telescope in the world. To handle this telescope of 10.54m focal length, and the dome, 14m in diameter, two assistants were usually provided to aid the observer. The story goes that Palisa used to send his assistants to bed at midnight, but continued to observe

until the break of dawn, handling the instrument all alone. Palisa discovered further 94 asteroids at Vienna, all by visual observations, using the 27" and the 12" refractor. In addition, Palisa discovered eight objects that were included by Dreyer in the NGC catalogue, as well as four nebulae listed in the IC. [4]

Figure 2: Portrait of Johann Palisa**.**

In 1883, he joined the expedition of the French academy to observe the total solar eclipse on May 6 of that year [5]. During the eclipse, he searched for the proposed planet Vulcan, which was supposed to circle the sun within the orbit of Mercury. In addition to observing the eclipse, Palisa collected insects for the Natural History Museum in Vienna. When he returned, he named minor planet (235) Carolina after the atoll of the Line islands, 450 miles northwest of Tahiti, where this expedition set up the instruments to observe the eclipse.

In 1885, Palisa offered to sell the naming right for minor planet (244) for L50 to raise funds for his expedition to the total solar eclipse of August 29, 1886. Apparently, this was not successful, as Palisa did not travel to the eclipse, and the minor planet was later named after the Indian goddess Sita.

Figure 3: View of the 27" Grubb Refractor at Vienna.
Image courtesy Vienna University Observatory.

At that time, there were no star charts available to support his search for new minor planets, so Palisa used to draw the maps on his own. At the end of the 19th century, Johann Palisa and Max Wolf in Heidelberg joined forces and worked on the Palisa-Wolf-Sternkarten. This work, which is the first photographic star atlas, was published between 1900 and 1908. Two years later, Palisa published his Sternenlexikon, a star catalogue covering the sky between declinations -1° and +19°. In 1908, Palisa became vice director of the Vienna observatory.

He retired in 1919, with the right to continue his observations at the observatory. For his work, Palisa was awarded with the Great Price of the Paris Academy. He was also honoured by minor planet (914) Palisana, discovered and named by Max Wolf, and by a lunar crater 33km in diameter. Palisa died in Vienna on May 2, 1925.
With 122 minor planets, Palisa is still the most successful Austrian discoverer of asteroids, as well as the most successful visual discoverer in the history of minor planet research.

The discoveries of Johann Palisa

Palisa's discoveries remain targets of modern research: Minor planet (153) Hilda is the prototype of the Hilda asteroids, orbiting the sun in 3:2 resonance with Jupiter. Asteroid (216) Kleopatra hit the headlines in 2000, when observations with the Arecibo Planetary Radar fount it to have an unusual dog-bone shape. In 1993, the Galileo spacecraft flew by (243) Ida, the NEAR spacecraft passed by (253) Mathile in 1997, and asteroid (140) Siwa will be fly-by target of ESAs Rosetta mission in 2008. Palisa's most famous discovery is probably asteroid (719) Albert. Being only the second NEA found, it was lost only a few days after its discovery. The Amor-type asteroid was finally recovered in 2000 by the Spacewatch project.

Appendix

Table 1: lists all solar system objects discovered by Palisa, in the order of the date of discovery.

Object Designation	Date of Discovery	Place of Discovery
(136) Austria	1874 03 18	Pola
(137) Meliboea	1874 04 21	Pola
(140) Siwa	1874 10 13	Pola
(142) Polana	1875 01 28	Pola
(143) Adria	1875 02 23	Pola
(151) Abundantia	1875 11 01	Pola
(153) Hilda	1875 11 02	Pola
(155) Scylla	1875 11 08	Pola
(156) Xanthippe	1875 11 22	Pola
(178) Belisana	1877 11 06	Pola
(182) Elsa	1878 02 07	Pola
(183) Istria	1878 02 08	Pola
(184) Dejopeja	1878 02 28	Pola
(192) Nausikaa	1879 02 17	Pola
(195) Eurykleia	1879 04 19	Pola
(197) Arete	1879 05 21	Pola
(201) Penelope	1879 08 07	Pola
C/1879 Q1 (Palisa)	1879 08 21	Pola
(204) Kallisto	1879 10 08	Pola
(205) Martha	1879 10 13	Pola
(207) Hedda	1879 10 17	Pola
(208) Lacrimosa	1879 10 21	Pola
(210) Isabella	1879 11 12	Pola
(211) Isolda	1879 12 10	Pola
(212) Medea	1880 02 06	Pola
(214) Aschera	1880 02 29	Pola
(216) Kleopatra	1880 04 10	Pola
(218) Bianca	1880 09 04	Pola
(219) Thusnelda	1880 09 30	Pola
(220) Stephania	1881 05 19	Vienna
(221) Eos	1882 01 18	Vienna
(222) Lucia	1882 02 09	Vienna
(223) Rosa	1882 03 09	Vienna
(224) Oceana	1882 03 30	Vienna
(225) Henrietta	1882 04 19	Vienna
(226) Weringia	1882 07 19	Vienna
(228) Agathe	1882 08 19	Vienna
(229) Adelinda	1882 08 22	Vienna
(231) Vindobona	1882 09 10	Vienna
(232) Russia	1883 01 31	Vienna

(235) Carolina	1883 11 28	Vienna
(236) Honoria	1884 04 26	Vienna
(237) Coelestina	1884 06 27	Vienna
(239) Adrastea	1884 08 18	Vienna
(242) Kriemhild	1884 09 22	Vienna
(243) Ida	1884 09 29	Vienna
(244) Sita	1884 10 14	Vienna
(248) Lameia	1885 06 05	Vienna
(250) Bettina	1885 09 03	Vienna
(251) Sophia	1885 10 04	Vienna
(253) Mathilde	1885 11 12	Vienna
(254) Augusta	1886 03 31	Vienna
(255) Oppavia	1886 03 31	Vienna
(256) Walpurga	1886 04 03	Vienna
(257) Silesia	1886 04 05	Vienna
(260) Huberta	1886 10 03	Vienna
(262) Valda	1886 11 03	Vienna
(263) Dresda	1886 11 03	Vienna
(265) Anna	1887 02 25	Vienna
(266) Aline	1887 05 17	Vienna
(269) Justitia	1887 09 21	Vienna
(273) Atropos	1888 03 08	Vienna
(274) Philagoria	1888 04 03	Vienna
(275) Sapientia	1888 04 15	Vienna
(276) Adelheid	1888 04 17	Vienna
(278) Paulina	1888 05 16	Vienna
(279) Thule	1888 10 25	Vienna
(280) Philia	1888 10 29	Vienna
(281) Lucretia	1888 10 31	Vienna
(286) Iclea	1889 08 03	Vienna
(290) Bruna	1890 03 20	Vienna
(291) Alice	1890 04 25	Vienna
(292) Ludovica	1890 04 25	Vienna
(295) Theresia	1890 08 17	Vienna
(299) Thora	1890 10 06	Vienna
(301) Bavaria	1890 11 16	Vienna
(304) Olga	1891 02 14	Vienna
(309) Fraternitas	1891 04 06	Vienna
(313) Chaldaea	1891 08 30	Vienna
(315) Constantia	1891 09 04	Vienna
(320) Katharina	1891 10 11	Vienna
(321) Florentina	1891 10 15	Vienna
(324) Bamberga	1892 02 25	Vienna
(326) Tamara	1892 03 19	Vienna
(569) Misa	1905 07 27	Vienna
(583) Klotilde	1905 12 31	Vienna
(652) Jubilatrix	1907 11 04	Vienna
(671) Carnegia	1908 09 21	Vienna

(14309) Defoy	1908 09 22	Vienna
(687) Tinette	1909 08 16	Vienna
(688) Melanie	1909 08 25	Vienna
(689) Zita	1909 09 12	Vienna
(703) Noemi	1910 10 03	Vienna
(710) Gertrud	1911 02 28	Vienna
(711) Marmulla	1911 03 01	Vienna
(716) Berkeley	1911 07 30	Vienna
(718) Erida	1911 09 29	Vienna
(719) Albert	1911 10 03	Vienna
(722) Frieda	1911 10 18	Vienna
(723) Hammonia	1911 10 21	Vienna
(724) Hapag	1911 10 21	Vienna
(725) Amanda	1911 10 21	Vienna
(728) Leonisis	1912 02 16	Vienna
(730) Athanasia	1912 04 10	Vienna
(734) Benda	1912 10 11	Vienna
(750) Oskar	1913 04 28	Vienna
(782) Montefiore	1914 03 18	Vienna
(783) Nora	1914 03 18	Vienna
(794) Irenaea	1914 08 27	Vienna
(795) Fini	1914 09 26	Vienna
(803) Picka	1915 03 21	Vienna
(827) Wolfiana	1916 08 29	Vienna
(828) Lindemannia	1916 08 29	Vienna
(867) Kovacia	1917 02 25	Vienna
(876) Scott	1917 06 20	Vienna
(902) Probitas	1918 09 03	Vienna
(903) Nealley	1918 09 13	Vienna
(932) Hooveria	1920 03 23	Vienna
(941) Murray	1920 10 10	Vienna
(964) Subamara	1921 10 27	Vienna
(975) Perseveranti	1922 03 27	Vienna
(996) Hilaritas	1923 03 21	Vienna
(1073) Gellivara	1923 09 14	Vienna

Table 1: This table lists all solar system objects discovered by Johann Palisa. [6,7]

References

1. Plank, S.: Seinerzeit-Spezial: Johann Palisa
http://www.astro.univie.ac.at/~wuchterl/Kuffner/ 2001/seinerzeit_spezial.html

2. Albrecht, R.; Maitzen, H.-M.; Schnell, A.: Early asteroid research in Austria, Planetary and Space Science, 49, 777-779 (2001)

3. Schnell, A.; Haupt, H.: Kleine Planeten, deren Namen einen Österreichbezug aufweisen, Sitzungeberichte der Österr. Akademie der Wissenschaften, Abt. II, 204, 185-257 (1995)

4. Steinicke, W.: List of NGC/IC observers
http://www.ngcic.com/observers/persons.htm

5. Palisa, J.: Bericht über die während der totalen Sonnenfinsternis vom 6. Mai 1883 erhaltenen Beobachtungen, Sitzungsbericht der kaiserlichen Akademie der Wissenschaften, 2. Abt., 88, 1883

6. Minor Planet Center: Discovery Circumstances of Numbered Minor Planet
http://cfa-www.harvard.edu/iau/lists/NumberedMPs.html

7. Meyer, M.: Catalogue of Comet Discoveries
http://www.comethunter.de/cocd2002.html

Observations of Comets: Tools and Perspectives

Gyula Szabó
University of Szeged, Dept. of Experimental Physics
H6720 Szeged, Dóm tér 9, Hungary, szgy@mcse.hu

1. Introduction

The well-equipped astronomer, having made comet observations of excellent quality, wish to extract the most characteristic and best measurable parameters. The aim is to have long-term observations of comparable parameters that well show the evolution of comets: the coma and tail, dust and gas production during the visibility. As we wish to characterize the comet itself, easily measurable parameters are required that are independent either on the equipments used or on the geometrical configuration of the Sun-Earth-Comet system during the observations.

We review size and brightness characterizations of the coma and tail by surface photometry, while the so-called Afrho quantity will help us measure the dust production independently on the observation circumstances. The filtering and calibration problems do not seem to supply the amateur narowband photometry, however, we shortly review this technique as well. Specially processed images emphasise several local details in the coma, and as they result representative images, this tool can be very promising in future amateur astronomy, too. Finally, we show the necessity of an archivation system that will maintain the images, calibrations and reductions so that the valuable observations will not to be lost for the detailed examinations.

2. Sizes, brightnesses and profiles

Both the coma and the tail of a comet diminishes to the edges, that is why the size and brightness determinations are ambiguous. The visual observer see brighter and bigger comets with smaller telescopes, so several empirical re-calibrations are required while merging the data of different observers. This is while visual observers detect the coma and the tail extending a point where the characteristic surface brightness diminishes under their limit surface-brightness magnitude. Surfaces fainter than this cannot be distinguished from the sky background. This limit magnitude, certainly, highly depends on the observation circumstances, the sky and the telescope, so different observers see quite different parts of the same object.

With help of digital image processing, unambiguous characterization of the coma size is straightforward: one selects a surface brightness that is well measurable on the image but is faint enough to show the faint halo of the coma. As the custom, 20, 22 and 25 magnitudes per square arcseconds are used, with other values also acceptable. The observed parameter is the extension of the comet surface where the surface brightness is over the selected limit, this is further referred as, for example, 22-magnitude size. In practice, the brightness of the comet is measured by increasing seria of circular apertures, so the fluxes of the individual shells can be measured. The flux of the quite extended surfaces are divided by their size, resulting the flux of the unit area (square arcsecond). The average surface brightness is calculated with help of the comparison star.

We have to note that surface brightness, referring to a really extended surface, is in practice measured in considerably large apertures, so the quantity can be much better measured as stars. For example, if we have and image where stars of 22 magnitudes are measurable with less than some tenth of magnitude error, we may hope that even the 25-magnitude size is to be measured quite well. However, the sky surface brightness is rarely fainter then 21 magnitudes in the optical, so we often have to measure 1 or 4 magnitudes below the sky background. That is why we emphasise that these measurements require quite precise calibrations.

For a more detailed analysis, one can extract cross sections from the images. For this, a promising tool is to use a code for spectral reduction. The window is traced along the comet, e.g. on the radial line that directs to the Sun. Flux needs converting into magnitudes as described above. On this diagrams, one can see not only the extension of the comet, but a section of its surface brightness map, let us say its brightness profile, which can include some useful characteristic details, e.g. solar jets that cannot be recognized by the determined size itself. If we measure the dust and gas components separately, e.g. with narowband filters or at last using Johnson I and V, the profile of the two components can be compared. Dust components will often decrease faster toward the Sun: the effect of the radiation pressure and the solar wind is responsible for this phenomenon.

Total brightness of the coma is properly measured within the specified coma radius, e.g. the 25-magnitude size. Though it is simple to be measured, this brightness depends on the distances in the Earth-Sun-comet geometry (via the visible brightness of the Sun at the position of the comet), so it does not characterize the comet the best.

3. Coma morphology

Surface photometry of images can address coma morphology (such as radial coma profiles and non-radial features, also called as coma profiles and azimuthally renormalized images, see e.g. Lederer et al 1997, Larson & Slaughter 1991), and also may yield estimated nuclear radii (e.g. Luu & Jewitt 1992, Lamy & Tóth 1995, Lowry et al. 1999). An appropriate selection of medium- and narrow-band filters centered on different wavelengths can separate the dust continuum from emission by gas. Differences in gas and dust components reveal the effect of radiation pressure on different types of particles (a good example of combined quantitative coma analysis can be found, e.g. in Schulz et al. 1993).

The coma is built up by the gas just blowing out of the nucleus. Having considered the ideal coma, namely a spherically symmetric and homogeneous flow with seeing effects negligated, simply proves that the slope of the logarithmic coma profil (d [log surface brightness on R radius] / d [log R], or d log B(R) / d log R) is exactly -1. Or, if you express the profil as the differenciate of surface brightness in magnitudes to the natural logarithm of the sampling radius, the slope is -1.08.

In practice, comets have narrower profiles than the ideal case of -1, usually between -1 and -2. That is because the solar wind and radiation pressure push the matter toward the antisolar direction and make the coma more compact.

As it has been seen, though surface brightness can be simply measured in the coma, this value depends on the radius that we used for the determination. Finally, we are to find a new parameter, the Afrho (Section 3.1.), which will be suitable for later examinations. The coma profile and the logarithmic profile of the Afrho are simply connected, as the Afrho-profile is exactly 0 for the ideal coma, and their difference is exactly 1 for every kind of comae.

If one has determined the coma profile, the modeled coma can be built up. Honestly, that will go on an inverse problem as the observed coma is somewhat more diffuse as the real one because of the smoothing effect of seeing and the motion of the comet during the exposure. So one has to calculate cylindrically symmetric comae and as the second step, blur and trace them by the seeing (deduced from stellar profiles) and the motion (calculated from the apparent velocity and the exposure time). When the resulted profile fits the observed outer coma, the model coma is accepted.

This coma usually does not fit the inner coma, but underestimates the flux. That is caused by the solid nucleus itself. So, the comparison of the coma model and the observations will result the magnitude of the nucleus as the superfluous light in the inner coma. In practice, the direct way is preferred: the model coma contains a nucleus with its brightness as a free parameter. The model nucleus is suggested to be a blurred and traced point source having the appropriate magnitude. This way, the free parameters of the coma model are its total brightness, its slope and the brightness contribution from the nucleus.

3.1. The Afrho

There exists an observable which is independent of the observation circumstances, namely the Afrho. It is defined as the relative linear filling factor of dust along the observation direction with rho collision parameter to the nucleus. So, we can write

$$Afrho[cm] = F(comet)*(2*D*R)^2 /F(sun)*1/rho$$

where D and R signs geocentric and heliocentric radius to the comet, F(sun) is the (terrestrially observed) flux of the Sun in the selected waveband, F(comet) is the detected flux of the comet, while rho is the collisional length of the observation line (the distance between the direction of the observation and the nucleus itself).

In the case of the ideal coma, the Afrho does not depend on the rho radius. In this case, the observer could have used only one Afrho parameter, even, without the referring rho specified. In practice, Afrho does slightly depend on rho: as it is mentioned above, the logarithmic slope of Afrho is exactly 1-more than the one of the logarithmic coma profile. So the comet is optimally characterized by the set of some rho-Afrho data pairs covering the whole coma. Time development of Afrho will show the varying matter production, while the spatial derivates of Afrho refer to the physical state of the comet.

4. Complex examinations

Selected examples will help us show some detailed examinations of comets. The serious may select splendid of tools to observe the comet evolution. The most important is to have homogeneous and continous time-coverage, so it would be advisable to observe less comets in more details continously instead of collecting few data of several comets.

Hereafter, we present some tools commonly used in, e.g., galaxy morphology (see eg. Ravindranath et al. 2001 for recent discussion). Presented data were obtained at Calar Alto Observatory, 1.23 m telescope, Gunn filters and selected interference comet filters such as CN (blue), C2, CO+. Telescope was tracked onto the comet instead of sidereal tracking so the apparent motion of the comet does not affect the results. So as to eliminate the starry background, images were first processed with the stellar-model subtraction tool of IRAF (in practice we made a PSF-photometry, and used the resultant images as star-free ones), and as the second step, the appropriate images were median-combined. Afrho was measured in Gunn r, where few emission lines affect the dust continuum, so the detected flux is considered to be proportional to the dust density. Obseravtion of gas evolution included the calculation of the individual gas production rates with help of spectrophotometry, and, on the other hand, comparison of the gas and dust profiles. Observations were made in August, 2000. For further details on circumstances, and calibartions of interference filters see Szabó et al., 2002.

To extract the surface brightness change across the nucleus, we used the apextract task from the TWODSPEC package in IRAF. A 5-arcsecond-wide aperture was shifted through the coma across the nucleus in two sampling directions. One of them was the solar-antisolar line (hereafter referred as radial section), the other perpendicular to the radial direction (hereafter referred as tangential section).

Azimuthally renormalized images are similar to the residual images defined by the difference of the coma image and an analytic radial profile. Here, instead of an analytic fit, we simply used the radial coma image resulting from an azimuthally averaged coma image. They are also similar to the Sekanina-sections as well. Bright positive areas in the residual image refer to matter excess while dark negative values show tenuous areas. This method emphasizes the presentation of special phenomena, such as the ellipticity of the coma, jet or spin structures. To describe these features, we extracted surface brightness profiles from the residual images, just as we did for the original images.

For physical conclusions, the strength of spatial variations must be characterized. We calculated local intensity ratios for the negative and positive peaks of azimuthally renormalized images. They are given by the peak intensities with respect to the normalised coma intensity at the same position.

The images are rotated in a such way the solar direction is to the right. The left subpanels show the observed images, while the right subpanels are azimuthally renormalized images. Graphs show radial sections of surface brightness profiles (middle) in standard Gunn r and C2. C2 is plotted with respect to the zero magnitude of Gunn g. Normalized intensity of spatial variations is shown in the bottom. Local intensity ratio (lc) of spatial variations is expressed in percents at positive and negative peaks. Crosses refer to the radial section while solid line shows the tangential section. The images are 150 arcsec times 150 arcsec for 19P and 100 arcsec times 100 arcsec for 29P and C/2000 A2.

So as just to illustrate the efficiency of these tools, we summarize our conclusions in the followings. The cited literature (mainly IAU Circulars) helped us overview the evolution of comets and present our data as the result of the previous history. For quantitatively detailed discussion and comparisons, see Szabó et al. 2002.

4.1. 19P/Borrelly

This comet belongs to the Jupiter family, with an orbital period of about 7 years. It is the prototype of the Borrelly-type class of comets (defined by Fink et al. 1999), known for its low C2 production. The 1994 perihelion was studied by A' Hearn (1995), who determined several production rates. A detailed structural analysis of its coma and nucleus is presented by Lamy et al. (1998) based on observations taken during the same apparition. They have determined a prolate spheroid nucleus model with 4.4 times 1.8 km semi-axes. The estimated fractional active area is 8%. Our observations were made about two months before the Deep Space-1 spacecraft encountered this comet in September, 2001.

Images at relative high airmasses and under pre-twilight conditions were taken because of the unfavorable elongation. The night of the best transparency conditions was selected for observations, although the seeing was larger than 2 arcsec.

Although the slope of the profile (-0.98) suggests an isotropic and steady-state coma, the inner structure was quite complex. The nucleus was far from the coma center, shifted to the antisolar direction. Dust components formed a compact cloud in the inner 30 arcsec around the coma and formed an impressive tail with forked structure. Gas components flowed to the solar direction, with almost no gas observed in the tail. Surface photometry showed that the surface brightness of the inner coma decreased faster in the antisolar direction (2 magnitudes in 7.5 arcs on the r images) and slower toward the Sun (2 magnitudes in 11 arcsec). The outer coma became quite regular: it faded by 5 magnitudes in 53 arcsec to the antisolar direction and 37 arcsec to the solar one.

As the azimuthally renormalized image shows, the behavior of the inner coma is due to a jet-like outflow to the antisolar direction containing 16% of the total flux. This feature is detectable through 45 arcsec on the radial cross section, which implies a proper length of 65000 km on the assumption that the jet is thin and lies on the solar radius. A comparison between the Gunn r and Comet C2 profiles suggests that it consists solely of gaseous components. The tail is quite long and could be detected even beyond the border of the image.

29P/Schwassmann-Wachmann 1

This unusual comet is well-known for its unpredictable outbursts (see Enzian et al. 1997 and references therein). The nucleus seems to be perhaps the largest one known in the Solar System, while its albedo is often estimated to be over 15\% -- much higher than is measured for ‘c0’sual’’nuclei (Jewitt 1990). Jets of the comet in outburst suggest rotational effects. Several observers have tried to determine the rotation period: the most recently published values are 14 and 32 hours (Meech et al., 1993).

We observed the comet during its 2001 outburst, which was first detected by Nakamura et al (2001) on May 17.69, 2001. During our observations and reductions, the main difficulty was the crowded sky-field in the Milky Way. Our star-subtraction procedure removed about 3500 stars brighter than about 21 magnitudes from the 10 arcmin times 10 arcmin field.

Three months after the outburst the comet was 12.68 magnitudes in Gunn r, thanks to its position at opposition and high activity. Due to the distance to the Earth, its coma was quite compact: its surface brightness decreased 2 magnitudes in 16 arcsec and 5 magnitudes in 35arcsec. The latter value corresponds to a diameter of 260000 km. On the azimuthally renormalized image, the well-known jet shows a spiral-like matter-rich and matter-poor part, with local contributions +37% and -77%, respectively. The spinning shape is attributed to rotation of the nucleus.

A ring-like structure, also visible with help of surface photometry, is not included in the non-radial part as it vanishes by subtracting the azimuthal average from the coma image. The jet ends at 21 arcsec, while this faint ring is suspected to be at 1 arcmin distance from the nucleus, having 22 mag/squarearcsec surface brightness. We believe that the low counts in CN, CO+ and C2 filters originate from the continuum, and considering the estimated errors, only higher limits of the emission rates can be reported.

C/2001 A2 (LINEAR)

The comet was in the very focus of the scientific interest during the summer of 2001: as of September, 2001, there have been 25 IAU Circulars issued describing the evolution of this interesting comet. At the end of March, the comet brightened 4 magnitudes in 4 days (Mattiazzo et al., 2001). By the end of April, a double

nucleus was detected (Hergenrother et al., 2001). Further fragmentation was reported by Schuetz et al. (2001), and a CN jet was reported by Woodney et al. (2001). At the second half of July, the comet diminished 3 magnitudes and rapid light variations were observed; these are explained by Kidger et al. (2001) as the separation of small, short-lived splinters that may not have been directly observable.

By the time of our observations, the total apparent magnitude decreased below eleventh magnitude, and none of the multiple nuclei was detectable on our images. Despite the calm behavior suggested by the run A2a (on 13th August, 0:14 UT), a slight increase of activity was detected on A2b images (on 15th August, 0:00 UT). During the A2c run (on 16th August, 0:28 UT}, production rates of CN and C2 increased by a factor of 4, while dust production and Afrho did not vary much. The most surprising event between the nights is the variation of the shape of C2 profile. The radiation pressure-dominated profile with narrow center turned into a quite extended, symmetric profile with little central hump. Some parts of the C2 surface were brighter than the Gunn r continuum. That suggests a similar outburst of activity in C2 and CN as was reported by many observers during the previous weeks (Kidger et al. 2001).

The Gunn r profile did not changed significantly between the two runs. In the central 7 arcsec, the surface brightness falls by 2 magnitudes, while on the solar side it decreases by more than 5 magnitudes in about 70 arcsec. On the antisolar side the coma evolves into an impressively bright and wide, V-shaped tail, which is brighter than 22 mag/squarearcsec when it leaves the field of view. As the tail character suggests merely dust components, the tail itself has also not been disturbed much by the observed small outburst. Altogether, the general morphology of C/2001 A2 is quite similar to the observed behavior of 19P/Borrelly. An important difference is that in the case of C/2001 A2, neither type of jet has been detected, and the azimuthally renormalized image shows a tail rich in dust and detectable until the nucleus.

Although the contribution of spatial variations parts slightly decreased during the outburst, the ratio of local contributions at minimum and maximum remained constant (i.e. 0.224-0.217 vs. 0.159-0.151) within an error of 4%. That may be explained by a spherically symmetric outburst. In this case, the absolute values of non-radial parts do not vary, but their contribution decreases as the absolute value of the radial part increases. Quantitatively, the radial part of the dust coma is increased by 39%. In this case, the brightness of the inner coma should increase -0.29: that agrees with the observed value (-0.24) within the expected errors.

A spherical outburst might be caused by uniformly increasing activity on the whole surface of the nucleus, though the little fractions of active area commonly observed in comets seem to contradict this view. Alternatively, matter ejected in fans above the active area can be blended to globular shape if we assume a fast-rotating nucleus. The assumption of a fast-rotating nucleus agrees with the observed break-up of small fractions of the nucleus. The measured 162--191 cm Afrho is smaller than 288 cm measured by Schleicher (2001), which is simply explained by the lower level of activity.

5. Discussion

Comet morphology is a progressive field of professional astronomy and offers promising results for the amateur as well. However, the professional astronomer rarely gets time on large telescopes enough for the detailed study, including spectrophotometry and spectral-resolved morphology. However, the homogeneous time-covered amateur observations may modify, even significantly alter the results of detailed observations. Vice versa, the detailed observations can many times help in understanding the previous evolution of the comet, even when it is presented by few and moderate-quality previous observations.

Therefore, we encourage the public observatories and the amateurs to continuously publish homogenous data on comets. For this, the evolution of rho-Afrho quantity pairs seems to be the best observable. Its time evolution shows to the dust (so the matter production) of the comet; while the spatial differences of Afrho (i.e. its rho-dependence) describe the coma profile, and offers study the effect of the solar wind and the radiation pressure. The most interested observer can try to do surface photometry, specially processed images, surface sections or emission exploration with narowband filters.

However, it would be useful to have a free-access archivation system where these data are collected. Original and processed images often contain important additional data (jets, spinning fans, antitails, etc.) that cannot be expressed so simply as e.g. the Afrho. That is why the archivation of the observed images seems to be also necessary.

So as to help the amateur-professional cooperation, now we are to design such an archivation. We plan to collect all the calibration data and the rho-Afrho pairs into a big table. The available images are to be cross-referred to the table via links. In spring, 2003, hopefully the first steps of the project will be made. Until the archivation is ready, I would like to ask the comet observers to by a filter set for comets (e.g. a Johnson-filter set and a C2 filter, that latter is 99$ at Lumicon), and to get familiar with Afrho. A code (written by Antonio Milani) which calculates the Afrho based on calibration data and fluxes is now available upon a request to the author (szgy@mcse.hu).

As the further perspective, I consider a closer cooperation of observers who work on comet morphology. Quite soon, all these observatories ought to establish a filter sequence which is transformable to a standard system. This is the principal condition of making homogeneous data. If these observatories buy some comet filters as well, and gas production parameters will be also measured, they should also have included into the archieves. We hope that these observations will be frequently used by the professional analyses as well, and will help in better understanding of comets.

6. Literature

A' Hearn, M. F., Millis, R. L., Schleicher, D. G., et al. 1995, Icarus, 118, 223 (A95) NASA ADS
Fink, U., Hicks, M. P., & Fevig, R. A. 1999, Icarus, 141, 331 NASA ADS
Hergenrother, C. W., Chamberlain, M., Chamberlain, Y., et al. 2001, IAUC, 7616
Jewitt, D. 1990, ApJ, 351, 277 NASA ADS
Kidger, M., Ferrando, R., Manteca P., et al. 2001, IAUC, 7679
Lamy, P. L., & Tóth, I. 1995, A&A, 293, L43 NASA ADS
Lamy, P. L., Tóth, I., & Weaver, H. A. 1998, A&A, 337, 945 NASA ADS
Larson, S. M., & Slaughter, C. D. 1992, Asteroids, Comets, Meteors 1991, 337-343
Lederer, S., Campins, H., & Osip, D. J. 1997, EMP, 78, 131
Lowry, S. C., Fitzsimmons, A., Cartwright, I. M., & Williams, I. P. 1999, A&A, 349, 649
Luu, J. X., & Jewitt, D. C. 1992, AJ, 104, 2243 NASA ADS
Mattiazzo, M., et al. 2001, IAUC, 7605
Nakamura, A., Hale, A., Kadota, K., & Yoshimoto, K. 2001, IAUC, 7640
Ravindranath, S., Ho, L. C., Peng, C. Y., et al. 2001, AJ, 122, 653 NASA ADS
Schleicher, D. 2001, IAUC, 7653
Schuetz, O., Jehin, E., Bonfils, X., et al. 2001, IAUC, 7656
Schultz, R., A'Hearn, M. F., Birch, P. V., et al. 1993, Icarus, 104, 206 NASA ADS
Szabó, Gy., Kiss, L.L., Sárneczky, K., Sziládi, K., 2002, A&A 384, 702
Woodney, L. M., Schleicher, D. G., & Greer, R. 2001, IAUC, 7666

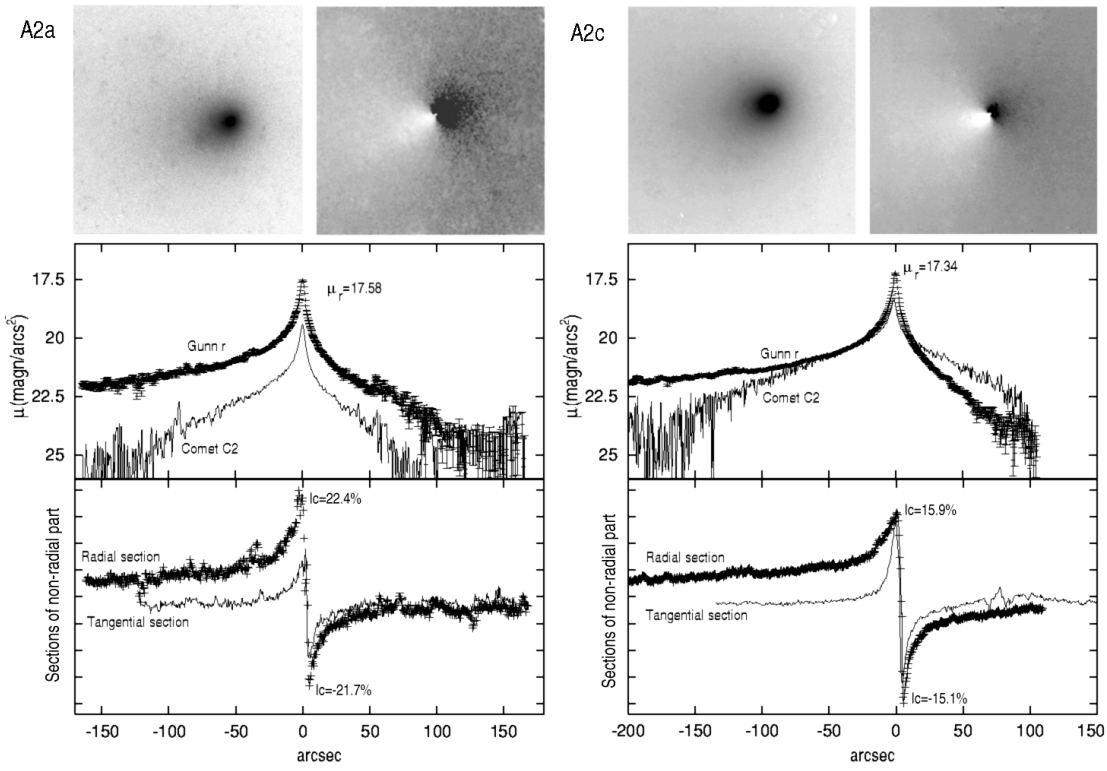

Figure 1: Comets 19P (left) and 29P (right).

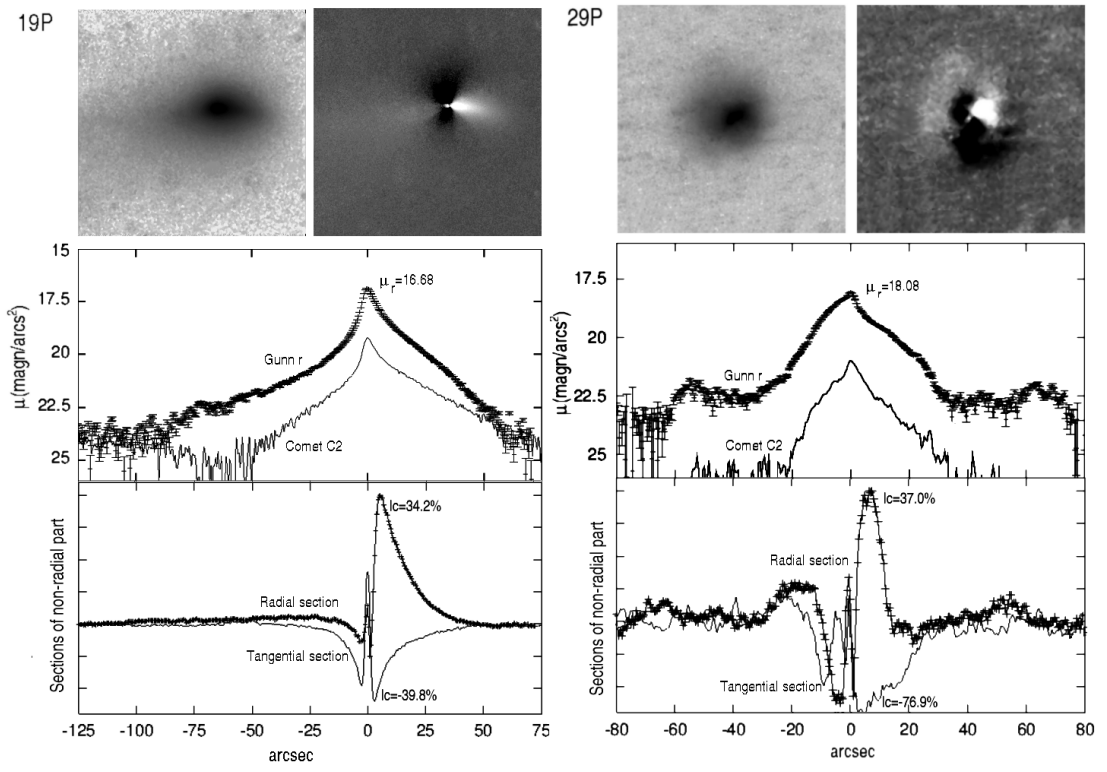

Figure 2: Comet C/2001 A2 on 13th (left) and 16th (right) August 2001.Note the strong change of C2 profile.